

FinFem-project report

Authors: Kimmo Päiväsaari, Jarno Kaakkunen, Martti Silvennoinen, Pasi Vahimaa (UEF)
Petri Laakso, Raimo Penttilä, Päivi Heimala, Ilkka Vanttaja, Matti Lehtimäki (VTT)

Confidentiality: Public

Report's title	
FinFem-project report	
Customer, contact person, address	Order reference
TEKES	
Project name	Project number/Short name
Nano structures and applications with fs laser technology	26206 FinFem
Author(s)	Pages
Kimmo Päiväsaari, Jarno Kaakkunen, Martti Silvennoinen, Pasi Vahimaa (UEF) & Petri Laakso, Raimo Penttilä, Päivi Heimala, Ilkka Vanttaja, Matti Lehtimäki (VTT)	84
Keywords	Report identification code
Nano Structures, Femtosecond, Laser, Industrial Applications	VTT-R-08007-10
Summary	
<p>In this project goal was to utilize femtosecond laser processing to achieve even as small as nanoscale features. Self organizing structures were produced with less than wavelength spacing in variety of materials. Also the principles of how to control this effect into some extinct were found out. Nanoscale particles were done into liquid media. Nanoscale particles that are produced during laser ablation with femtosecond laser were analyzed and results correlated well with knowledge from literature. Particles can be well under 100 nm which is in the true nanometer scale.</p> <p>Project goals were set in the beginning of the project and during project those goals were met pretty well even though further studies would be needed to fully understand nature of femtosecond laser processing and all related phenomena. Functional surfaces were a big part of the project and especially the hydrophobic and hydrophilic properties were pursued. From the mold as high as 152° contact angles were measured. On the other hand also hydrophilic surfaces were also made when contact angle could not be measured due drop spreaded over very large area. Using novel optical means to enhance processing speed with fs-laser was utilized successfully and when compared to literature processing speed could be increased by several orders of magnitude.</p> <p>To conclude all results in this report we could say that goals were met but a lot is still needed to do if total understanding is pursued.</p>	
Confidentiality	Public
Lappeenranta 10.10.2010	
Written by	Reviewed by
Kimmo Päiväsaari, Senior Researcher, UEF	Pasi Vahimaa, Professor, UEF
Raimo Penttilä, Research Scientist, VTT	Timo Määttä, R & D Manager, VTT
	Risto Kuivanen, Vice President, R & D, VTT
VTT's contact address	
Distribution (customer and VTT)	
Modines, Okmetic, Savcor Alfa/Cencorp, Stora Enso, Thermo Fischer, TEKES, UEF, VTT	
<p><i>The use of the name of the VTT Technical Research Centre of Finland (VTT) in advertising or publication in part of this report is only permissible with written authorisation from the VTT Technical Research Centre of Finland.</i></p>	

Preface

Project “Nano structures and applications with fs laser technology” (FinFem) was carried out between 2008 and 2010. Project was carried out by UEF (University of Eastern Finland in Joensuu) together with VTT’s research groups in Lappeenranta and Espoo.

Project was funded by TEKES with participating companies and VTT.

Steering group consisted of following people

Modines Kari Rinko
Okmetic Kari Myrberg
Savcor Alfa/Cencorp Anssi Jansson and Jari Ketoluoto
Stora Enso Nina Miikki
Thermo Fisher Niina Sande
TEKES Kalevi Pölönen
UEF Timo Jääskeläinen and Pasi Vahimaa
VTT Timo Määttä

Project manager was Kimmo Päiväsaari UEF. In addition project involved a number of different researchers from VTT and UEF. Writers of this report would like to acknowledge the steering group and all companies in the project for active steering and good cooperation through out the project.

Lappeenranta 1.11.2010

Authors

Contents

Preface	2
1 Introduction.....	5
2 Goal.....	7
3 State of the art.....	8
3.1 Fundamentals of femtosecond laser technology.....	8
3.1.1 “Long”- and “short”-pulse ablation.....	8
3.1.2 Physics of the fs-ablation	9
3.1.3 Self-organized surface structures	10
3.1.4 Process parameters and atmosphere influence.....	12
3.1.5 Applications of fs-pulses	13
3.1.6 Femtosecond laser system	13
3.1.7 Generation of femtosecond laser pulses.....	14
3.1.8 Pulse Amplification.....	15
3.2 Markets and trends VTT.....	16
3.2.1 1970s to 1980s: dye lasers	16
3.2.2 Early 1990s: Ti:sapphire and other solid-state lasers.	17
3.2.3 Early 1990s to present: fiber and disk lasers.	17
3.2.4 Materials processing	18
3.2.5 Commercial lasers	19
3.2.6 Ultrafast laser prices	20
3.2.7 Ultrafast laser forecast	20
3.3 Conclusion of markets and trends.....	21
3.4 Typical ultrafast laser applications	21
3.4.1 Diamond machining	21
3.4.2 Silicon surface modification.....	22
3.4.3 Drilling of metals	23
3.4.4 Biomedical stent cutting	24
3.4.5 MEMS micromachining	24
3.4.6 Photomask repair.....	25
3.4.7 Fused silica ablation	26
3.4.8 Thin film patterning	27
3.4.9 References.....	28
3.5 Workstations	28
3.5.1 Purchasing a workstation.....	30
3.5.2 Laser integrators in the ultrafast laser field	31
4 Methods.....	31
4.1 Laser Equipment at VTT	31
4.1.1 Femtosecond laser system	31

4.1.2	SPI G3 20 W pulsed fiber nanosecond laser	32
4.1.3	Lumera Rapid 2 W picosecond laser	33
4.2	Laser Equipment at JoFy	33
4.3	Femtosecond laser parameter tests in silicon	34
4.4	Femtosecond laser parameter tests in tool steel.....	35
4.5	Femtosecond laser parameter tests in nickel.....	35
4.6	Laser parameter tests with picosecond and nanosecond lasers in silicon, tool steel and nickel	36
4.7	Laser drilling tests on silicon	36
5	Results	37
5.1	Femtosecond laser parameter tests in silicon	37
5.2	Femtosecond laser parameter tests in tool steel.....	41
5.3	Femtosecond laser parameter tests in nickel.....	47
5.4	Laser parameter tests with picosecond and nanosecond lasers in silicon, tool steel and nickel	50
5.5	Comparison of rectangle depths made with different lasers.....	57
5.6	Holes in silicon	58
5.6.1	Basic drilling tests	61
5.6.2	Water assisted drilling.....	64
5.6.3	Drilling using diffractive optics.....	67
5.7	Nanoparticle measurements	68
5.7.1	Introduction and goal	68
5.7.2	Description	68
5.7.3	Measurements and results.....	71
5.7.4	Nanoparticle generation in solution.....	74
5.7.5	Summary.....	75
5.8	Functional surfaces.....	76
5.8.1	Hydrophobic surfaces	76
5.8.2	Controlling the cell adsorption using structured surface.....	80
6	Conclusions.....	81
	References	83

1 Introduction

FINFEM project target is to create new nano- and microscale laser processing techniques by using a femtosecond laser. To map out the possible applications and specific advantages ablation can bring to the industrial processes. The objectives defined by industrial partners range from the traditional material removal to the generation of the functional surfaces. Joensuu University did coordinate the project and made basic research on laser-matter interaction together with international partner Laser-Laboratorium Göttingen. VTT Laser processing team assisted in basic research and developed the micro- and nanomachining processes to industrial applications. Industrial partners in the project were Okmetic, Thermo Fischer scientific, Stora Enso, Modines and Cencorp.

Creating of the micro- and nanostructures is one of the main fields in the scientific research today. There are many elaborate manufacturing processes for writing different structures, for example, electron beam lithography and optical lithography. However, usually these traditional techniques demand several stages of pre- and postprocessing for final nanostructured product. Also the equipment for these techniques are usually very expensive and demands strict clean room conditions. In some applications these restrictions can be avoided using direct laser ablation to the surface structuring. In laser ablation such energy density can be created on the material that the surface is removed by evaporation. Advantages of this technique is the need of the less manufacturing steps, possibility to structure material with curved surface and materials that are otherwise hard to process. Sometimes the laser matter interaction itself can produce the structures with new desired properties. A wide range of material properties can be changed including wetting, frictional and absorption behaviour by structuring the surface with micro- and nanosized features.

Nanoscale features could be utilized when combining electronics and mechanics (MEMS), electronics and biotechnology (diagnostics) and when making medical implants and instruments, optical components, functional surfaces (lubrication, friction control, lotus effect, optical functional surfaces, chemical catalysts and bioactive surfaces). Driving forces in this are the economic and society based trends like raising demand for elderly people enabling technologies. Also one additional driving force is high need for new functionalities in different gadgets, instruments and machines. Femtosecond pulse width ($f_s = 1 \times 10^{15}$ s) lasers enable machines to produce electronics and medical components and instruments up to nanoscale level.

Laser development has been rapid over the last decade which leads to continuous price reduction of equipment. Using optical means to divide the beam enable increase the processing speed close to industry's demanding needs. Femtosecond processing makes it possible to machine all known materials with high precision without heat input and melt formation during processing. It is also possible to make processing inside material which enables making of different channels or doing 3D polymerization in organic ceramics. Short pulse laser like picosecond and femtosecond laser have enabled processing of the most demanding materials

and applications. For example with an fs-laser with pulse width of 100 fs can produce intensity of hundreds of terawatts per square centimetre. In practise this kind of energy density vaporized all known materials. This kind of straight vaporization with out melt regime is called ablation. Besides metallic and plastic materials it is possible ablate ceramics, semiconductors and dielectric materials. Short pulse duration minimizes the heat effect to the surrounding material which makes the thermal load negligible and the best quality and smallest features are possible to be done. This is then called cold ablation. Interferometric ablation can be applied very well to making periodic micro and nanofeatures. In interferometric ablation beam is divided in to multiple beams with diffractive optical element and then combined with imaging optics to sample surface. Interference pattern is then replicated to sample surface as surface structure. This enables to produce large areas of grating structure fast with low repetition laser straight to e.g. metallic surface. In Figure 1 there is one grating like surface on polished steel surface.



Figure 1. VTT-logo made with grating like structures.

In addition fs-laser interaction can make together with interacting material nanostructures which may have wanted properties. As an example in Figure 2 there is nanostructures made with fs-laser ablation on steel.

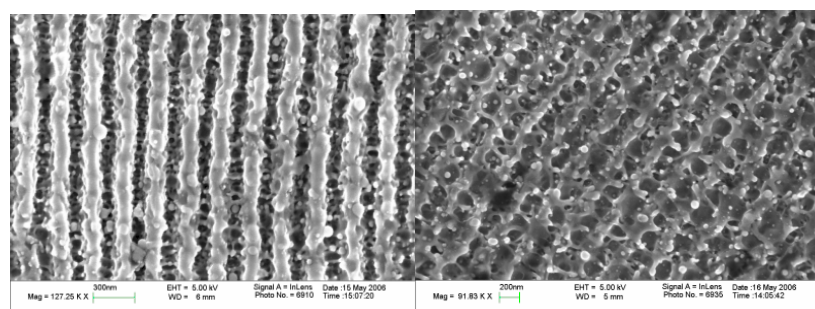


Figure 2. Nanostructures made with femtosecond laser

Material surface properties can be modified with certain surface structure. These properties can be wetting, friction or absorption. Applications in which it is essential to increase the surface area vs. volume may also have new applications (fuel cells, biomedical implants etc. Especially reflection and absorption control are very interesting applications e.g. in solar industry. Example of this kind of periodic functional steel surface ablated interferometrically is presented in Figure 3. This surface combining material surface properties can be modified with certain surface structure. These properties can be wetting, friction or absorption. Applications in which it is essential to increase the surface area vs. volume may also have new applications (fuel cells, biomedical implants etc. Especially reflection and absorption control are very interesting applications e.g. in solar industry. An example of this kind of periodic functional steel surface ablated interferometrically is presented in Figure 3. This surface combining micro and nanostructures changes from diffractive to absorbing when the structures are deep enough. This ablated surface reflects only 5 % back of visible light. Phenomenon is almost non wavelength dependent at VIR_NIR region.

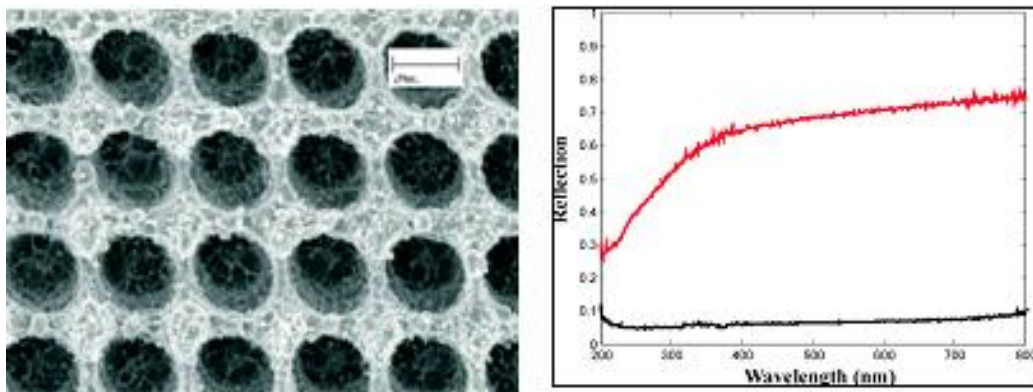


Figure 3. Surface covered with micro and nano features. Measured reflection spectrum from non texturized (red) and texturized (black) surface.

Joensuu University started fs-laser ablation in 2005 with low repetition rate laser. In TEKES funded NAARMU project a lot of ablation research was done. During this project University invested in modern fs-laser with 800 nm wavelength and 3.5 mJ pulse energy. University has all the needed analysing tools for these nano and micro surfaces. University's strong field is the laser-matter interaction and surface modification with interferometric ablation.

VTT Laser processing team has a strong competence on laser materials processing. Covered research topics are: laser processing of materials with various types of lasers, surface engineering, engraving, heat treatments, marking, drilling, cutting, laser welding of numerous materials etc. VTT will contribute to the project in terms of femto, pico and nanosecond surface processing with different strategies. During project VTT will rent an fs-laser for six months and build a laser processing cell close to industrial setup to be able to serve industry's cases in the project.

2 Goal

FINFEM project target was to create new nano- and microscale laser processing techniques by using a femtosecond laser with novel optical means. Optical

solutions were e.g. interferometer based diffraction optics. These optical solutions enabled true nanoscale fs-ablation. This makes it possible to pursue more efficient and fast processing for the industry. Another aim was to be able to make feasible large area fs-processing using optics developed during project. These optics are needed due fs-laser processing is done with fairly low repetition rate but with high pulse energy which could be spreaded to wider area to increase processing speed. In addition goal was to seek possible industrial applications for fs-laser processing in Finland. Fs-laser process was developed further to minimize heat effects and burr. One part of project was to make functional surfaces with hydrophobic and hydrophilic properties. Joensuu University had close research cooperation together with international partners Laser Labor Göttingen and Moscow Lomonosov state University. One researcher visited in Göttingen for one year beginning from February 2009. Research report of this exchange is a separate appendix 1 (Jarno Kaakkunen, Laser ablation using femtosecond pulses in UV-wavelength range). During project several researchers visited Joensuu University from Moscow Lomonosov State University.

3 State of the art

3.1 Fundamentals of femtosecond laser technology

Powerful, ultrashort optical pulses, with durations of a few hundreds femtoseconds or less, are of interest for numerous scientific applications, such as nonlinear optics and optical sampling of ultrafast phenomena. These femtosecond pulses also allow material processing with minimum thermal effects, optical communication, imaging of biomedical and chemical reactions. Femtosecond laser has many qualities that previous pulsed lasers lacked: no heat production in ablation, chemical reactions can be observed in femtosecond time scale and terahertz spectroscopy is possible due to the femtosecond laser pulses. In laser ablation, very large peak power provided by shorter pulses enables not only ablation of the smaller features, but also ablation of virtually any material.

3.1.1 “Long”- and “short”-pulse ablation

With relatively long pulses, like nanosecond it is already possible to move into direct ablation of the various materials in a micro-size region. This range pulses are suitable for ablation of few tens of microns structures, but even then some problems occurs. Depending on material it might either crack (e.g. silicon) or properties of the surrounding area of the ablation might be changed by heat flow (Figure 4a). This is the major problem of these lasers in micro-machining that additionally leads into the new problems. Because of the heat diffusion even if laser spot is focused into size of few microns, we are ablating about 10 time’s bigger areas. This melting has also other disadvantages. Heat is affected in much larger area than smallest structures that can be ablated. This area is also called Heat Affected Zone (HAZ). This influences into upcoming ablations properties and can also influence on optical properties of the material. Also the edges of the ablation zone are not well defined and walls of burr can be formed next to it.

These problems can be avoided by moving into even shorter pulses, down to femtosecond region (Figure 4b). These pulses with only length of few microns are so short that matter does not have time to move away from them, like in a case of the longer pulses. This means that pulse length is shorter than the heat diffusion time. Therefore, instead of debris formation matter is directly evaporated into electron and ion plume giving us clean surface around ablation area. Because there is no heat effected zone, the matter is not formed around ablation area and there are neither micro-cracks.

Because energy does not have time to diffuse away, micromachining has high efficiency. Amplified ultrashort pulses are packed only with energy in range of mJ, but because of the short length of pulses the peak power raises into gigawatts and therefore also the intensity can easily rise in terawatt per cm^2 range. This means that temperature increases in tooling area far beyond evaporation point till so called plasma region.

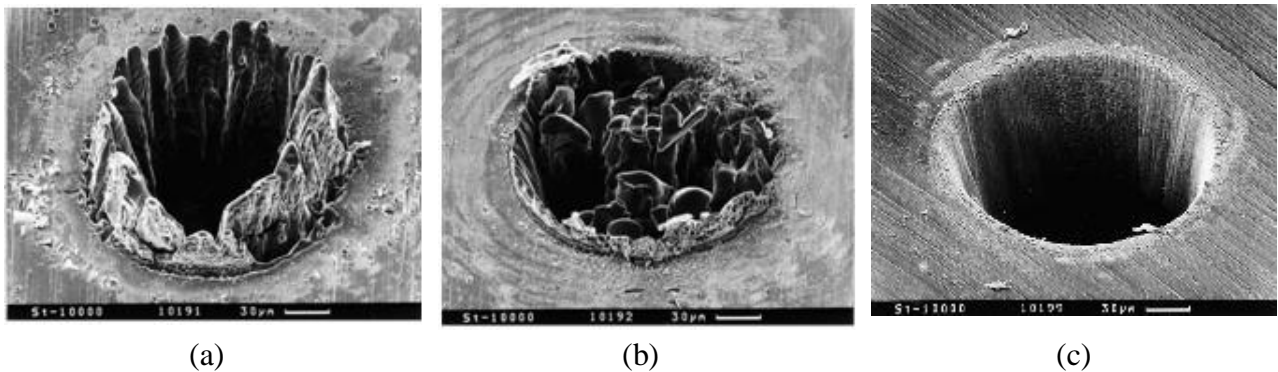


Figure 4. Hole drilling in a steel foil made using different laser pulse lengths, (a) nanosecond, (b) picosecond and (c) femtosecond pulses (Chichkov, C. Momma, S. Nolte, F. von Alvensleben and A. Tünnermann, *Appl. Phys. A: Materials Science & Processing* 63, 109-115 (1996).).

As a conclusion the main physical differences of the ultrashort pulse ablation over the nanosecond ablation are as follows:

- High peak power enables ablation of virtually any material.
- Using of ultrashort pulse minimizes heat affected zone. This enables ablation of smaller features and minimizes formation of molten zone, recast layer, micro cracks and shock wave.

3.1.2 Physics of the fs-ablation

There is no unambiguous explanation for fs-ablation mechanism, because it is very complex phenomenon including strongly coupled optical, thermodynamic, energy transfer and mechanical processes. The simplified physical model of the femtosecond ablation process can be described as follows. In the first stage of the ablation the laser energy is absorbed into solid sample by free electrons via the inverse Bremsstrahlung. This raises the temperature of the electron subsystem compared to the lattice temperature. This is followed by a rapid relaxation of the temperature difference between the two subsystems leading to phase transformation of the laser affected zone. Thereafter matter is separated from the

sample surface and this plasma is then expanded into ambient. Well known way to describe the temporal and spatial evolution of the electron (T_e) and lattice temperatures (T_i) is one-dimensional two-temperature diffusion model:

$$C_e \frac{\partial T_e}{\partial t} = \frac{\partial Q(z)}{\partial z} - \gamma(T_e - T_i) + S$$

$$C_i \frac{\partial T_i}{\partial t} = \gamma(T_e - T_i)$$

$$Q(z) = -k_e \frac{\partial T_e}{\partial z}$$

$$S = I(t)\alpha \cdot A \cdot \exp(-\alpha z)$$

where, $Q(z)$ is heat flux, $I(t)$ the laser intensity, S laser heating source, A surface absorptivity, α material absorption coefficient, C_e and C_i are the heat capacities of the electron and lattice, respectively. γ is the electron-phonon coupling coefficient and k_e the electron thermal conductivity.

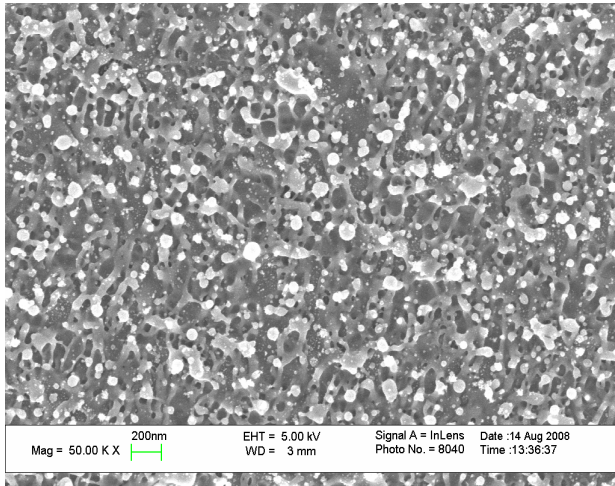
There are two major mechanism, avalanche ionization and multiphoton ionization, which are considered for free electron generation. Avalanche ionization dominates in lower intensities and multiphoton ionization becomes significantly strong in higher intensities. Avalanche ionization consist series of (collisional) impact ionization, were one free electron produces two free electrons. After critical density laser energy is absorbed mainly through inverse Bremsstrahlung and resonance absorption mechanism. Also the material removal itself is not trivial and two different mechanisms are considered for explanation, thermal vaporization and Coulomb explosion. According to these two mechanism femtosecond ablation can be divided into two regimes, strong and gentle ablation. In strong ablation, were intensities are significantly higher than ablation threshold, thermal evaporation is dominant and respectively in gentle ablation, were intensities are near ablation threshold, Coulomb explosion in dominant.

3.1.3 Self-organized surface structures

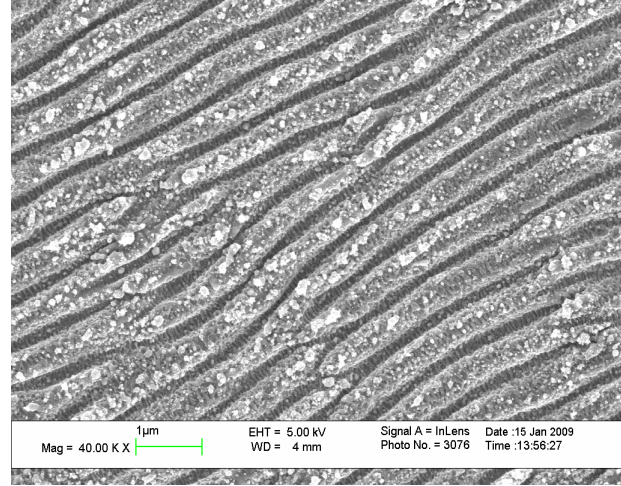
During the femtosecond ablation different kind of self-generated structures appear. With low values of fluence (pulse energy per area) various nano-size structures start to grow on the matter (Figure 5a). By increasing the pulse number and fluence the matter begins to orientate according to polarization, forming so called Laser Induced Periodic Surface Structures a.k.a. LIPSS (Figure 5b). Furthermore if using high energies or high pulse numbers different form micron-size structures start to cover the matter (Figure 5c and d).

Nano-size ripples are the first visible indication on matter's surface about the ultrafast and ultrashort laser ablation. Different form nano-structures start to cover the material well before total evaporation. Although these structures seem to be randomly formed, they have certain shapes. Usually structures are round shaped balls that are connected with rims. Those are formed by extremely rapid material heating and cooling process. Femtosecond irradiation heats the matter to plasma which is rapidly cooled down, causing the formations seen in the surface. Plasma formation is not uniform and therefore local plasma centrals start to appear

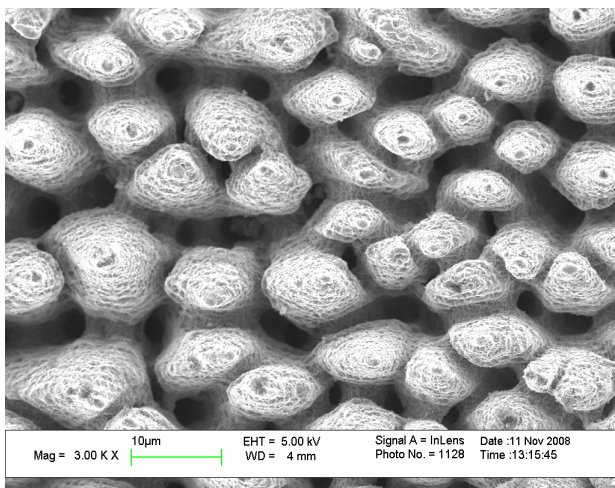
causing nano-craters. Matter starts to evaporate from the surface, but because of rapid cooling it re-solidifies in nano-sphere shape. Some of these spheres might explode during the evaporation and hence causing different nano-rims and splashes.



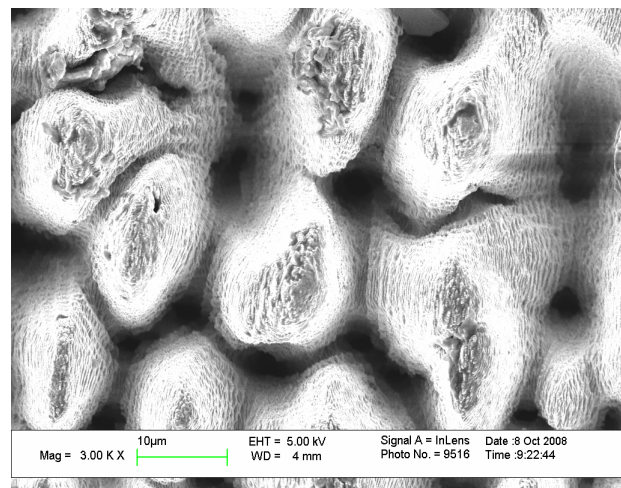
(a)



(b)



(c)



(d)

Figure 5. Different kind of self-generated structures in steel. (a) are generally formed nano-structures, (b) is laser induced periodic surface structures (LIPSS), (c) is so called “coral”-structures and (d) is higher magnification of the (c).

Other type of phenomena during femtosecond ablation is LIPSS. For certain pulse parameters the surface starts to orientate perpendicular to the polarization of the beam. This means that matter starts to orientate like linear binary grating. Pattern is not perfect, because it has some irregularity points where line ends or divides into two parts. This grating like structures direction can be controlled with polarization of the pulses in a case of the linear polarization. Added to different form linear polarizations, this effect has been seen to happen also with elliptically polarized light. It is well known that for linear p-polarization the period of the grating Λ can be estimated as follows

$$\Lambda = \frac{\lambda}{1 \pm \sin\theta}$$

where λ is wavelength of the pulses in vacuum and θ is incidence angle of the pulses. Respectively for the s-polarization

$$\Lambda = \frac{\lambda}{\cos \theta}$$

In literature there are also other kind of variations about these formulas, but these are the most common and used estimations. As these formulas shows the LIPSS period can be controlled with changing the wavelength or irradiating the surface in various angles.

Ablation of matter using higher femtosecond pulse fluencies causes additional self-organized structures in micro-scale. Certain shape micro-size canyons a.k.a. “coral”-structures start to cover ablated surface randomly. Like in the case of the nano-ripples, size of these structures can be controlled with laser parameters within certain limits. These structures are usually covered with both nano-ripples and LIPSS.

3.1.4 Process parameters and atmosphere influence

Ablation quality, efficiency and speed can be controlled with laser parameters such as pulse length, fluence, repetition rate, wavelength, etc. Also external properties such as atmosphere, temperature, humidity etc. has an influence on ablation.

Pulse wavelength has influence, not only into size of the minimum feature size caused by diffraction limit, but also into self-organized structures. By using shorter wavelengths we are able to focus our beam into smaller area. Added to this size of the all self-organized structures, such as LIPSS, are influenced by wavelength. It also influences on various materials ablation rates, because different material has various optical properties for each wavelength. Naturally propagation and behavior of the different wavelength pulses in for example lenses etc. are totally different.

Fluence of the pulses has huge influence on ablation. Ablation with above ablation threshold causes only thermal effects into matter and no evaporation can be observed. Ablation with lower fluencies, but still higher than ablation threshold, we can ablate nice precise structures without any cracks. In some materials, such as silicon, too high fluence can cause cracks. Naturally with higher fluence ablation rate is faster, but amount of the debris is then higher. Unlike with long pulse ablation, short pulse caused debris can be afterwards removed. With high repetition rates, it might be that material has not totally recovered from last shot and there for the ablation is not the same than with lower repetition rates. Other thing is that evaporated material can influence on beam path and shape of the next pulse.

3.1.5 Applications of fs-pulses

Femtosecond pulses can be used in various applications. Not only in laser ablation, drilling, machining, cutting, etc., but also for example in spectroscopy, terahertz applications, etc. Femtosecond ablation can be used in direct micro-machining, but also in ablation inside (transparent) the materials. Also various interferometric setups can be applied and this possibilities for example security marking and fabrication of various optical devices as fiber Bragg gratings, waveguides, couplers, etc. Femtosecond pulses can be also use for fabrication of stamps for various mass production methods, like injection molding or hot embossing.

Different self-organized femtosecond ablated structures has several functionalities and they can be used in various applications. For example high absorption surfaces can be made just ablating the target with focused pulses. Previously mentioned LIPPS can be applied for example in security marking. Also wettability properties of the materials can be changed with using previously mentioned “coral”-structures.

Material tooling with femtosecond pulses is not only limited on micro- and nano-machining. They can be also applied in material coating and nano-particle generation. It has been shown that uniform and flat coatings can be done with various materials, mostly from metals but also from dielectrics. Other property of the fs-pulses is that they can be used in nano-size particle generation. When material is irradiated using them small particles are released from the material and when this process is taken into the liquid environment even smaller few nano-size particles can be generated.

3.1.6 Femtosecond laser system

Femtosecond optical pulse is an electromagnetic pulse in a time scale of 10^{-15} seconds and is made with lasers. Typical femtosecond laser system consists of oscillator, pulse stretcher, amplifier and pulse compressor as shown in Figure 6. Oscillator is used for generation of the femtosecond signal. This can be done by using suitable gain medium and mode-locking technique inside the oscillator. Usually femtosecond pulses coming out of the oscillator are in nJ range and this is too low value of energy for most applications. Pulse is usually amplified with succeeding gain stages. In order to gain medium to withstand the generated intensities the femtosecond pulse must be stretched to the picoseconds range before amplification. After amplification pulse is compressed again to the femtosecond range and pulses with several mJ can be generated using this method.

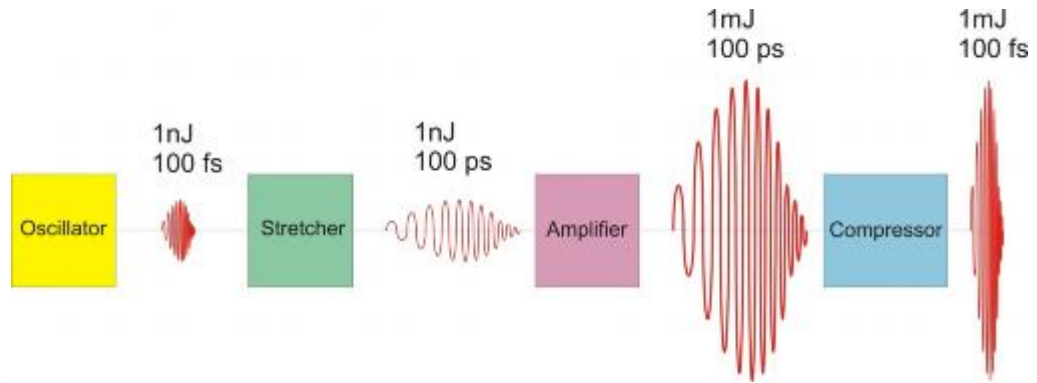


Figure 6. Schematics of the femtosecond laser system.

3.1.7 Generation of femtosecond laser pulses

A laser is constructed from three principal parts: an energy source, a gain medium, and mirrors that form an optical resonator. A laser's bandwidth of operation is determined primarily by the gain medium that the laser is constructed from, and the range of frequencies that a laser may operate over is known as the gain bandwidth.

Femtosecond pulses are mainly generated either in solid state femtosecond oscillator or in femtosecond fiber oscillator. In solid state oscillators the most popular gain medium is Titanium-Sapphire (Ti:Al₂O₃ or Ti:S) crystal. The wide gain bandwidth of Ti:S makes it especially suitable for generation of signals with wide spectrum needed for generation of ultra short pulses. Ti:S oscillator uses a self-focusing nonlinear optical effect for mode-locking operation and generation of femtosecond optical pulses. Dispersion control inside the oscillator is important for the pulse-shortening process and it is typically controlled by a prism pair. The schematics of the Ti:S femtosecond oscillator is shown in the Figure 7.

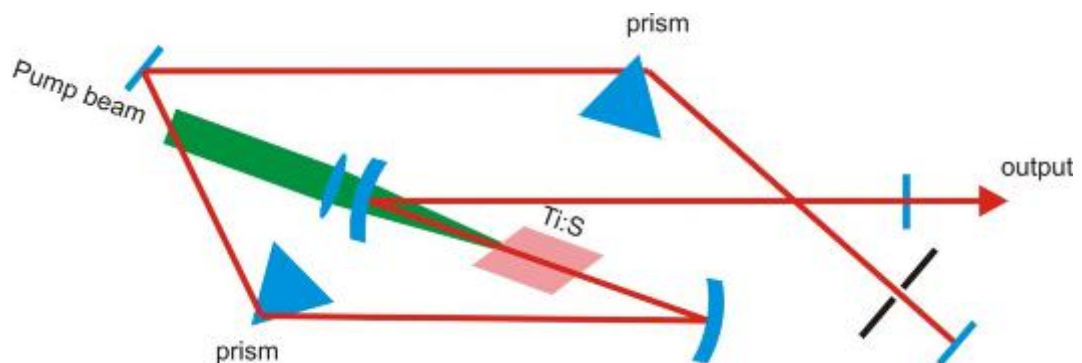


Figure 7. Ti:S femtosecond oscillator.

Although the oscillator based on the Ti:S crystal is efficient, it requires some space to make suitable length to the oscillator and recently more compact designs based on the fiber oscillators are getting more popular as a femtosecond source component. As an example of the femtosecond fiber oscillator, in Figure 8 is shown the schematics of the oscillator based on the Erbium fiber. The oscillator of the fs-Er: fiber laser is built up as a ring, that includes a short free-space section in order to establish mode-locked operation and to generate ultrashort pulses. In this

process, the nonlinear polarization rotation inside the fiber section is exploited to achieve pulsed operation. This mechanism is self-starting and self-stabilizing, i.e. mode-locked once, the Er: fiber laser is capable to run continuously without further alignment.

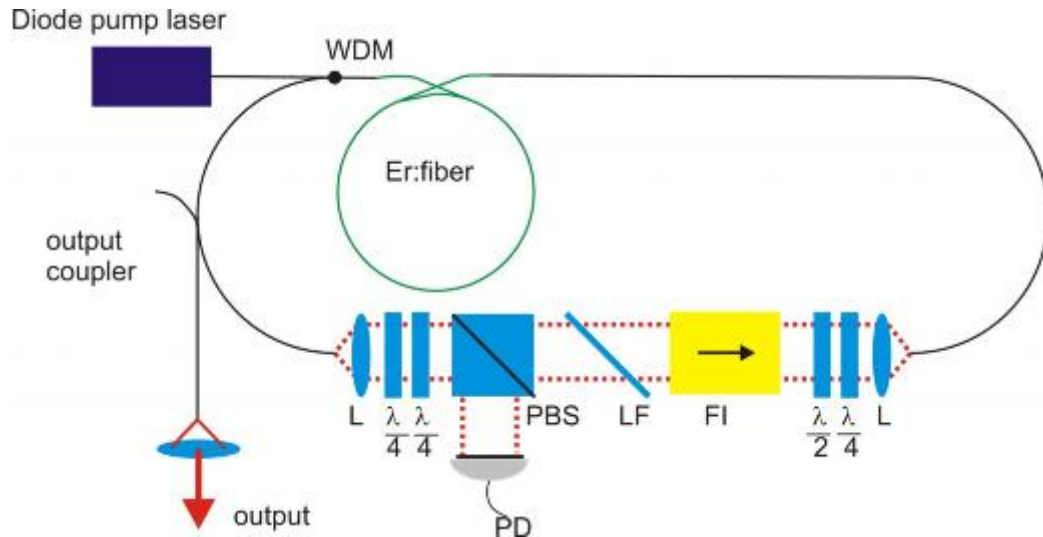


Figure 8. Er: fiber femtosecond oscillator. WDM wavelength division multiplexer, PBS polarizing beam splitter, L coupling lenses, LF Lyot filter, FI Faraday isolator, PD photodiode .

3.1.8 Pulse Amplification

Many applications demand more energy per pulse than what oscillators can give out. The energy of ultrashort pulses can be increased through amplification. However, high peak intensities of the amplified pulses are problematic because they can trigger nonlinear distortion of the pulse or can even cause optical damage to the amplifier. To avoid these limitations, chirped pulse amplification can be used. It consists of stretching the incoming pulse to a considerably longer duration in time with a strongly dispersive element prior to amplification. The temporal intensity of the pulse is thus reduced to a level that avoids damaging effects. Pulses are typically stretched to tens of picoseconds or more in order to minimize nonlinear effects. After amplification, the pulse is recompressed to its initial duration by an element of opposite dispersion. Actual amplification is usually done in the Ti:S solid state crystal and either regenerative (regen), multipass (MPA) or combination of both can be used as an amplifier. This amplification can be as high as 10^6 times the energy of original seed signal pulse. Pulse energies of several mJ can be obtained using combination of the regenerative and multipass amplifiers where the output of the regen acts as an input for a multipass amplifier. In Figure 9 is shown the schematics of the regen amplifier consisting of Ti:S crystal, oscillator and pulse picker. Pulse picker select and synchronises the incoming seed pulse for amplification and it is made by placing a Pockels cell (PC) and polarizing mirror (P) inside the oscillator. The principle of the multipass Ti:S amplifier is shown in Figure 10. Like its name says the pulse is made to pass multiple round trips through Ti:S crystal and is amplified in every pass.

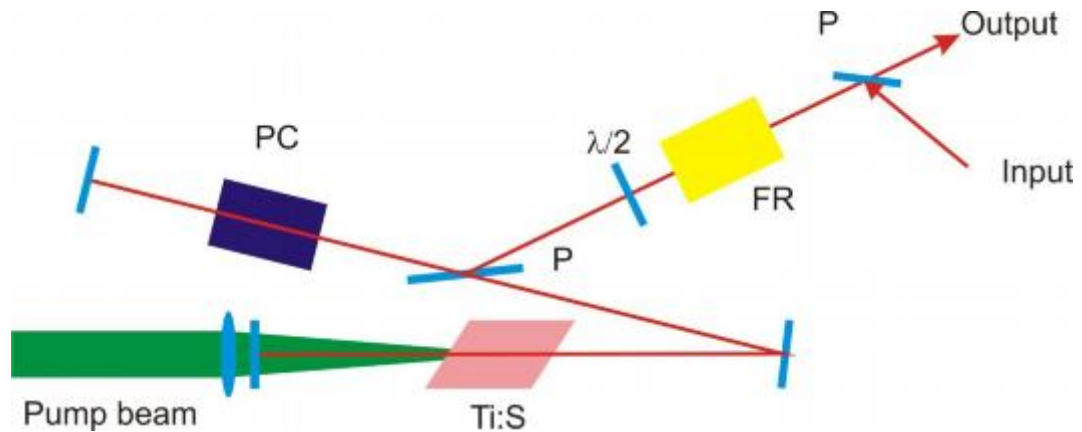


Figure 9. Schematics of the femtosecond pulse regenerative amplifier. Ti:S titanium sapphire crystal, PC Pockell's cell, P polariser, FR faraday rotator.

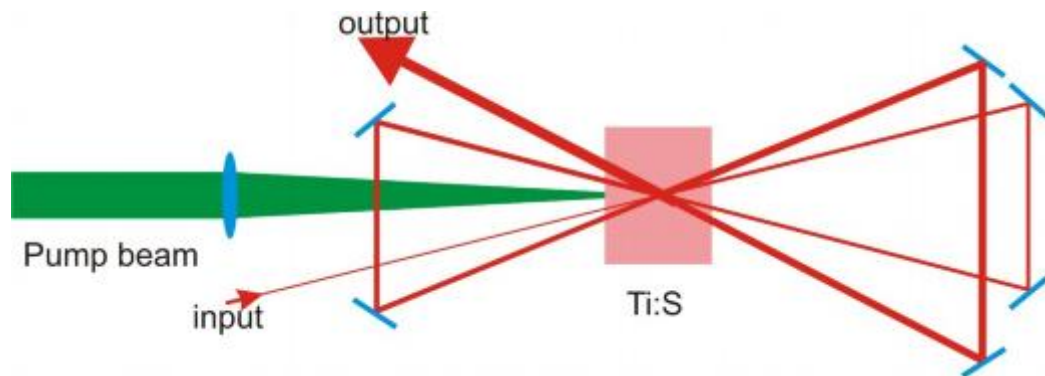


Figure 10. Schematics of the femtosecond pulse multipass amplifier.

3.2 Markets and trends VTT

Ultrafast lasers have been making their coming a long time and technology has grown a lot but still in laser microprocessing of materials the breakthrough is to come. For example the eye surgery business is already heavily relying on ultrafast laser processing but material processing is not.

Ultrafast lasers have matured since the nineteen sixties but other lasers have been the major business area for the whole time.

3.2.1 1970s to 1980s: dye lasers

Mode-locking was introduced in the 1960s, with solid-state lasers achieving picosecond pulses. Early femtosecond lasers using dye lasers and active mode-locking were introduced in the 1970s. The pump sources were initially argon-ion lasers and, later, solid-state lasers. The dye laser emission is centered in the visible range, depending on the dye that is used.

Ultrafast lasers based on dye lasers enabled new applications, but they are notoriously difficult to work with, exhibiting poor reliability and low output power. Dye lasers are still sold for exotic and tunable wave-lengths, but they form a very narrow niche of the laser market and they are no longer used for ultrafast lasers.

3.2.2 Early 1990s: Ti:sapphire and other solid-state lasers.

Commercial ultrafast Ti:sapphire lasers were introduced in the early 1990s, improving reliability and output power over dye lasers. Mode-locking expanded from active to passive, including the use of SESAM materials. The pump sources were argon-ion lasers and, later, green diode-pumped solid-state lasers. The fundamental Ti:sapphire emission is centered around 780 nm.

Ti:sapphire lasers are now relatively mature in the ultrafast market. They have the broadest gain bandwidth of any material today, assuring their place in the market indefinitely, particularly for providing the narrowest pulse widths and the highest peak power.

Commercial ultrafast lasers using diode pumping of solid-state materials were introduced in the late 1990s, including the use of Nd:YAG, Nd:YVO₄, Yb:YVO₄, and Nd:glass. The use of diode pumping reduced the size, cost, and complexity of ultrafast laser systems.

Ti:sapphire lasers are the core systems in research facilities around the world due their good properties for making research.

3.2.3 Early 1990s to present: fiber and disk lasers.

Fiber lasers are a variation on diode-pumped doped glass lasers, but using Yb- or Er-doped glass fiber instead of glass rods. The fundamental emission of Yb-doped fiber is also around 1 micron, while that of Er-doped fiber is around 1.5 micron. The first ultrafast fiber lasers appeared in the early to mid-1990s but were overshadowed by Ti:S lasers. More recently, fiber lasers are beginning to be better appreciated, and a number of start-up companies have appeared since 1999 to commercialize them alongside the early entrants. Fiber lasers offer a more compact, more robust, and less expensive alternative to Ti:sapphire designs. They are well suited for many applications, but they are not the best choice for the highest peak power or the narrowest pulses. Innovation also continues in ultrafast solid-state laser design. TRUMPF and Time-Bandwidth Products now each offer an ultrafast (picosecond) diode-pumped disk laser. These lasers are notable for their quite high average powers of 50 W. The fundamental emission of the disk lasers is centered around 1 micron.

Fiber-based designs confound earlier categories of laser types. Before fiber lasers appeared on the market, ultrafast lasers used free-space designs. Today, however, ultrafast lasers may use not only all-solid-state or all-fiber designs, but also fiber laser oscillators with solid-state amplifiers, or solid-state oscillators with fiber amplifiers. The mix of fiber stages with solid-state stages in MOPA designs points out the complexity of ultrafast technology.

Nowadays fiber lasers can produce laser powers up to one kilowatts when repetition rate is high (tens of Megahertz) [1,2]. This company is a spinoff from Fraunhofer ILT. Company name is Amphos GmbH.

In the future fiber laser may take a bigger role in the industry so that fiber laser is coupled with external pulse compressor to get the short pulses without danger of damaging fibers.

3.2.4 Materials processing

Ultrafast lasers are useful for many microfabrication processes. Ultrafast lasers are very well suited for precision materials processing, where the cut quality is very important. This includes precision cutting, precision drilling, scribing, dicing, fuse blowing, etc. They all involve finely featured material removal with high-quality cuts and minimal damage to the surrounding material. Precision fabrication processes often use Q-switched lasers but may also use CW, modulated CW, or ultrafast lasers. Average output powers range from a few watts to about 150 watts. The price for lasers for precision fabrication can range from about 40 000 to 100 000 € for general-purpose tools based on CW or Q-switched lasers, to 300 000 € or more for more specialized systems. Highly specialized systems (such as for semiconductor wafer fabs) can cost as much as millions of euros or more.

However, ultrafast lasers are not useful for traditional micro-fabrication, such as microwelding. Ultrafast lasers do not provide a particular advantage for highly thermal processing, such as thick metal cutting, welding, surface treatment, or material deposition. Such processes require a build up of heat and long interaction times. Ultrafast femtosecond lasers are also not useful for microfabrication processes where throughput is more important than cut quality. Throughput and cut quality are always issues, but the alternatives may be more cost-effective. For example, ultrafast lasers may be useful for scribing semiconductor material, but a Q-switched laser or diamond saw is likely to be preferred for cutting completely through the material. However, the throughput can be improved as the average power of ultrafast lasers increases. Nowadays picosecond laser offer almost the same throughput that nanosecond laser only the system price is limiting factor for maybe not using ps-laser. Femtosecond lasers tend to be too high cost for high throughput applications still.

Existing and potential applications can be done with ultrafast lasers but could be done using ns-lasers currently. These applications could be repair of photolithographic mask patterns, displays, and memories, scribing thin-film dielectrics for electronics, solar cells, and displays, trimming of MEMS devices or precision parts, die and package singulation, other material cutting and singulation, surface texturing, via hole drilling, drilling holes in fuel injector nozzles, inkjet printer nozzles and feed holes, other precision drilling applications, stent cutting, cutting biodegradable stents and other polymers, microfabrication inside of transparent materials, inserting pixels inside of photolithographic masks, explosives and weapons processing, laser direct imaging (LDI), machining molds, 3D lithography and glass welding.

3.2.5 Commercial lasers

The market share of ultrafast lasers has been dominated by two companies, Coherent and Newport, well known for their Ti:sapphire lasers and accessories. But much of the growth in the market is still to come, with gains expected from fiber and disk lasers, expansion into new picosecond and femtosecond applications, and entry of some players new to the ultrafast market. **Error! Reference source not found.** lists some key femtosecond laser suppliers.

Table 1. Femtosecond laser suppliers

SUPPLIER	LOCATION	www
Alnair Labs	Japan	www.alnair-labs.com
ALPHALAS	Germany	www.alphalas.com
Amplitude Systemes	France	www.amplitude-systemes.com
Calmar Optcom	USA	www.calmarlaser.com
CDP	Russia	www.cdpsystems.com
Clark-MXR	USA	www.cmxr.com
Coherent	USA	www.coherent.com
Cyber Laser	Japan	www.kr.cyber-laser.com
Del Mar Photonics	USA	www.dmphotronics.com
FEMTOLASERS	Austria	www.femtolasers.com
Fianium	UK	www.fianium.com
High Q Laser	Austria	www.highqlaser.at
IMRA America	USA	www.imra.com
KMLabs	USA	www.kmlabs.com
Light Conversion	Lithuania	www.lightcon.com
Menlo Systems	Switzerland	www.menlosystems.com
MPB Communications	Canada	www.mpbc.ca
Newport (Spectra-Physics)	USA	www.newport.com
PolarOnyx	USA	www.polaronyx.com
Quantronix	USA	www.quantronixlasers.com
R&D Ultrafast Lasers	Hungary	www.szipocs.com
Thales Laser	France	thales.nuxit.net
Time-Bandwidth	Switzerland	www.time-bandwidth.com

3.2.6 Ultrafast laser prices

Ultrafast lasers have always been expensive equipment due their complex nature.

Large high pulse energy Ti:sapphire ultrafast lasers typically range from under 150 000 to 300 000 € or more but can range to as much as 500 000 € or even 1 million each. This is for the laser itself (including its many subsystems), and not for the overall system product assembled around it. Really low average power (tens of milliwatts) femtosecond systems with high repetition rate can have price of tens of thousands of euros. Fiber-based ultrafast lasers range from under 40 000 € to as much as 300 000 €, but lower price means normally really modest powers. The low price presumes a commitment to a large order of lasers. One comment that sums the pricing nicely was that “it’s hard to do femtoseconds and low energy pulses, or picoseconds and high energy pulses, but it’s really hard to do femtoseconds and high energy pulses.”

No top limit to the cost of ultrafast lasers. There is almost no limit to the cost of the largest ultrafast laser systems. Huge petawatt lasers for fundamental research can cost in the range of 12 million euros. The planned European Extreme Light Infrastructure (ELI) exowatt laser is expected to cost 116 million euros over five years, not counting annual operating costs and salaries of 8 million euros. However, these extremely large ultrafast lasers are assembled from subsystems. The assembly of such systems is more like the systems integration that laser customers do. Also, the one-off (single unit order) nature of these projects is more like contracted R&D than laser manufacturing.

3.2.7 Ultrafast laser forecast

Growth has been slow but steady. The ultrafast market has been mainly an R&D market for many years, and therefore a slowly growing one. Bio-medical instrumentation and semiconductor inspection extended the R&D applications into new segments. Now medicine and materials processing promise to expand the market further. But the laser market expands painfully slowly. Moreover, the over-all market is around \$370 million, while the growth is only coming from a few small segments. Thus, there are very interesting opportunities in those segments, but the net growth in the market is not especially impressive. Current economic conditions are not critical. The current economic slowdown will not help matters, but it will probably not hurt, either. Machine tools, surgical tools, instruments, and semiconductor inspection tools will continue to be sold, but perhaps at a slower rate. Just as important, however, is that systems with ultrafast lasers may offer cost or performance advantages that are as attractive, or more attractive, during recessionary times. For example, new ultrafast tools that can process materials without post-processing can offer a less expensive overall process. Or an ultrafast surgical tool that eliminates an excimer laser may be more cost-effective than the current approach.

Strong growth in the ultrafast laser market is expected, as fiber lasers enable lower-priced products, especially in the power range necessary for micromachining. As the prices drift downward, users will find more applications for ultrafast lasers. In some cases, ultrafast lasers will substitute for Q-switched lasers. In others, ultrafast lasers will substitute for non-laser techniques, such as

mechanical saws and surgical scalpels. In a few cases, ultrafast lasers may enable an entirely new application.

That said, ultrafast will remain mainly a “fine-toothed saw” that is useful for many precision applications but not less-demanding ones. The lower throughput and higher complexity of the ultrafast process will restrict it to those applications that require very high quality cuts, have specialty or heat-sensitive materials, and, as always, scientific, biological, and instrumentation applications. Lower unit prices cannot greatly expand the market, at least over the term of this forecast. Even if the lasers were free, they would not be used in most well-known laser applications.

3.3 Conclusion of markets and trends

The market is growing but slowly. Ti:Sapphire based systems are almost fully developed and their technology cannot be taken much further anymore. Their low repetition rate makes processing speed quite low and that is why different optical means are needed to apply to fully take advantage of the potential from this type of lasers. These optical means are studied in this project and maybe also in to next project. New optical device for making fs-laser processing faster is spatial light modulator which could enable many times faster processing. After all one has to keep in mind that accuracy comes with slow processing only. With fs-laser one can do worse quality than someone with ns-laser when parameters are selected in wrong manner. When fiber laser based systems develop a bit to be able to provide repetition rate together with fairly high pulse energy we will see ultrafast technology opening new applications and taking market share from nanosecond lasers.

For a long time everyone is saying that fs-lasers will come to production in the next five years but it seems to be so that it is always five years from now on. There are couple of job shops like www.micreon.de having femtosecond lasers in production but still it is nothing compared to the whole laser processing business.

3.4 Typical ultrafast laser applications

Since ultrafast lasers can machine virtually any material almost every machining task is possible with these lasers. High pulse energy lasers tend to be low repetition rate lasers and the application has to be such that machining time is not critical. This is why ultrafast lasers are used only when their unique properties are needed. This is why the market is specialized to niches.

This chapter tries to enlighten application area through several application examples.

3.4.1 Diamond machining

Machining of diamond tools for micro metal optics. Since diamond machining is difficult is femtosecond laser a good solution due all materials can be processed.

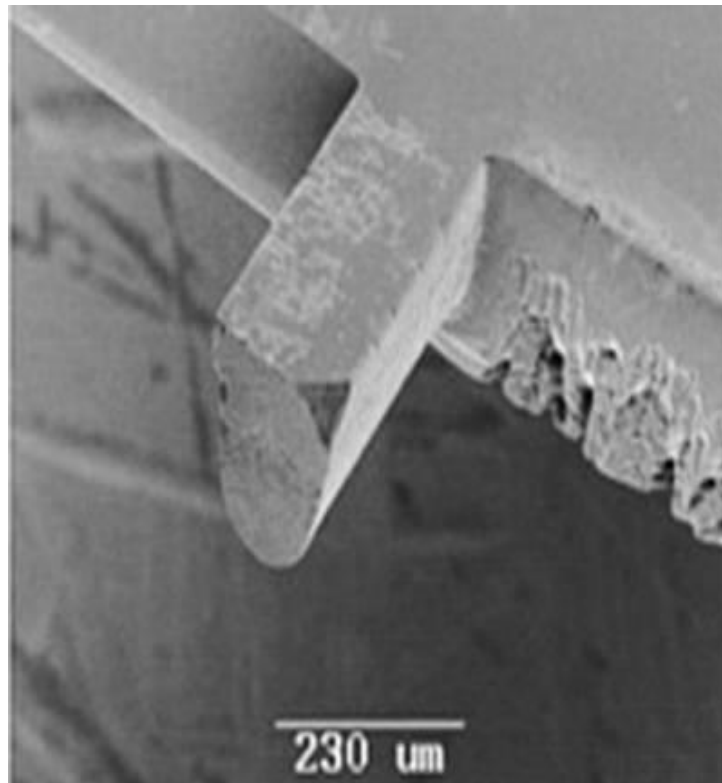


Figure 11. Diamond machining (www.kugler-precision.com).

3.4.2 Silicon surface modification

One of the most interesting applications for femtosecond laser in the electronic industry is the making of black silicon. Company SiOnyx in US has patented a technology for making certain surface structure on silicon surface to exploit unique atomic level alterations that occur in materials irradiated by high intensity lasers. Process employs a powerful, femtosecond laser that exposes the target semiconductor to high intensity pulses as short as one billionth of a millionth of a second in a chamber with sulphur hexafluoride (SF₆). Silicon subject to these intense localized energy events under goes two kinds of transformative change. The first is chemical: the atomic structure becomes instantaneously disordered and large quantities of sulphur from the gaseous SF₆ environment are “locked in” as the substrate re-crystallizes. The second change is structural: the physical surface transforms from a smooth, shiny wafer into a thin layer of nano and microstructured surface that is black. The confluence of these chemical and structural changes yields a unique new material that is a highly doped, optically opaque, shallow junction interface with optical properties never before observed.

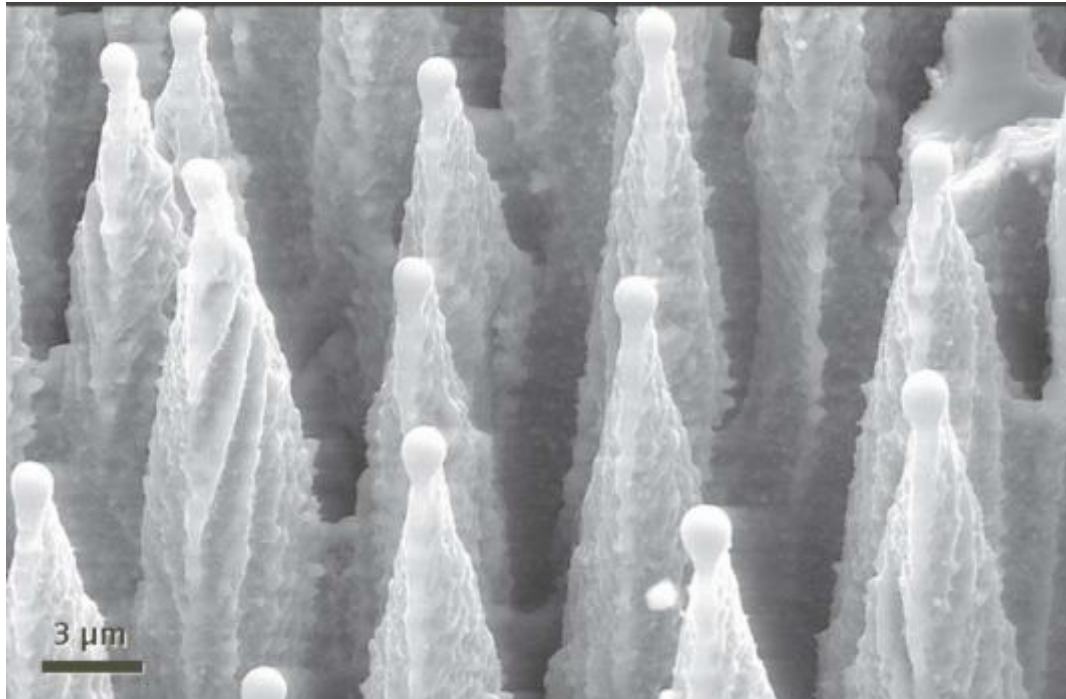
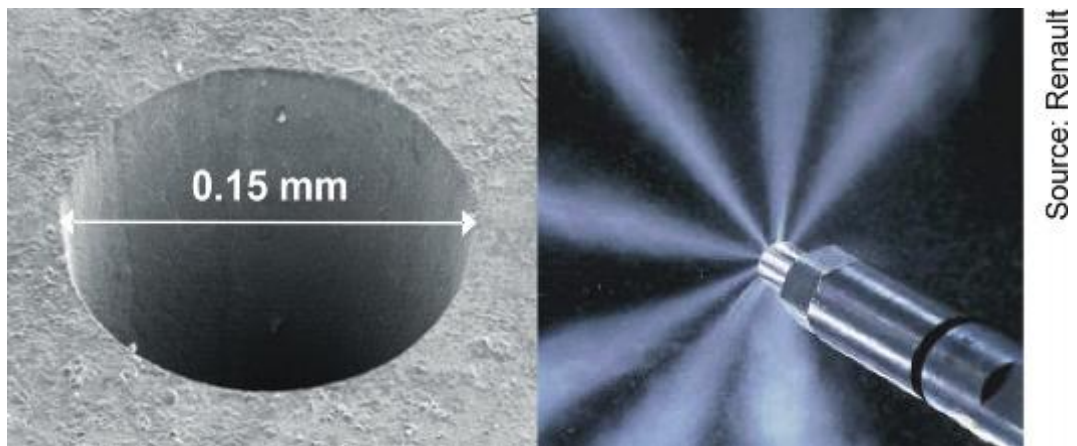


Figure 12. Silicon surface modification (<http://www.sionyx.com>)

Various research groups have used fs-laser to produce different kinds of surfaces because absence of melt in processing. Many of the research activities the processing speed is very modest.

3.4.3 Drilling of metals



Source: Renault

Figure 13. Drilled fuel injector (<http://www.laser-zentrum-hannover.de>)

Drilling with femtosecond lasers is really good application if really small and precise holes are needed. To enhance the hole quality drilling is to be done in vacuum chamber. Vacuum chamber helps in drilling due evaporated and/or melted material is free to evacuate from hole. If atmospheric pressure is present evaporated material and melt maybe attached to hole edges. Since fs-laser has really high peak powers one can utilize on the center of the beam to drill and this is why really deep holes with small diameters can be achieved in any material. Polarization control is important factor and with trepanning and helical drilling one can get more possible geometries to produced holes.

3.4.4 Biomedical stent cutting

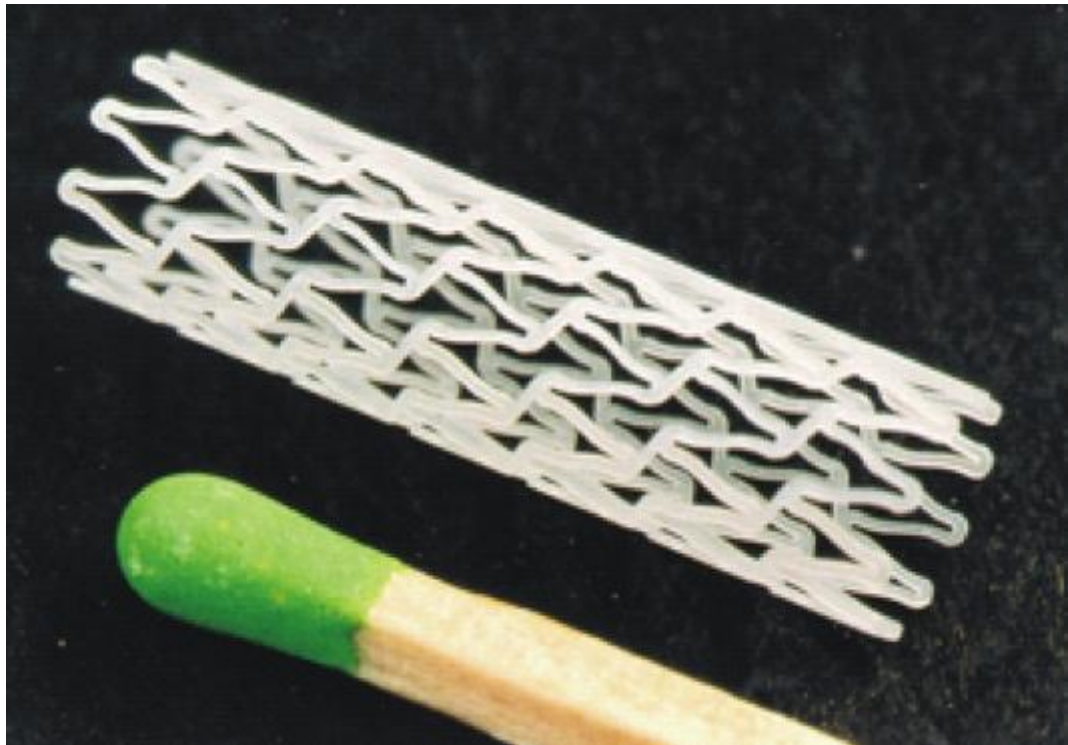


Figure 14. Laser cut bio-degradable stent (<http://www.laser-zentrum-hannover.de>).

Stent production is its own business area and they are nowadays normally done with fiber lasers. After laser cutting there are several steps to clean the edges due stent cutting quality is quite rough. Using femtosecond laser one can achieve better quality on metallic materials but the most benefits are gained when polymeric stents are produced even tough ns. UV lasers can also be used.

3.4.5 MEMS micromachining

When silicon or other dielectric materials are needed to be processed without HAZ or debris femtosecond laser might be a good choice. One must still use the low ablation rate processing parameters to get the best quality. This regime is normally below 10 J/cm^2 . Then typically one pass takes only some hundreds of nanometers material away in maximum. This is a region where there is no melt present. If higher intensities are used there will be melt present due the energy cannot evaporate all material and some of the material melts and starts boiling. This is called explosive boiling and it should be avoided in really high precision machining.

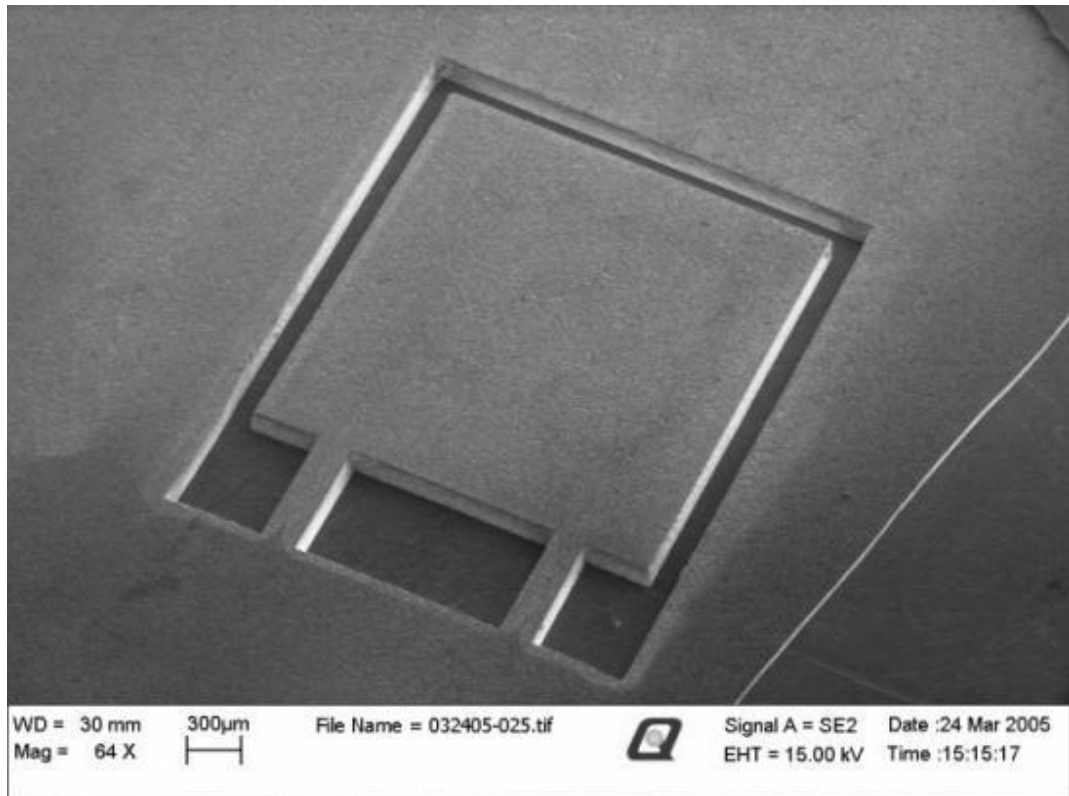


Figure 15. Laser direct written accelerometer (Quantronics).

3.4.6 Photomask repair

It is said that the femtosecond pulse does not bring any heat to the process is true when only the pulse width of the time is thought. 10 ps after the pulse has hit the material, the material starts to heat up if additional energy is present (additional to e.g. material evaporation). If correct parameters are used one can ablate material from on top of the other without damaging the lower one. In Figure 16 chrome is ablated from photomask in which substrate is fused silica.

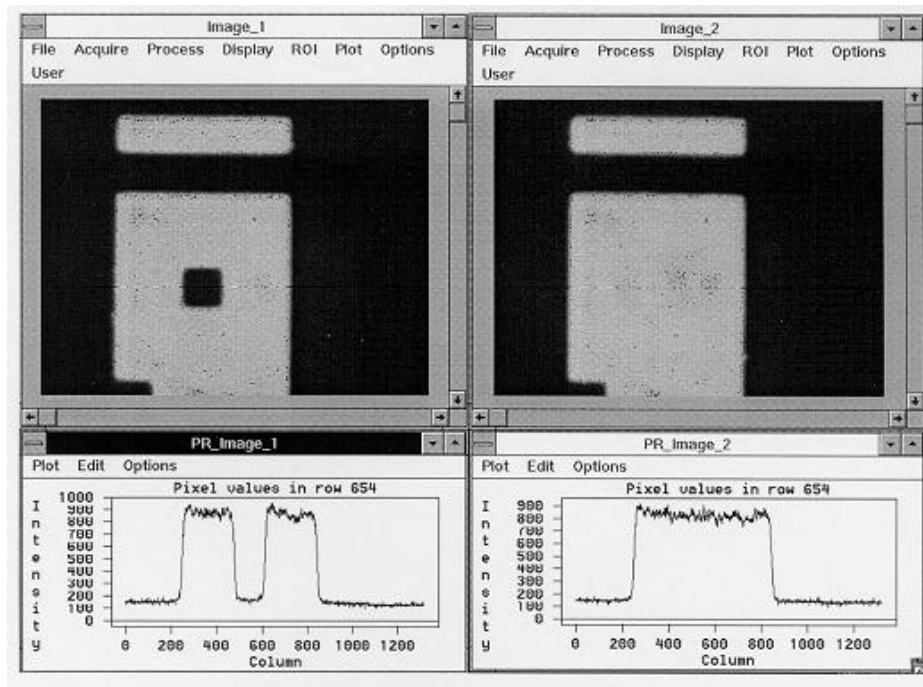


Figure 16. Photomask repair (Quantronics).

3.4.7 Fused silica ablation

Fused silica is challenging material for laser due the high band gap energy. With femtosecond laser it is possible to ablate fused silica even with 800 nm wavelength due intensity is so high that multiphoton absorption is possible. Of course using 2nd harmonic of Ti:sapphire wavelength the ablation works even better due 400 nm is absorbed by fused silica a bit better. 3rd harmonic 266 nm would be even better due fused silica absorbs a notable amount of the light at that wavelength. Problem is that the conversion efficiency from fundamental wavelength is quite poor.

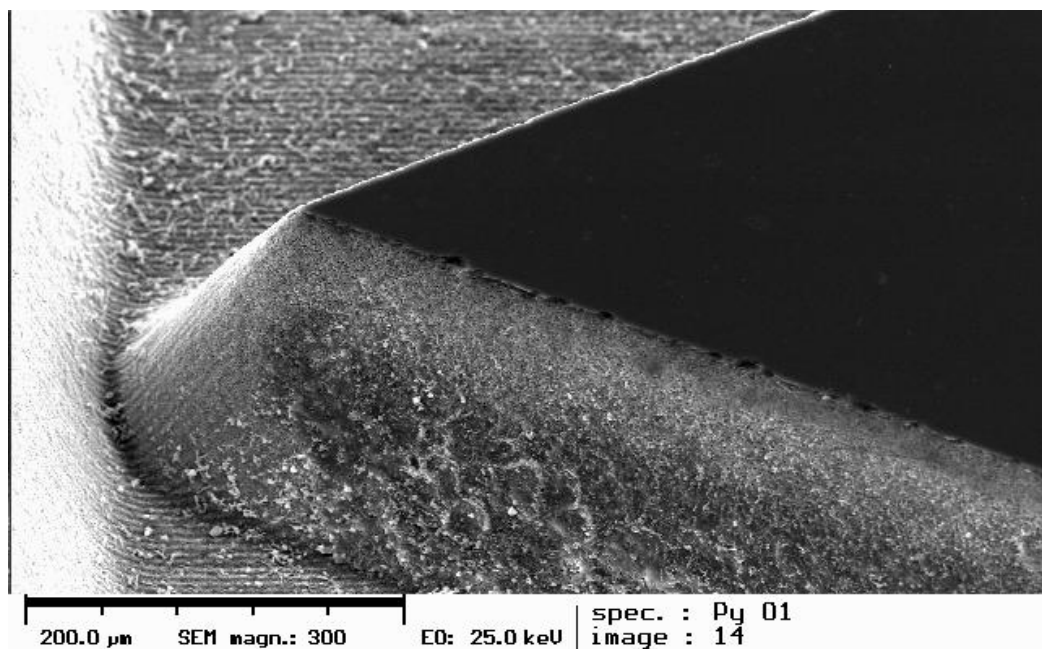


Figure 17. 3D-ablation of fused silica (<http://3d-micromac.com>)

3.4.8 Thin film patterning

Thin film patterning is one really growing area in the laser processing world. Also femtosecond lasers are good choices for the task but the price might be too high compared to productivity. In Figure 18 there is SiN coating ablated away to make electrical contacts on solar cell. Similar applications can be found in many electronic areas like TV and other display applications.

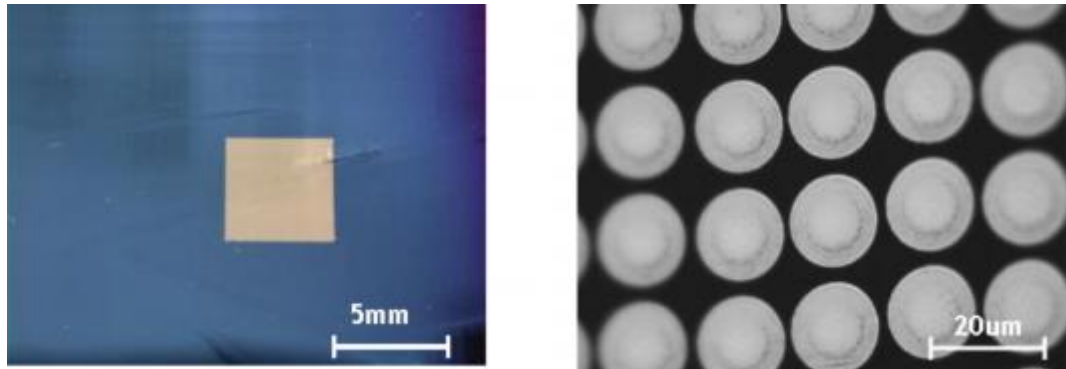


Figure 18. SiN ablation from Si-wafer (Quantronics).

Intra material marking or processing is also an area where ultra fast laser can also be utilized. For example this medical application where marking is needed inside material (fused silica). In this kind of application beam is focused so tightly that beam is only absorbed by the material in the focal region where intensity is high enough and non linear absorption is possible. That is why surface is not affected by the beam at all.

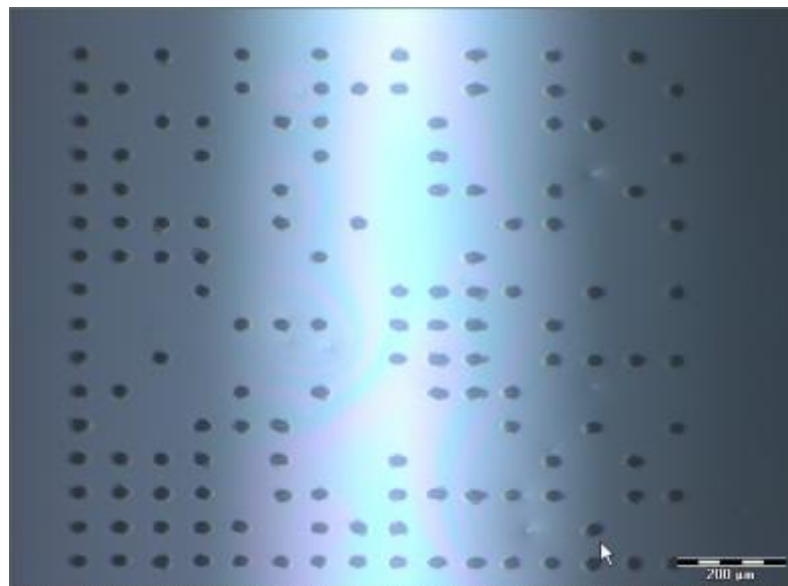


Figure 19. Intra glass marking for syringes in medical application (Quantronics).

3.4.9 References

- [1] 400W Yb:YAG Innoslab fs-Amplifier P. Russbuedt, T. Mans, G. Rotarius, J. Weitenberg, H. D. Hoffmann, and R. Poprawe Optics Express, Vol. 17, Issue 15, pp. 12230-12245 (2009)
- [2] www.amphos.de

3.5 Workstations

Femtosecond laser workstation as a production system does not differ a lot from normal laser workstation. At least all the same components can be found from both setups. Typical components in the system are laser, power source, cooling unit, attenuator, mirrors, beam expanding, focusing optics, cameras, power/pulse energy meter, software, enclosing, axes, jig with fixtures, polarization, slit.

If femtosecond laser is Ti:Sapphire based it normally runs at “full” power and the power which is used in the process is controlled by polarization angle and polarizing cube. This way the energy control can be made from program but it might take a second or two to change. When femtosecond laser is running at constant power it is stable. If green pump laser is driven at different values one can tune the output power also but then laser starts to be unstable.

Normally Ti:Sapphire based system is pulsed with electro optical modulator like pocket cell which is used to get the pulses out that are wanted to use. It is normal that laser leaks a bit because all lasers do that. For example in Lappeenranta the laser leaks 20 μ J pulses which will process material depending on optical configuration. This is why shutter should be used to prevent unwanted pulses to hit the processed sample. Also the eye safety is one issue why shutter should be installed.

Fiber laser based femtosecond laser typically have low pulse energies and high repetition rates. Due fiber nature of the system the beam wavelength is around 1 μ m. Workstation with fiber laser is a lot simpler due no additional mirrors are need and only focusing optics are needed. Fiber lasers rely on the master oscillator power amplifier technology and then output can be controller in electronic manner normally without external devices. To be able to be stable these lasers are typically set to one repetition rate and it cannot be changed easily. Of course exceptions are also available like amplitude systems laser which can be tuned in a wide range. Those on can also tune pulse length from hundreds of femtoseconds to couple picoseconds.

For online vision one would want to have camera behind the last mirror before focusing optics to see where beam will hit. Also this works as a visual evaluation of processed sample after wards.

Normally beam is steered with mirrors and then using lens beam is focused down to sample. It is also possible to use scanhead with f-theta optic to move the beam on a work area. Then one has to keep in mind that beam will hit sample in an

angle on the edges of the work area. Typically this angle is $\pm 12^\circ$. If telecentric optic is used on the scanhead this angle problem is avoided. Mirrors should be selected so that they do not cause chirp to femtosecond pulses. This means that if incorrect coatings are using in mirrors there is possibility that pulse width will increase.

Beam expander is needed to expand the beam before focusing to be able to focus beam down to as small as possible. Normally laser beam output is in the range that can be used in many cases but sometimes beam has to be enlarged to utilize full focusing potential.

Special optics like top hat optic can be used to modify the beam mode i.e. beam spatial profile. Then the high peak in the middle of the beam is transferred to flat top intensity to optimize ablation over the whole beam area. Diffractive optic can be used to focus beam into multiple spots or even complex geometries which will make processing faster and utilize the femtosecond high pulse energy.

If lens is used to focus the beam one needs to have axes moving the sample. Depending on sample size one needs to select axis dimensions. Axle accuracy has to be normally really to be able to process with high accuracy. Sometimes even nanoprocessing axes are needed in 3 dimensions (up to 5 or more axes). Depending on the repetition rate of the laser one needs to have different speeds on the axes. Ti:Sapphire laser is typically 1kHz laser and if 10 μm spots are wanted to be overlapped 50% it means that speed has to be 0.5 mm/s. Fiber laser operating at 1 MHz set totally different demands for axes. 1 MHz laser typically has low pulse energy and then pulses need to be overlapped a lot more.

Workstation in production has also software to verify the productivity and other important data about production. From keeping production in the same operating window one needs to have system that checks the laser power and beam quality every now and then to verify that system is working properly.

Femtosecond lasers need normally really stabile conditions as a basis for reliable operation. This means that the room where laser is should be kept in controlled temperature. Depending on laser manufacturer the system cooling could be done so that external heat does not affect laser operation. Thales for example cools the whole laser block down to wanted temperature. The laser is also encapsulated to that no air goes out or in. But for example Quantronics Integra is only cooled from base plate so external heat will generate problems. Also Quantronics is under not so dust proof cover and external dust may cause problems.

Since the femtosecond laser typically consists of several lasers the cooling is needed and this is done with water to air or water to water chiller. If heat is released to same room it might be a problem due heat load is quite big. Also water to air heat changed is quite noisy. These things are normally solved in laser workstations.

If laser workstation is placed in clean room facilities one needs to enclose the laser workstation well due a lot of particles will be in air due evaporation in laser process. This kind be handled with suction close ablation point.

It is said that laser processing does not make forces to sample but when really small MEMS components are machined one can measure forces due recoil force. Recoil force is produced when ablated material is ejected from the sample. This force is not big but when really thin materials and thin sections are in question material could be broken due momentum on sample. Typically jig and fixtures are needed to keep sample on its place when axes are moving and to have samples always on same spot. Really high precision needs camera based calibration and then jig accuracy is not enough.

Normally femtosecond lasers have certain polarization and it is known that in the polarization direction machining is faster than on against the polarization. This is why sometimes polarization is needed to be changed as depolarized be. In drilling it is beneficial to rotate polarization continuously during drilling to get round holes. Laser mode on the beam is almost always a bit elliptic and that is why mirror angles should be so that beam turns 90° in each corner not to make beam more elliptic. Anyway a slit can be used to cut edges of the beam away to get only the part of the beam into use that is known to e.g. ablate material. If the slit is put on the raw beam it might cause diffraction fringes on the image plane. This is why some researchers use vacuum chamber where they focus the beam through the slit and then collimate beam after the slit. This is how the fringes can be avoided. This cannot be done in air due air breakdown will happen quite easily with even modest powers.

3.5.1 Purchasing a workstation

Normally someone who is willing to invest on femtosecond laser system is seeking a laser solution for production challenges. Then it is good to keep couple of things in mind.

First is the price of the system is normally 2–x times higher than the laser itself. This is because integrator has to make functional system and integrate different components to fulfil customer needs.

Second is that there are a lot of integrators out there and safest solution is to buy the whole system from some integrator which can promise production with certain production rate with certain quality and show it over longer period before full payment. This is why because customer is not buying a laser system but customer is really buying a solution to their production challenge. Even though laser fulfils the specification but it might be so that it will not fulfil the productivity with the quality that is really needed.

Third is that one does not need to worry about the details of the system if integrator is selling complete system with wanted specs and needed productivity.

Our experience is that femtosecond Ti:Sapphire system is a lot more complex than rugged DPSSL picosecond laser and one will need someone who will take care of the system because much more things maybe go wrong with fs-laser than with ps or ns marking system.

3.5.2 Laser integrators in the ultrafast laser field

There are laser manufacturers who can also provide complete system to customer but there are also integrators who are willing to integrate femtosecond lasers. To mention couple femtosecond laser integrators here are few: 3D-micromac, Kugler precision, Oxford lasers, ESI, Lasea and TrackInside.

4 Methods

4.1 Laser Equipment at VTT

4.1.1 Femtosecond laser system

VTT rented a femtosecond laser setup for six months. Chosen system was from Quantronics. Selection of system provider was selected according to tenders. This femtosecond laser system from Quantronics is presented in Figure 20 and Figure 21. Laser is Integra C2.0 with maximum of 2 mJ pulse energy at 1 kHz repetition rate. Pulse width is 130 fs. Wavelength of the laser is 790 nm. Pulse energy is attenuated with external polarization dependant cube and computer controlled polarizing window. After pulse energy is attenuated the beam is divided into two beams. The other part of the beam goes to scan head and the other to normal processing head. Scanhead had to different optics f100 and f330 f-theta lenses. Fixed optics had f50 and f100 optics. VTT implemented online vision for the fixed optics after delivery.

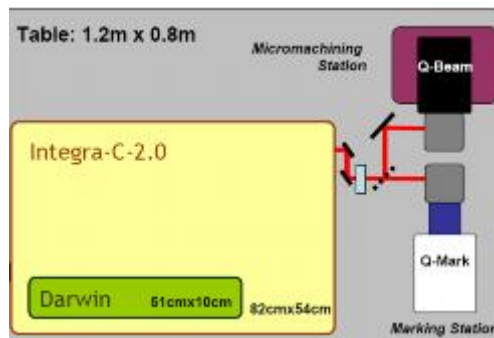


Figure 20. Schematic of system

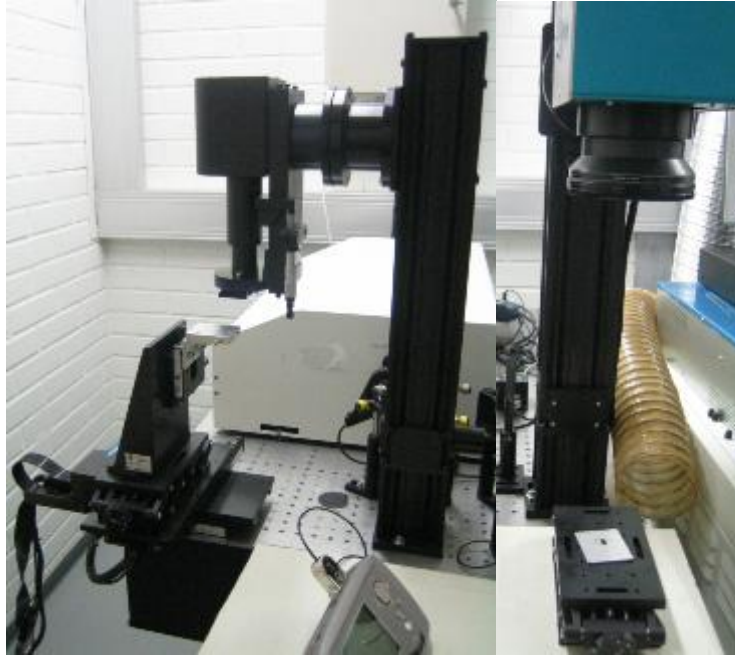


Figure 21. Actual setups of fixed two workstations.

Aerotech ALS-130 axes are used for sample positioning and movement in plane (x and y directions) together with NView software. The beam focus was adjusted to sample surface (z-movement) by Aerotech manual axis ATS-25-12DM. Scanhead is controlled via Quantronics Qmark-software.

4.1.2 SPI G3 20 W pulsed fiber nanosecond laser

The SPI G3.0 pulsed fiber laser module is a pulsed fibre MOPA (master oscillator power amplifier) laser with maximum average power of 20 W. Laser central wavelength is 1061.44 nm according to SPI test report. Laser can be operated also in CW mode if needed. Pulsing range is from 0 to 500 kHz. Laser pulse width can be tuned from 9 to 200 ns with 29 different variants. Laser was connected to detachable isolator to prevent back reflections damaging the laser. Laser was also equipped with high-capacity heat sink to enable stability if room temperature would change during marking tests.

The output beam from the laser is 3.2 mm and after isolator it is enlarged with variable expander 1-4x to be able to focus beam as small as possible. After expander beam is steered and focused with Scanlab HurryScanII with 14 mm aperture. Scanhead can be equipped with f100, f160, f254 f-theta lenses. Picture of the system is presented on the Figure 22. SCAPS SamLite was used to control the scanhead and in making the marking programs. Behind of the setup is the Rofin Nd:YAG laser.



Figure 22. SPI fiber laser optical setup.

4.1.3 Lumera Rapid 2 W picosecond laser

Lumera RAPID is an Nd:YVO₄ picosecond laser source. Used output wavelength of the laser was 355 nm. The focusing optic was telecentric with a nominal focal length of 100 mm, the diameter of the focal point was 20 μm and beam quality was $M^2 < 1.1$. A Gaussian beam profile was used in processing. Beam profile of used laser in focal spot is in the Figure 23.

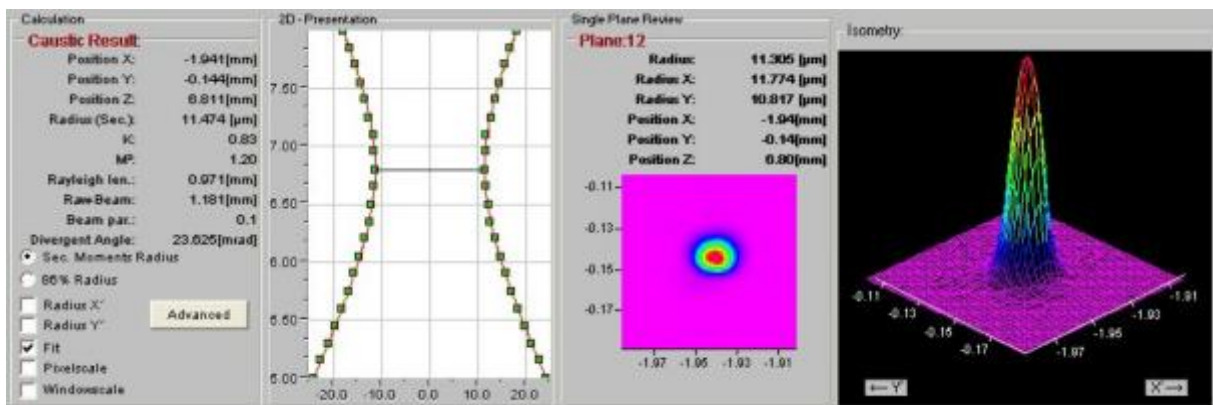


Figure 23. Beam profile of used laser.

4.2 Laser Equipment at JoFy

Quantronix Integra C femtosecond laser system was purchased to University of Joensuu during the project. System provides pulses of 120 fs with energy of 3.5 mJ at 1 kHz repetition rate. In Joensuu we had laboratory workstation with constantly changing setups. Mainly our setup consisted of laser system, energy control unit, beam expansion optics, computer controlled shutter and xyz-

translation table and different focusing and diffractive optics. Figure 24 shows different optical setups used in the experiments. In addition the vacuum chamber was manufactured in the department for testing the influence of the atmosphere to the process parameters.

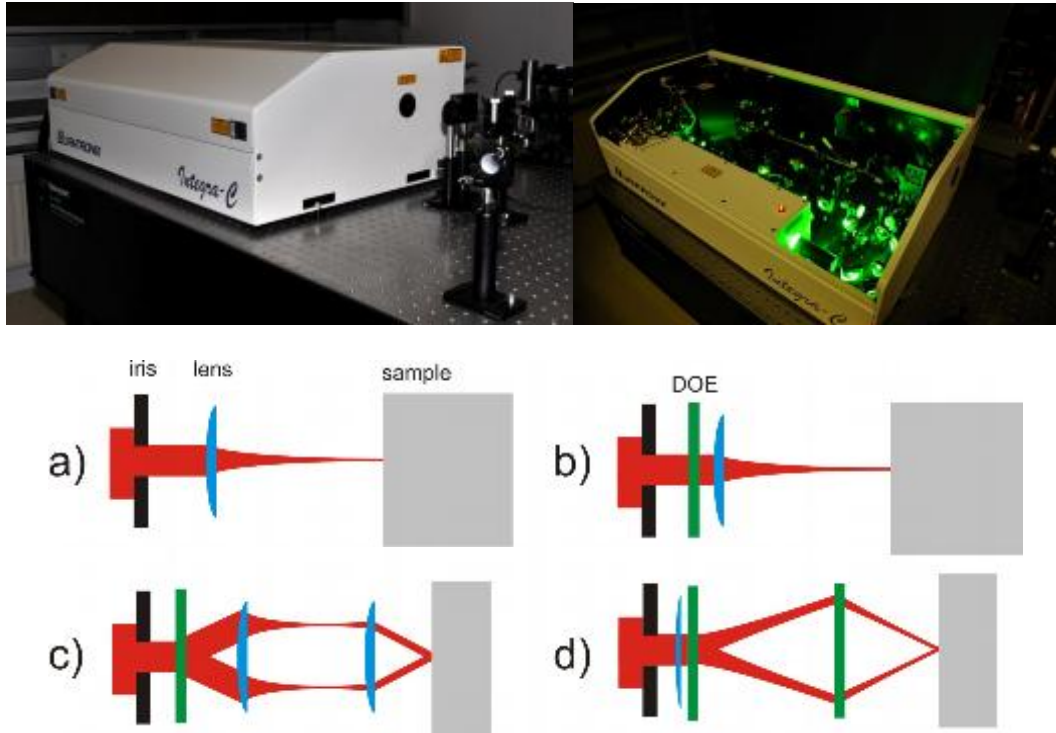


Figure 24. Different optical setups consisting lenses and diffractive optical elements (DOE) used in the ablation experiments. a) Direct focusing (spherical and cylindrical lenses). b) Diffractive optical element (image or multibeam). c) Interferometric ablation. d) Interferometric ablation with grating pair.

4.3 Femtosecond laser parameter tests in silicon

Parameter matrixes were made with VTT's fs-laser and scan head (100 mm optics) focused on the surface of the samples. Scanning speeds varied between 5–320 mm/s and hatch line distances between 0.01–0.10 mm (Figure 25).

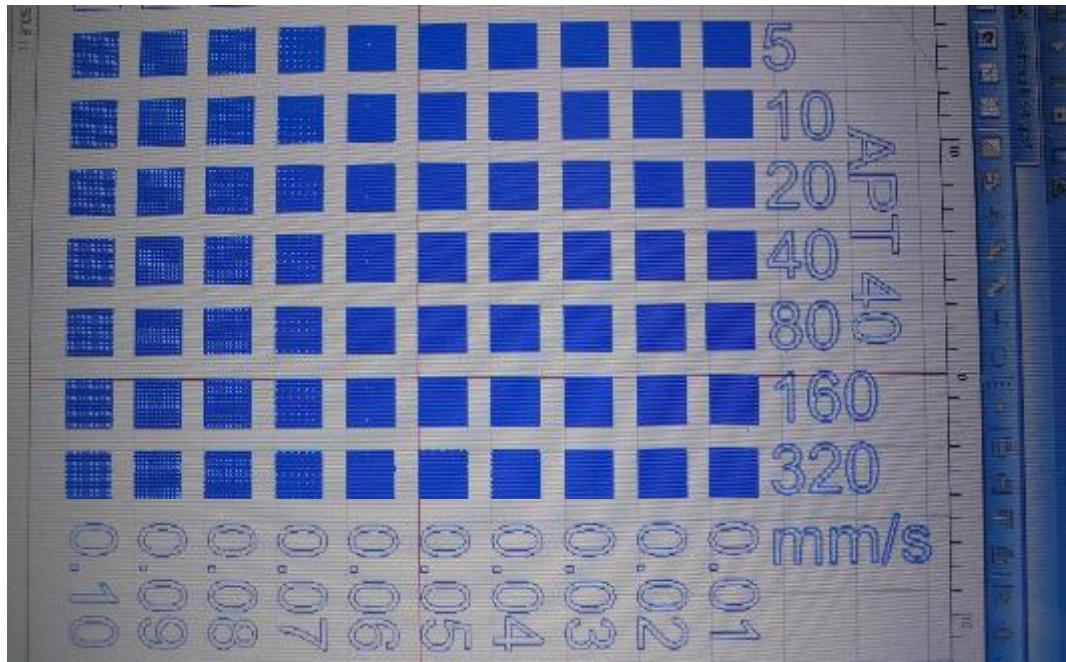


Figure 25. Laser parameter matrix on the PC display

The sizes of the rectangles in the parameter matrix were 2x2 mm. The rectangles were cross hatched (horizontally and vertically) and they were made without contours with power settings APT17–APT55 (10, 40, 125, 250, 500 and 800 mW).

Depths of the rectangles were estimated with an optical microscope.

4.4 Femtosecond laser parameter tests in tool steel

Parameter matrixes were made with fs-laser and scan head (100 mm optics) focused on the surface of the samples (polished tool steel). Scanning speeds varied between 1–320 mm/s and hatch line distances between 0.01–0.10 mm (Figure 25).

The sizes of the rectangles were 2x2 mm. The rectangles were cross hatched (horizontally and vertically) and they were made without contours with four power settings: APT60 (full power 800 mW), APT40 (500 mW), APT30 (250 mW) and APT25 (125 mW).

After laser machining the surfaces were washed with ultrasonic washing device. Depths of the rectangles were estimated with an optical microscope.

4.5 Femtosecond laser parameter tests in nickel

Parameter matrixes were made with fs-laser and scan head (100 mm optics) focused on the surface of the samples (0.1 mm thick nickel sheet). Scanning speeds varied between 1–160 mm/s and hatch line distances between 0.01–0.10 mm (Figure 25).

The sizes of the rectangles were 2x2 mm. The rectangles were cross hatched (horizontally and vertically) and they were made without contours with four power settings: APT60 (full power 800 mW), APT40 (500 mW), APT30 (250 mW) and APT25 (125 mW).

After laser machining the surfaces were washed with ultrasonic washing device. Depths of the rectangles were estimated with an optical microscope.

4.6 Laser parameter tests with picosecond and nanosecond lasers in silicon, tool steel and nickel

In order to compare femtosecond laser processing to other lasers, parameter matrixes were made also with VTT's picosecond laser and nanosecond laser.

Parameter matrixes for VTT's ps-laser (Lumera Rapid, wave length 355 nm) were made using 100 kHz repetition rate. Parameter matrixes for VTT's ns-laser (SPI 20 W fiber laser, wave length 1060 nm) were made with repetition rates 50 kHz and 100 kHz. With both lasers, scan heads were used (100 mm optics) focused on the surface of the samples (silicon wafer, polished tool steel and 0.1 mm thick nickel sheet). Scanning speeds varied between 10–800 mm/s and hatch line distances between 0.01–0.10 mm (Figure 25).

The ps-laser power was 0.6 W from the laser and 0.5 W on the sample. The ns-laser power setting 10 W gave 8 W on the sample.

Depths of the rectangles were estimated with an optical microscope.

4.7 Laser drilling tests on silicon

Test holes

Holes were made in coated and uncoated silicon wafers (diameter 150 mm, thickness 0.38 mm) with VTT's fs-laser (repetition rate 1000 Hz, wave length 800 nm):

- Linear x-y-table was used for wafer movements.
- Fixed optics with focal length 100 and 50 mm were used.
- Power settings APT20, APT25, APT30, APT40 and APT55 (20, 125, 250, 500 and 800 mW) were used.
- Number of laser pulses in test holes were 1, 2, 4, 8, 16, 32, 64, 125, 250, 500, 1000, 2000, 4000, 8000, 16000 and 32000 pulses.

Hole matrixes

According to measurements of test holes, 16 hole matrixes were made in 2 coated and 2 uncoated silicon wafers (see Table 2 and Figure 26):

- Hole groups (11x11 holes) were made with 0.5 mm pitch (group size 5x5 mm).
- All 121 holes of a group (e.g. A1) were made with same parameters.
- 1 mm space was left between hole groups (e.g. A1–B1 or A1–A2).
- Power settings APT25, APT30, APT40 and APT55 (125, 250, 500 and 800 mW) were used.

- Number of laser pulses in holes were 125, 250, 500, 1000, 2000 and 4000 pulses.

The hole matrixes (16 matrixes, 4 wafers) were sent to VTT Espoo for characterization.

Table 2. Laser parameters (APT power setting / number of laser pulses)

	A	B	C	D	E	F
1	55/125	55/250	55/500	55/1000	55/2000	55/4000
2	40/125	40/250	40/500	40/1000	40/2000	40/4000
3	30/125	30/250	30/500	30/1000	30/2000	30/4000
4	25/125	25/250	25/500	25/1000	25/2000	25/4000

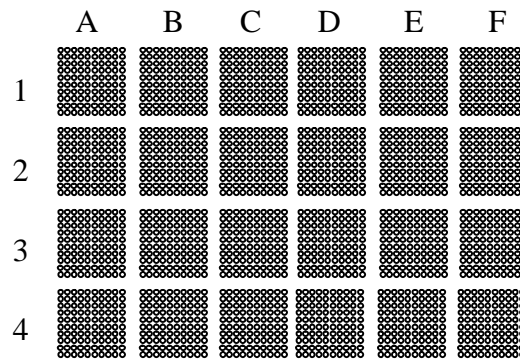


Figure 26. Hole matrix: 6x4 hole groups, 11x11 holes per group

5 Results

5.1 Femtosecond laser parameter tests in silicon

Parameter matrixes were made with fs-laser and scan head (100 mm optics) focused on the surface of the samples. Scanning speeds varied between 5–320 mm/s and hatch line distances between 0.01–0.10 mm (Figure 25 and Figure 27).

The sizes of the rectangles were 2x2 mm, and they were cross hatched (horizontally and vertically). The rectangles were made without contours with power settings APT17–APT55 (10, 40, 125, 250, 500 and 800 mW).

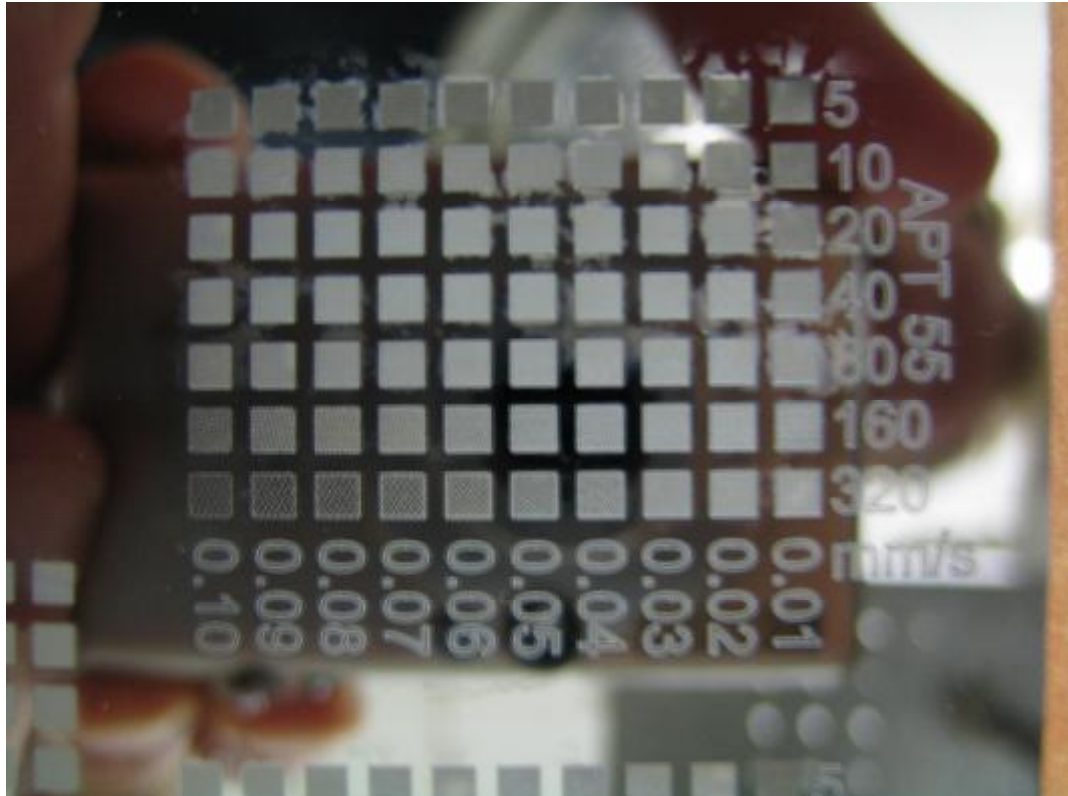


Figure 27. Parameter matrix made in a silicon wafer

The shape of the focal point can be seen in Figure 28 made with high speed and hatch distance.

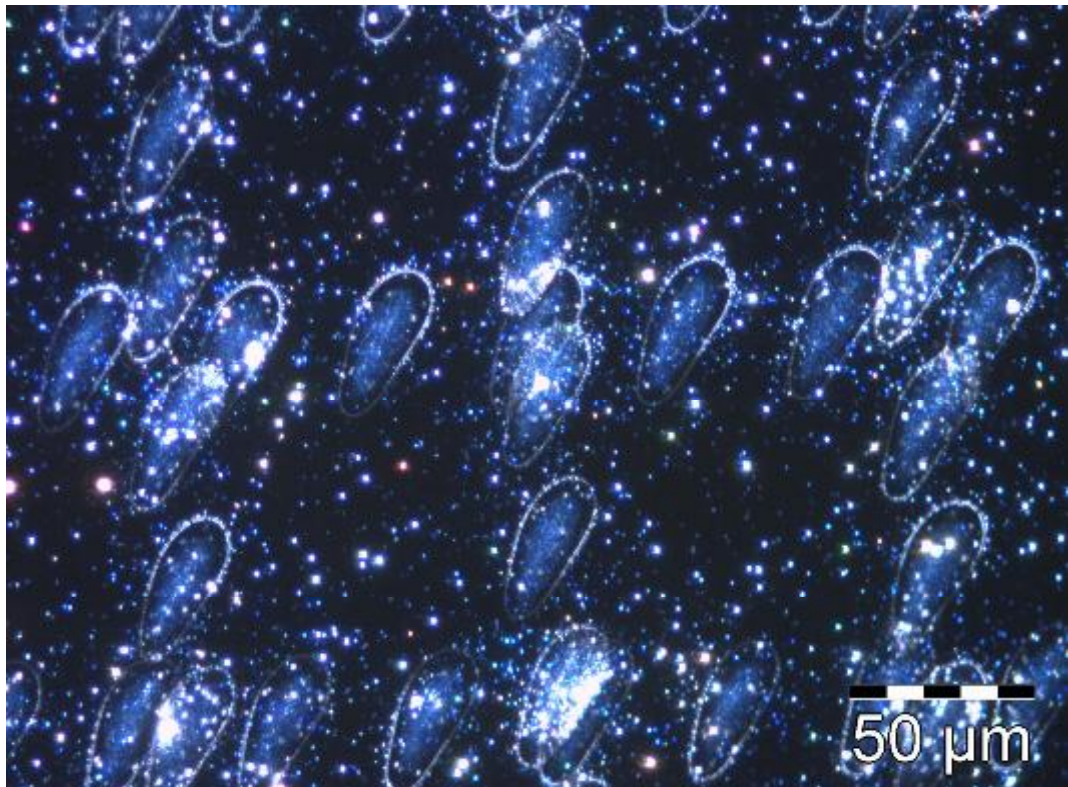


Figure 28. Power setting APT17, speed 40 mm/s, hatch distance 0.1 mm

The oval focal point makes different line widths in different directions and slanted line ends (Figure 29, Figure 30 and Figure 31).

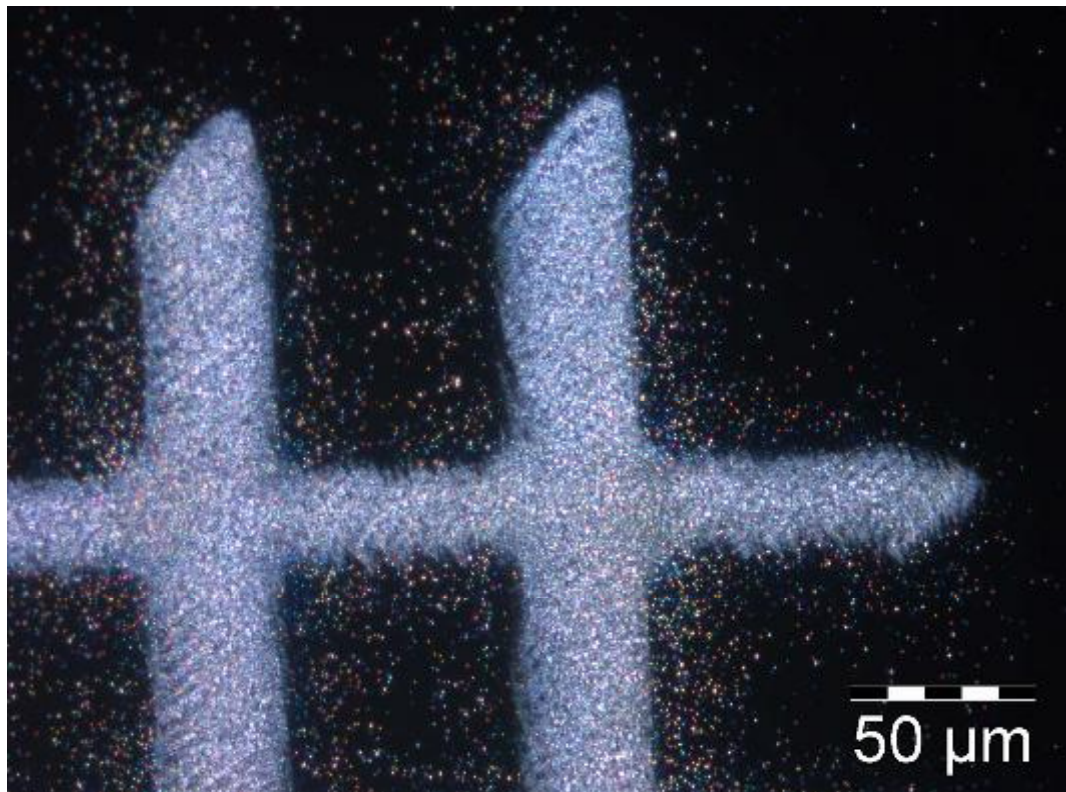


Figure 29. Power setting APT17, speed 5 mm/s, hatch distance 0.01

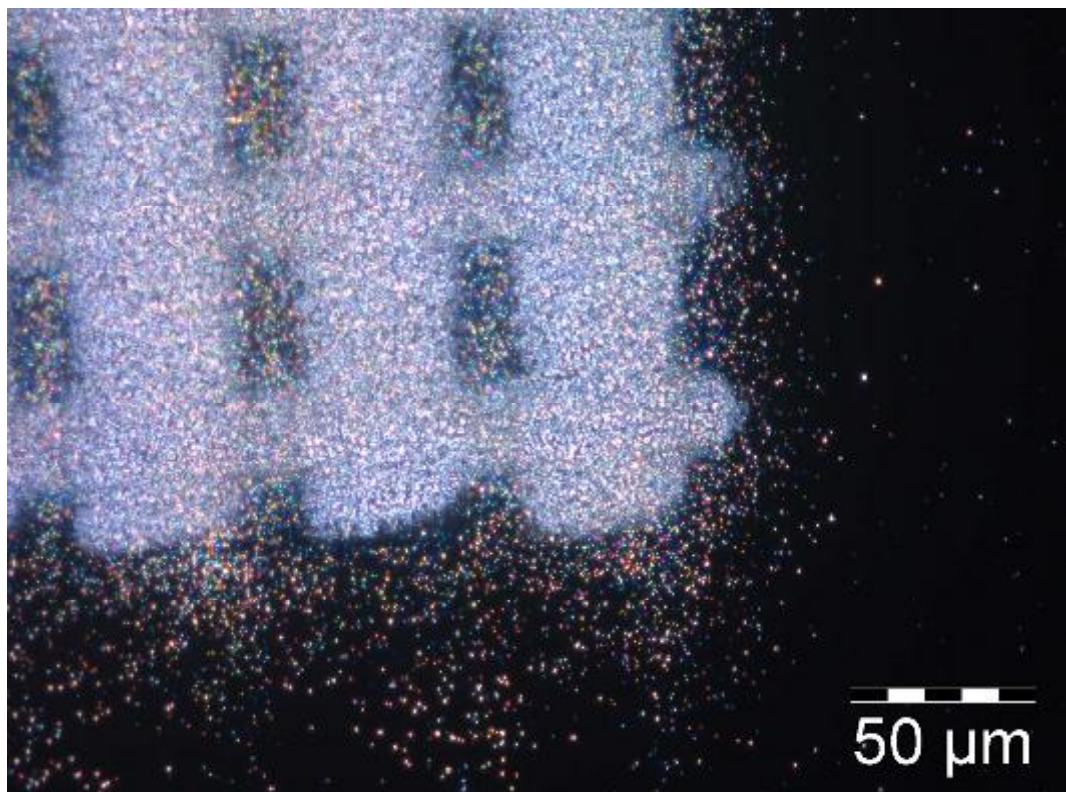


Figure 30. Power setting APT17, speed 5 mm/s, hatch distance 0.06 mm

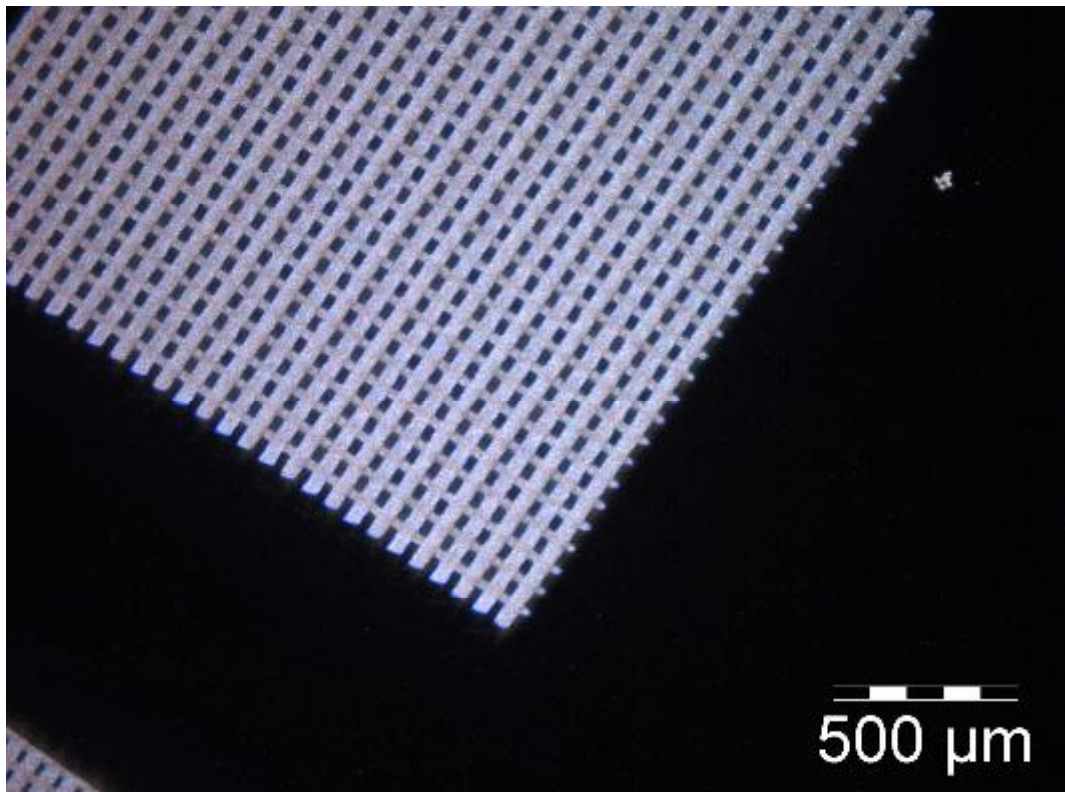


Figure 31. Power setting APT17, speed 5 mm/s, hatch distance 0.07 mm

Higher power makes the focal point larger (Figure 32).

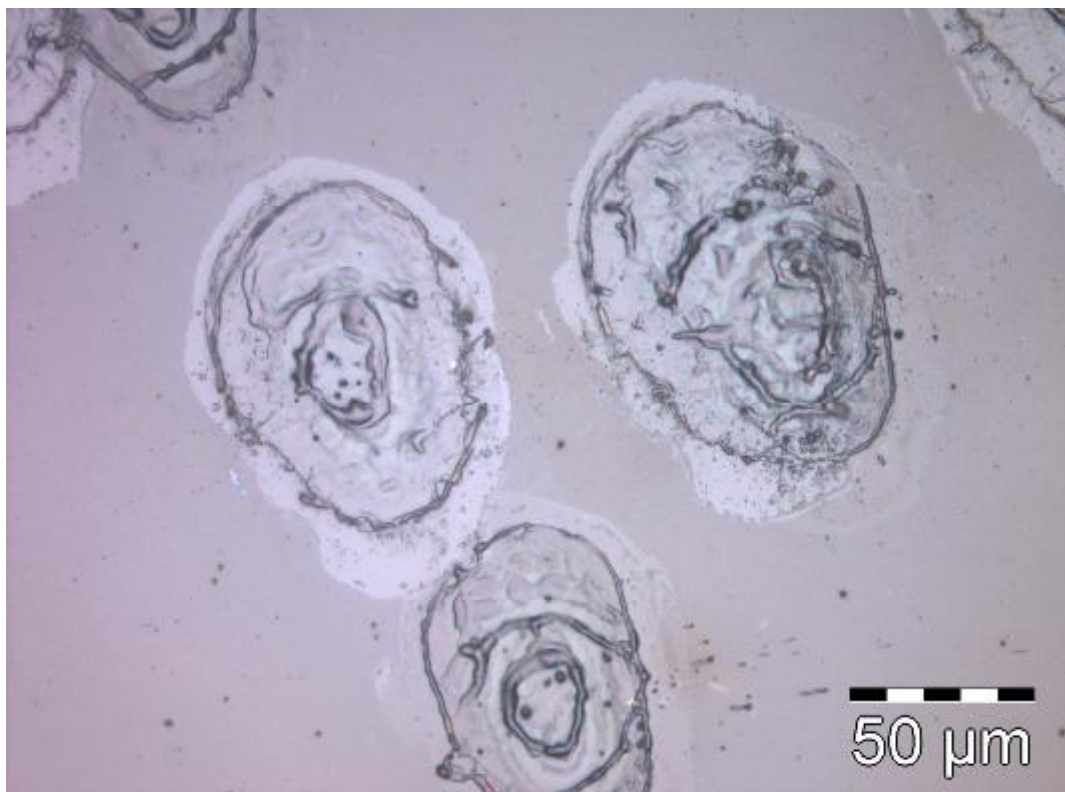


Figure 32. Power setting APT55 (full power), speed 320 mm/s, hatch distance 0.09 mm

Depths

Depths of the rectangles were estimated with an optical microscope [μm]:

2xAPT55 (800 mW)	0.01	0.02	0.03	0.04	0.05	0.06	0.07	0.08	0.09	0.10 mm
5 mm/s	90	40	30	25	20	15	15	10	10	5
10	40	20	15	10	10	5				
20	20	10	8	5	5					
40	10	5	3							
80	5									

APT55 (800mW)	0.01	0.02	0.03	0.04	0.05	0.06 mm
5 mm/s	40	20	15	10	7	5
10	20	10	5	3	2	
20	10	5				
40	5					
80	2					

APT40 (500 mW)	0.01	0.02	0.03	0.04	0.05	0.06 mm
5 mm/s	25	15	10	5	5	
10	10	8	5			
20	10	3				
40	5					

APT30 (250 mW)	0.01	0.02	0.03	0.04	0.05	0.06 mm
5 mm/s	15	5	5			
10	5					

APT25 (125 mW)	0.01	0.02	0.03	0.04	0.05	0.06 mm
5 mm/s	10	5	5			
10	5					

APT20 (40 mW)	0.01	0.02	0.03	0.04	0.05	0.06 mm
5 mm/s	5					

On power setting APT17 (10 mW) no measurable depth could be made.

5.2 Femtosecond laser parameter tests in tool steel

Parameter matrixes were made with fs-laser and scan head (100 mm optics) focused on the surface of the samples (polished tool steel). Scanning speeds

varied between 1–320 mm/s and hatch line distances between 0.01–0.10 mm (Figure 25 and Figure 27).

The sizes of the rectangles were 2x2 mm, and they were cross hatched (horizontally and vertically). The rectangles were made without contours with four power settings: APT60 (full power 800 mW), APT40 (500 mW), APT30 (250 mW) and APT25 (125 mW).

After laser machining the surfaces were washed with ultrasonic washing device.

The focal point shape can be seen in Figure 33 (high speed and hatch distance).

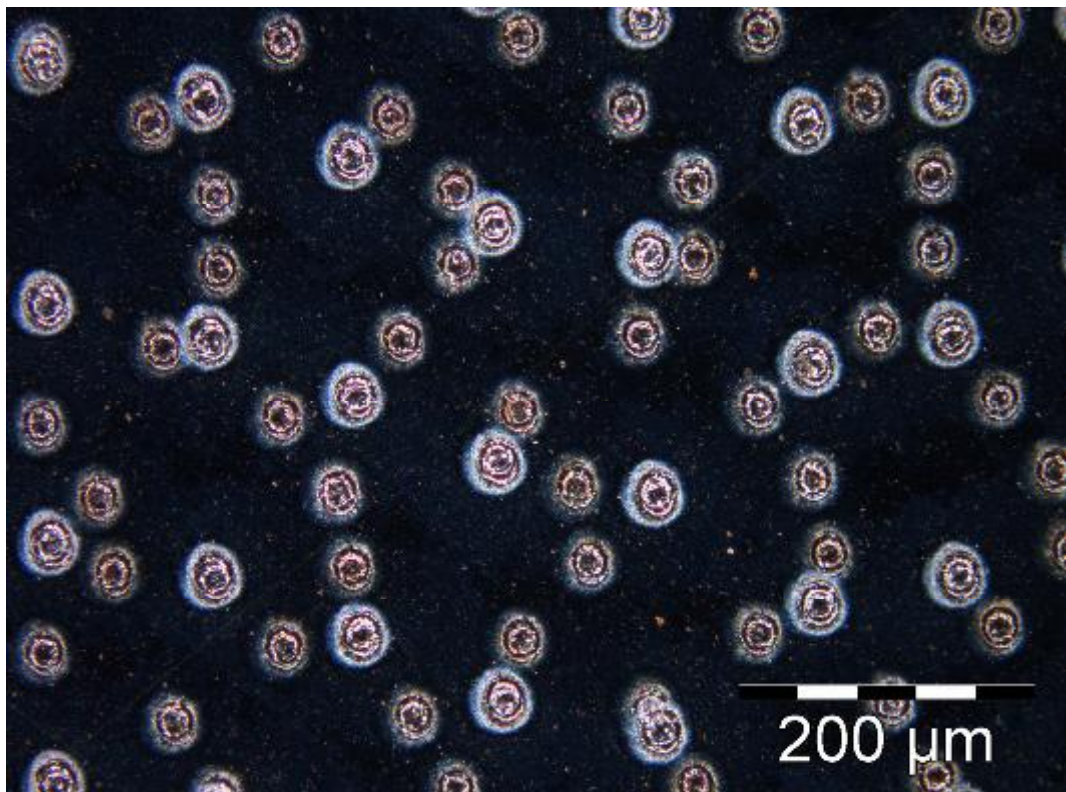


Figure 33. Power setting APT25, speed 160 mm/s, hatch distance 0.1 mm

Higher power makes the focal point larger (Figure 34).



Figure 34. Power setting APT60 (full power), speed 320 mm/s, hatch distance 0.1 mm

According to microscopic inspection, the surface quality depends mostly on hatch distance and speed and not so much on power. Following figures show examples of the surfaces.



Figure 35. Power setting APT25, speed 1 mm/s, hatch distance 0.01

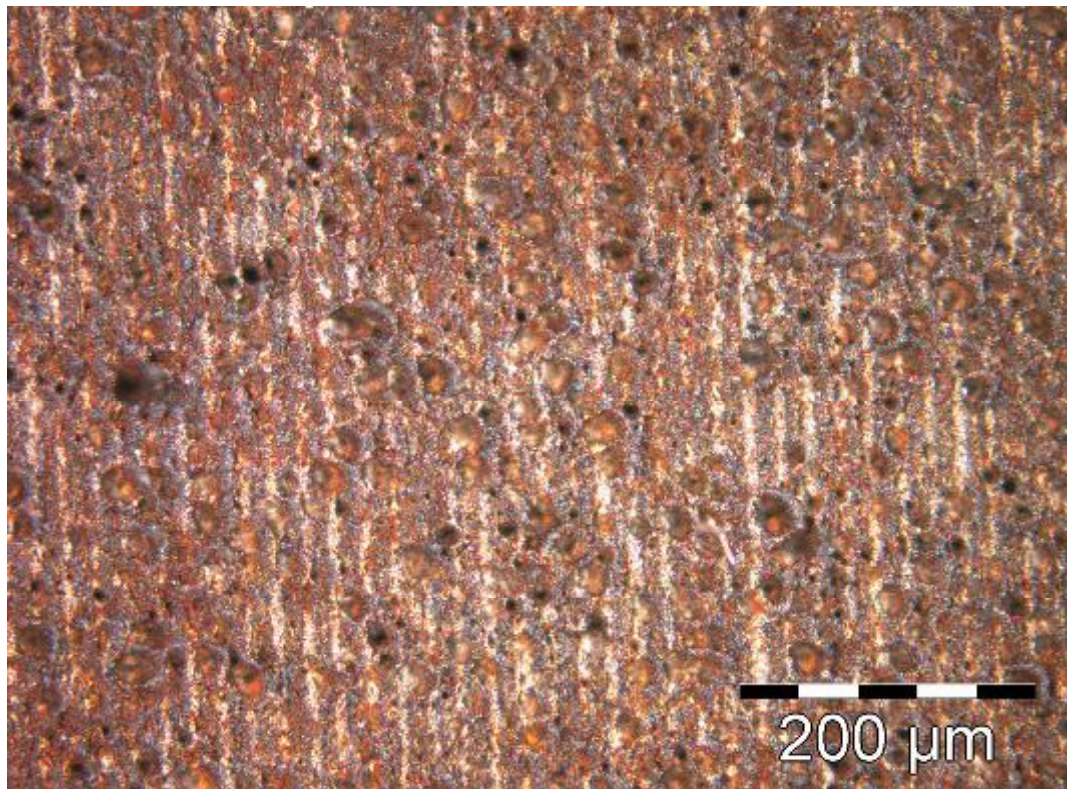


Figure 36. Power setting APT30, speed 2 mm/s, hatch distance 0.01 mm

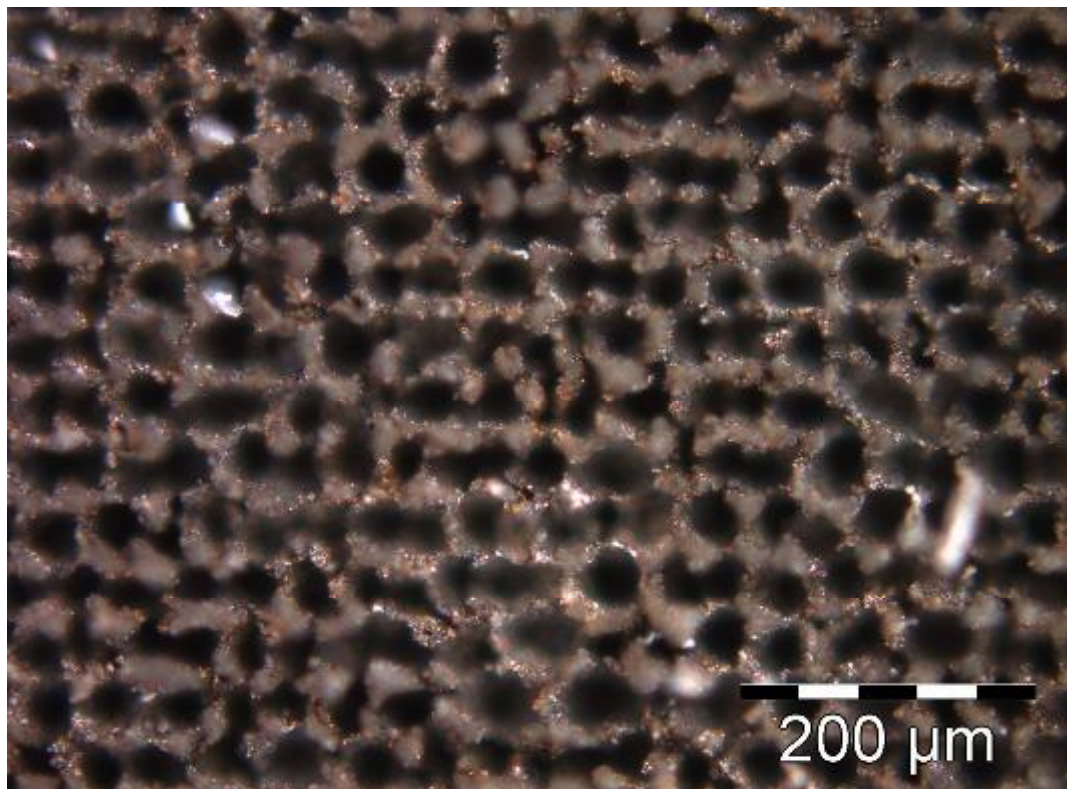


Figure 37. Power setting APT40, speed 1 mm/s, hatch distance 0.02 mm

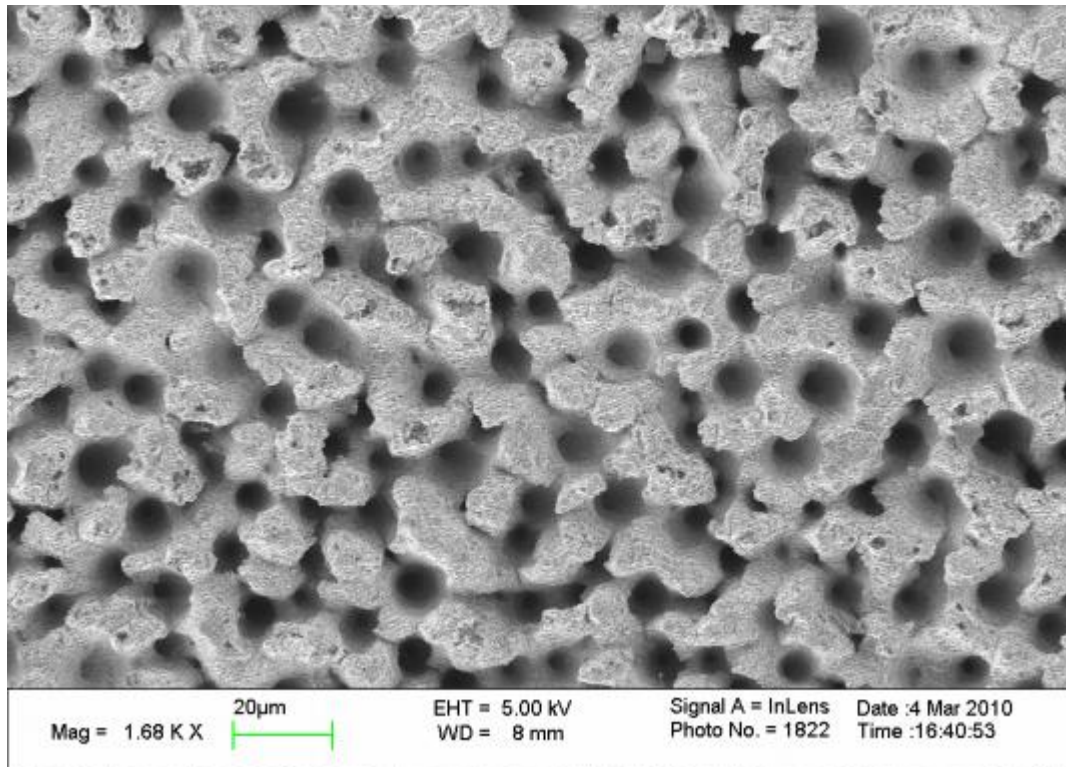


Figure 38. Fe: hatch distance 0.01 mm, speed 1 mm/s (femtosecond laser)

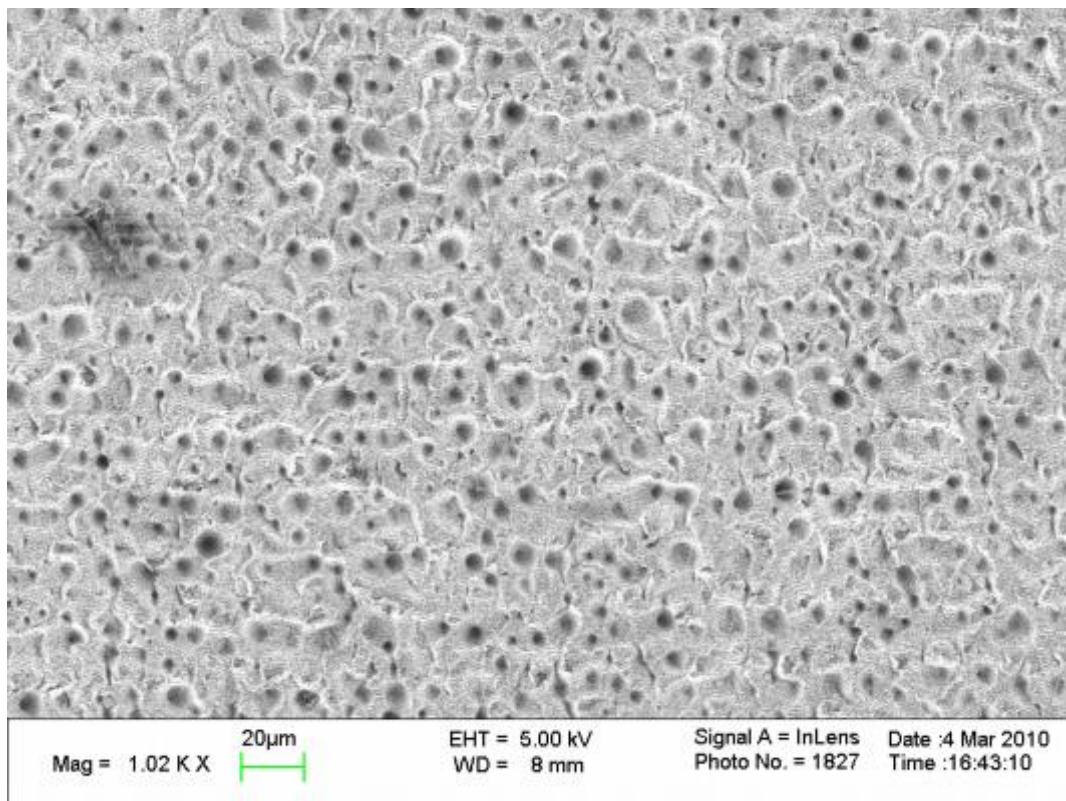


Figure 39. Fe: hatch distance 0.02 mm, speed 1 mm/s (femtosecond laser)

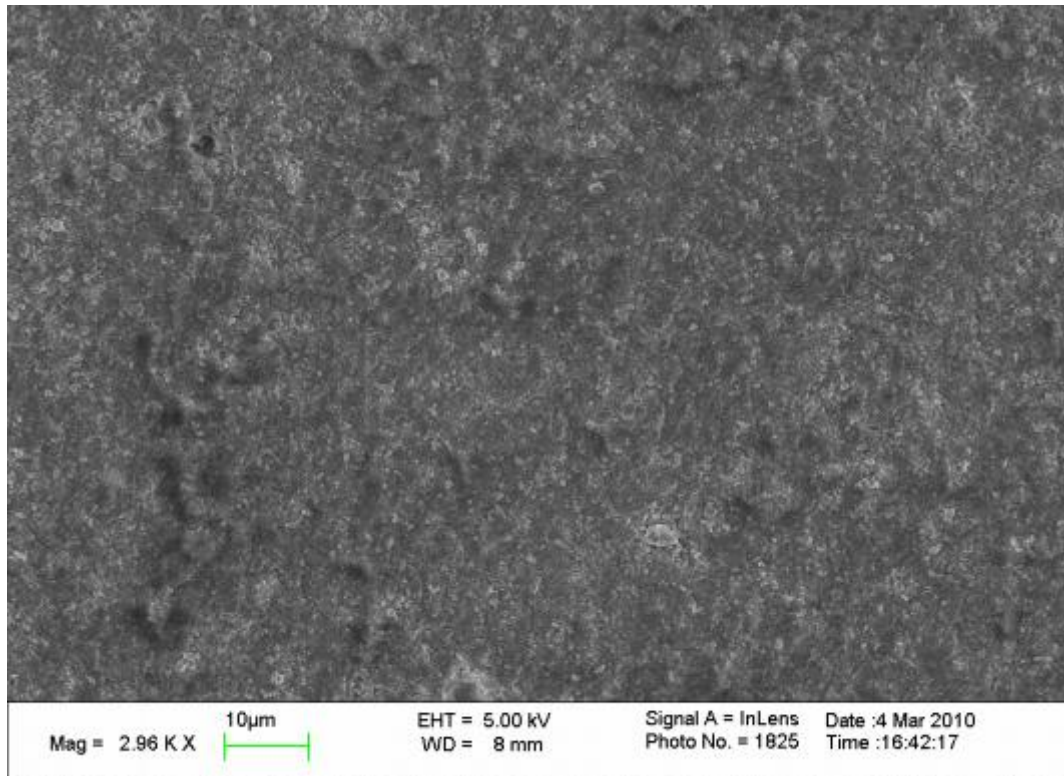


Figure 40. Fe: hatch distance 0.01 mm, speed 5 mm/s (femtosecond laser)

Depths

Depths of the rectangles were estimated with an optical microscope [μm]:

APT60 (800 mW)	0.01	0.02	0.03	0.04	0.05	0.06 mm
1 mm/s	80	40	30	25	20	20
2	40	30	20	20	15	10
5	20	15	10	10		
10	10					

APT40 (500 mW)	0.01	0.02	0.03	0.04	0.05	0.06 mm
1 mm/s	50	30	25	20	15	10
2	30	20	15	10		
5	15	10				
10	10					

APT30 (250 mW)	0.01	0.02	0.03	0.04	0.05	0.06 mm
1 mm/s	30	20	10			
2	20	10				
5	10					

APT25 (125 mW)	0.01	0.02	0.03	0.04	0.05	0.06 mm
1 mm/s	20	10				
2	10					

5.3 Femtosecond laser parameter tests in nickel

Parameter matrixes were made with fs-laser and scan head (100 mm optics) focused on the surface of the samples (0.1 mm thick nickel sheet). Scanning speeds varied between 1–160 mm/s and hatch line distances between 0.01–0.10 mm (Figure 25 and Figure 27).

The sizes of the rectangles were 2x2 mm, and they were cross hatched (horizontally and vertically). The rectangles were made without contours with four power settings: APT60 (full power 800 mW), APT40 (500 mW), APT30 (250 mW) and APT25 (125 mW).

After laser machining the surfaces were washed with ultrasonic washing device.

Following figures show examples of the surfaces made.

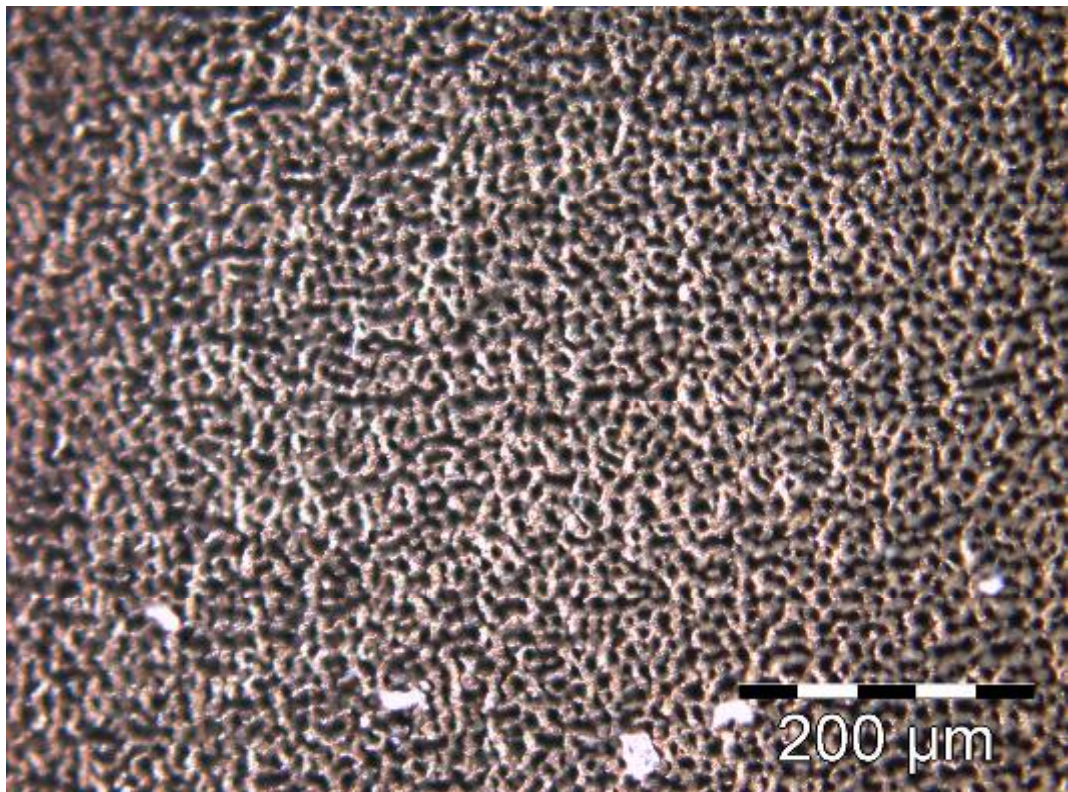


Figure 41. Power setting APT25, speed 1 mm/s, hatch distance 0.01

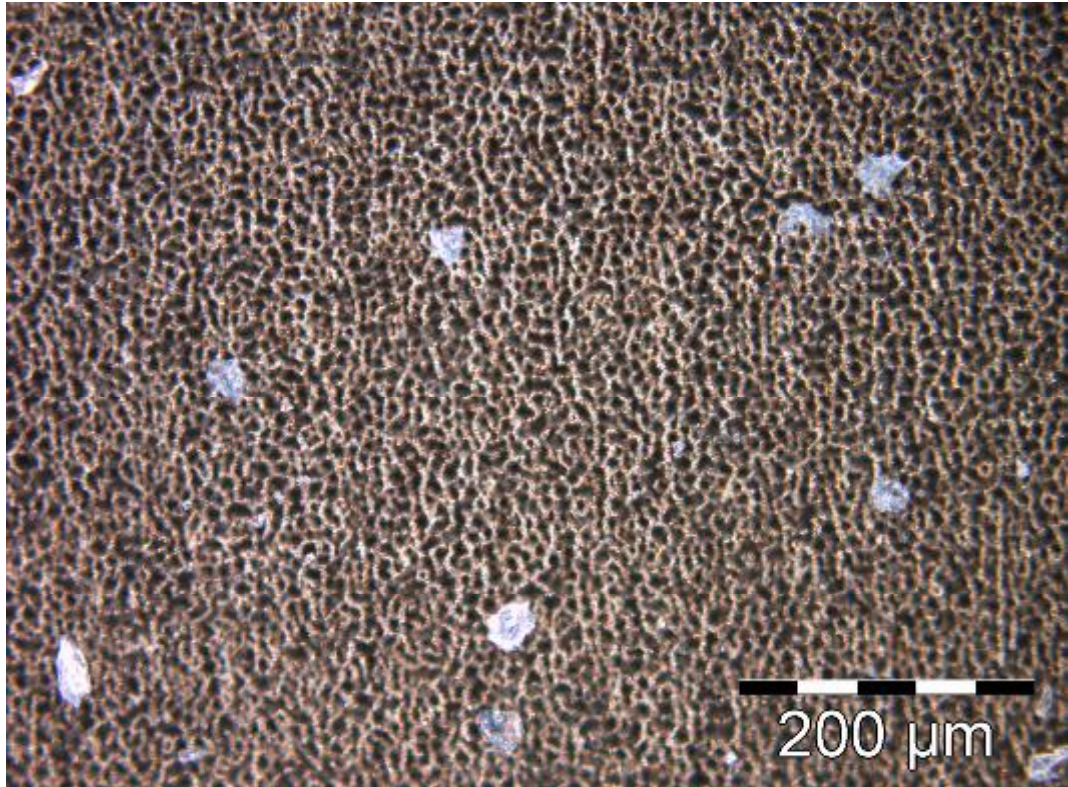


Figure 42. Power setting APT25, speed 2 mm/s, hatch distance 0.01 mm

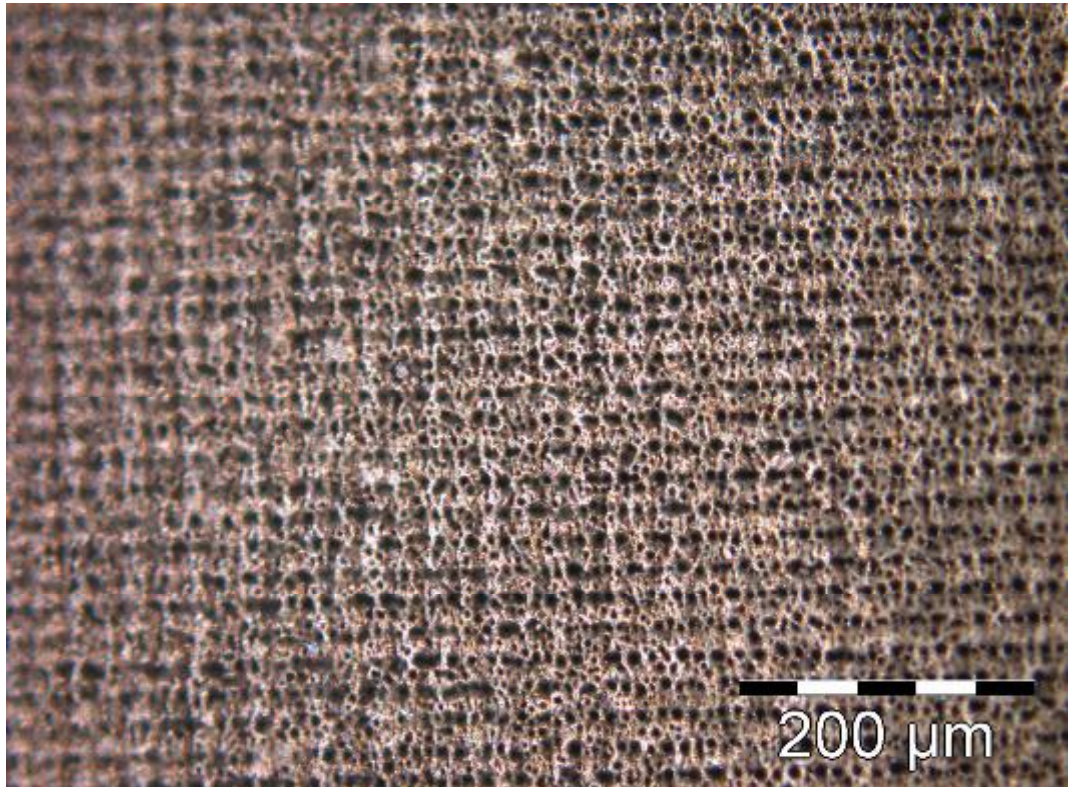


Figure 43. Power setting APT25, speed 1 mm/s, hatch distance 0.02 mm

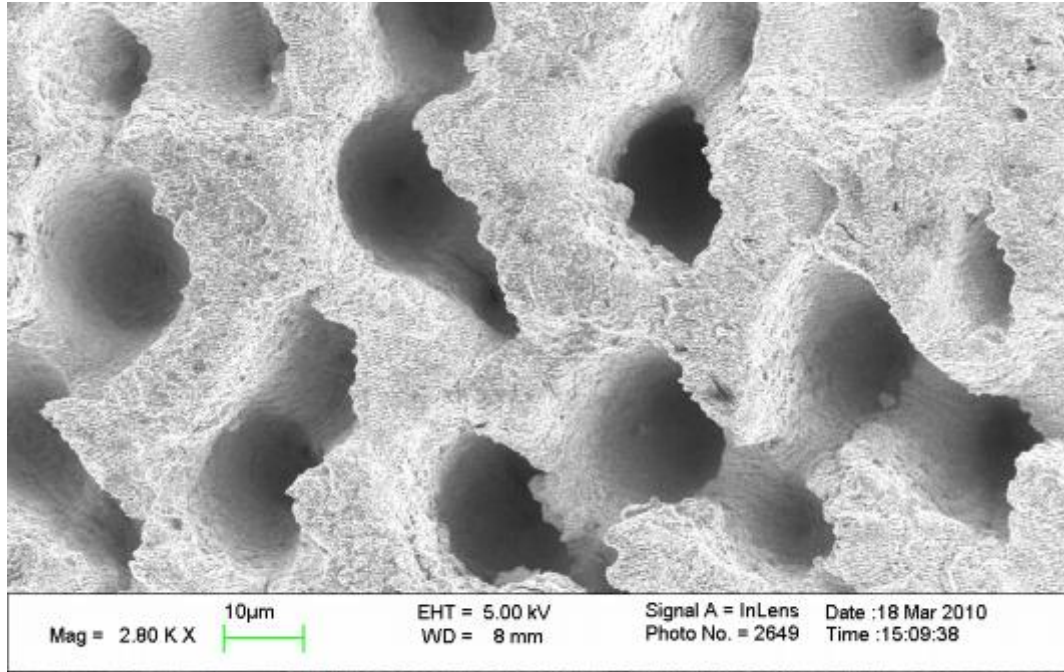


Figure 44. Ni: hatch distance 0.01 mm, speed 1 mm/s (femtosecond laser)

Depths

Depths of the rectangles were estimated with an optical microscope [μm]:

APT60 (800 mW)	0.01	0.02	0.03	0.04	0.05	0.06 mm
1 mm/s	90	30	20	10		
2	60	20				
5	10					
10						

APT40 (500 mW)	0.01	0.02	0.03	0.04	0.05	0.06 mm
1 mm/s	40	10				
2	20					
5	10					
10						

APT30 (250 mW)	0.01	0.02	0.03	0.04	0.05	0.06 mm
1 mm/s	20	10				
2						

APT25 (125 mW)	0.01	0.02	0.03	0.04	0.05	0.06 mm
1 mm/s	10					
2						

5.4 Laser parameter tests with picosecond and nanosecond lasers in silicon, tool steel and nickel

Parameter matrixes were made with ps-laser and ns-laser using scan heads (100 mm optics) focused on the surface of the samples (silicon wafer, polished tool steel and 0.1 mm thick nickel sheet). Scanning speeds varied between 10–800 mm/s and hatch line distances between 0.01–0.10 mm (Figure 25 and Figure 27). The ps-laser power was 0.6 W from the laser and 0.5 W on the sample. The ns-laser power setting 10 W gave 8 W on the sample.

Following figures show examples of the surfaces made.

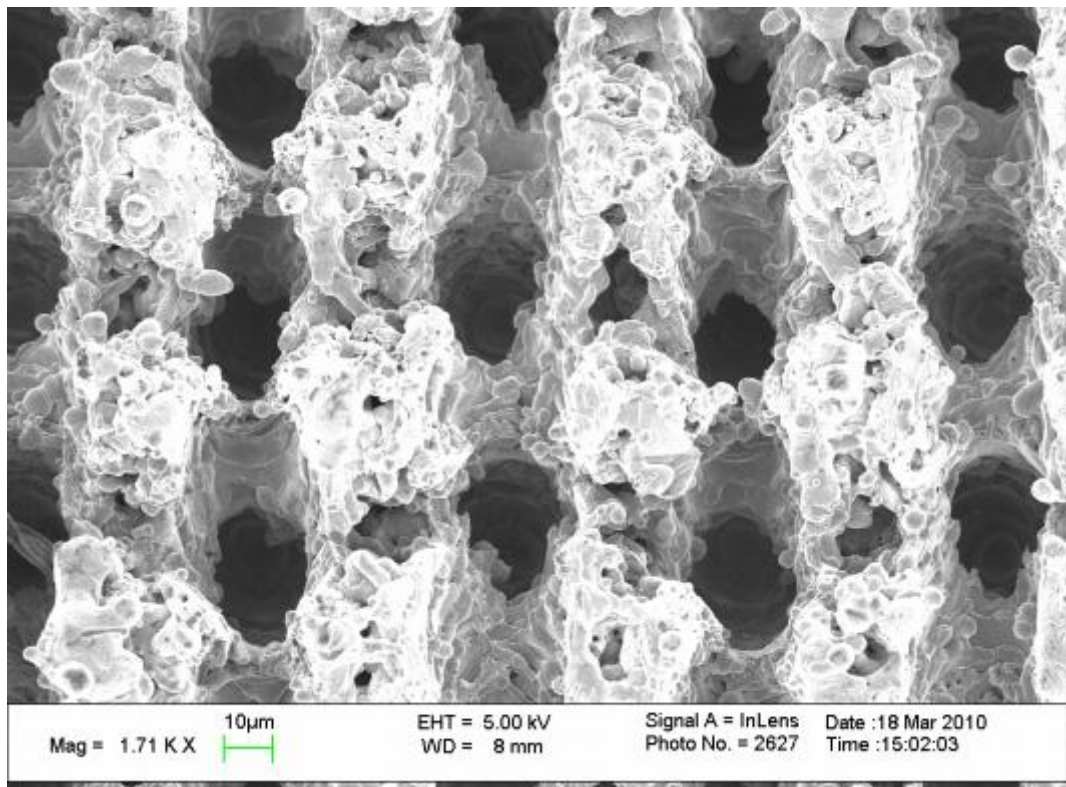


Figure 45. Ni: hatch distance 0.05 mm, speed 200 mm/s (nanosecond laser)

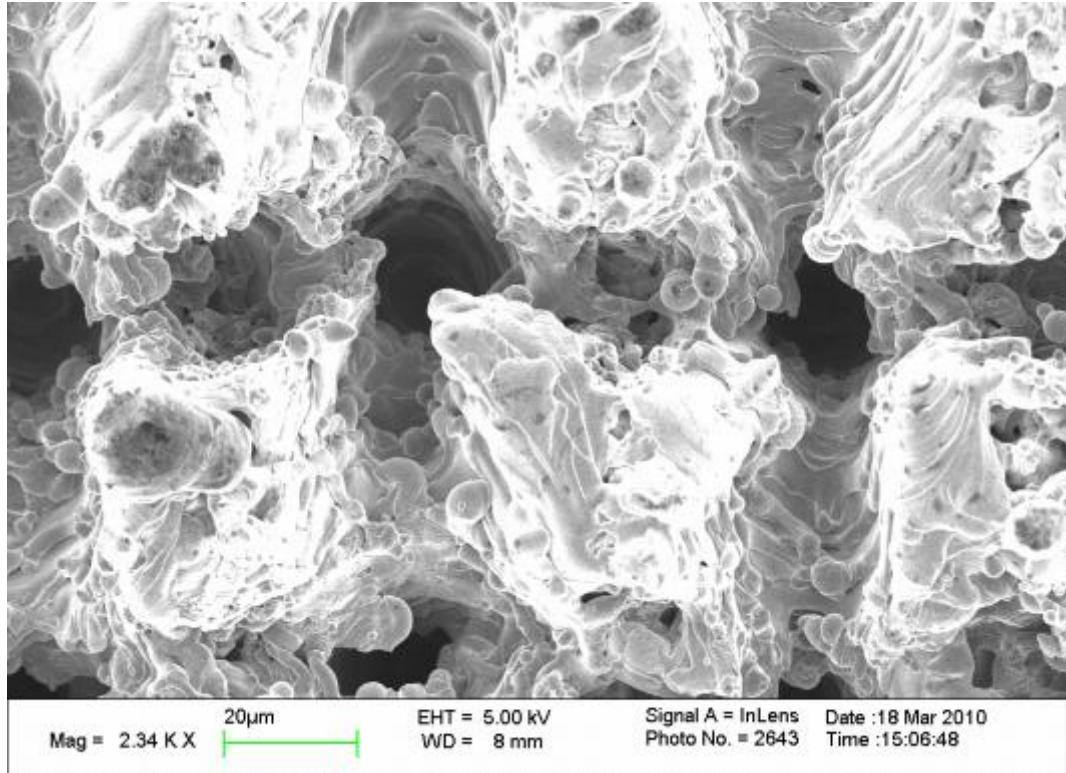


Figure 46. Ni: hatch distance 0.06 mm, speed 200 mm/s (nanosecond laser)

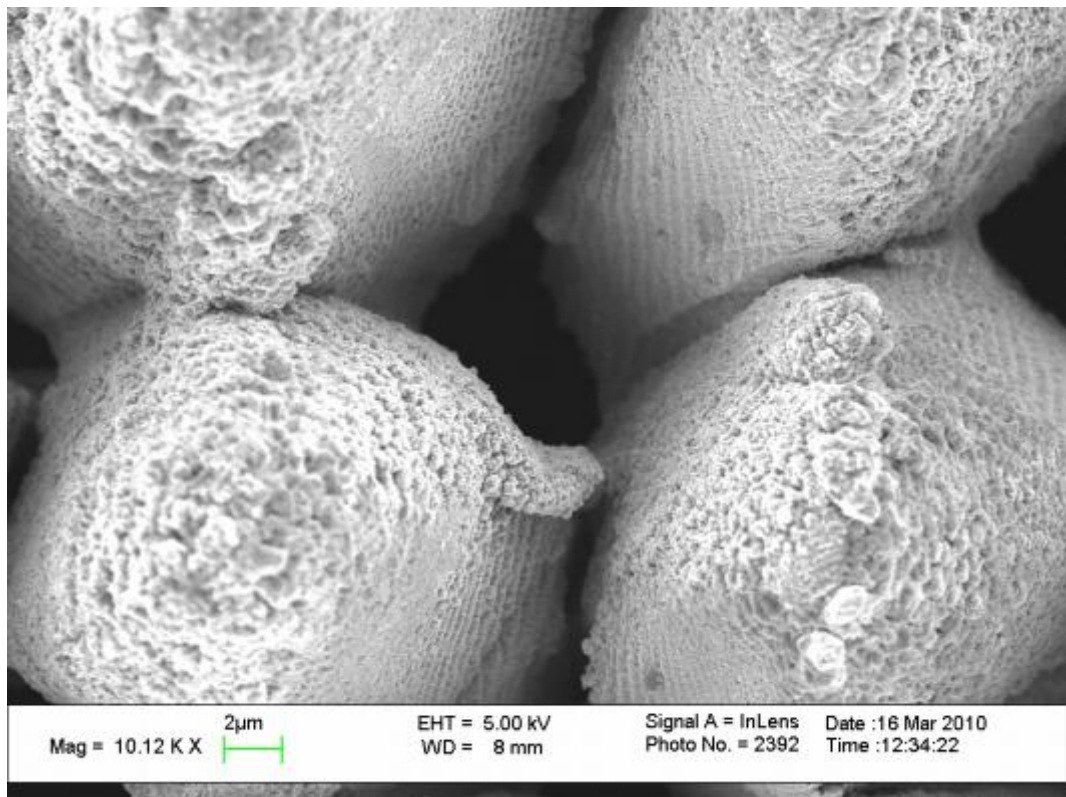


Figure 47. Ni: hatch distance 0.02 mm, speed 10 mm/s (picosecond laser)

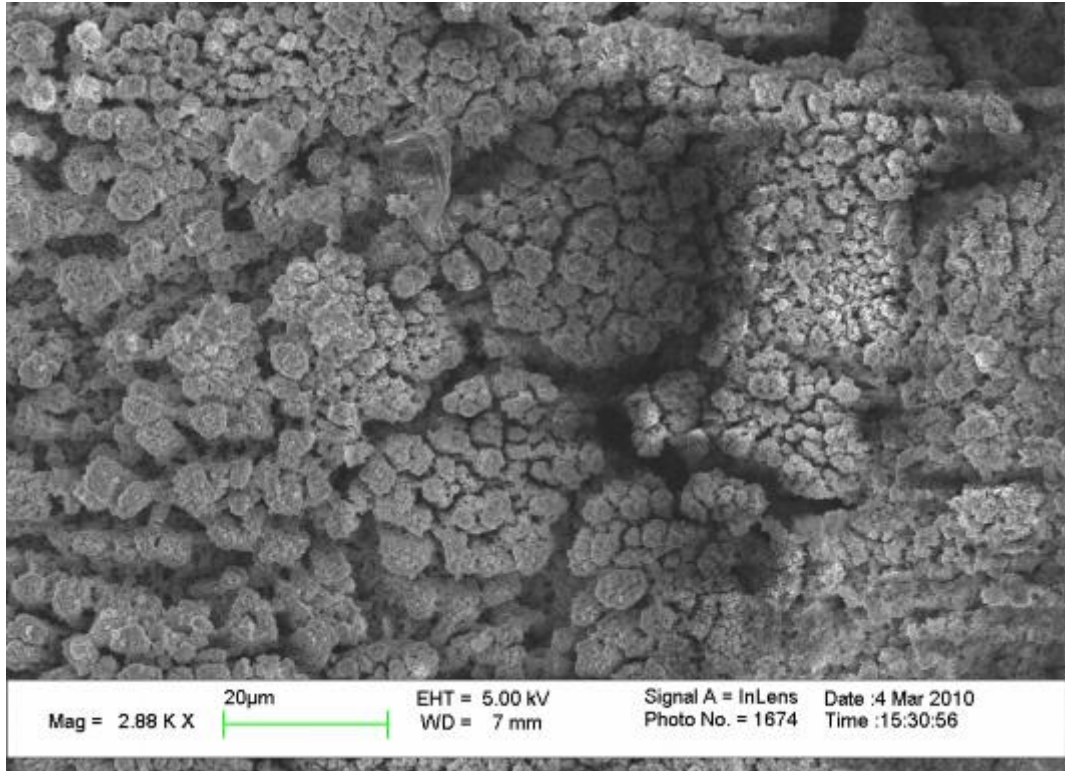


Figure 48. Fe: hatch distance 0.01 mm, speed 10 mm/s (nanosecond laser)

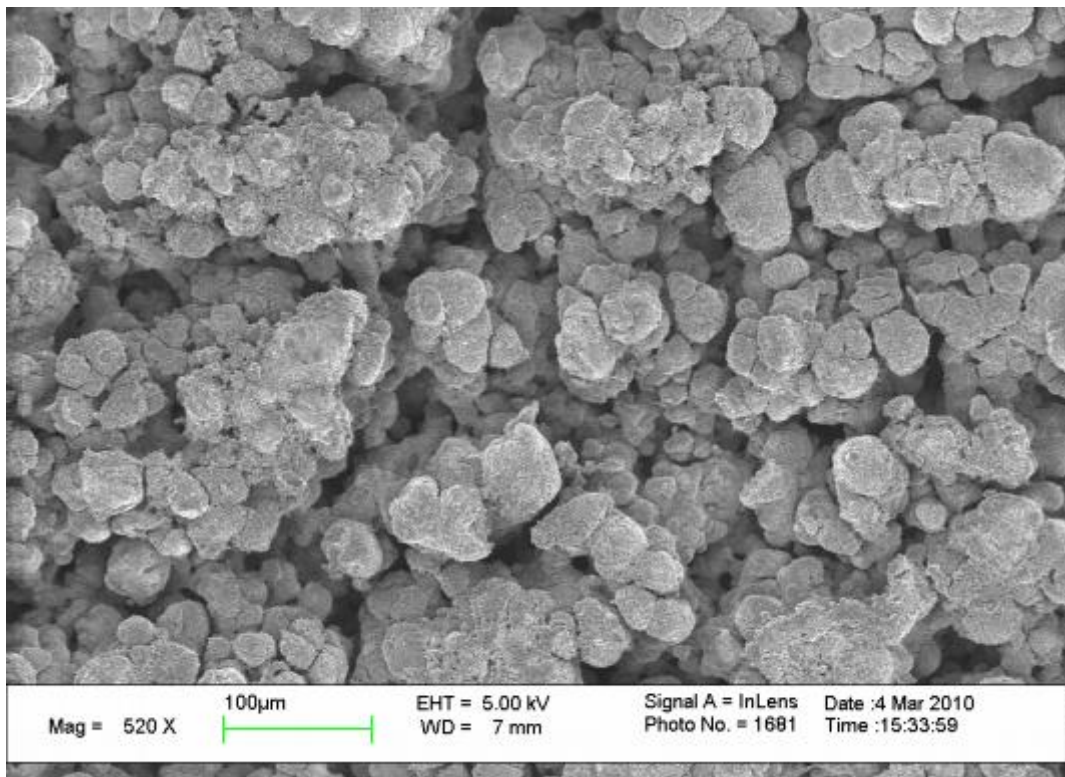


Figure 49. Fe: hatch distance 0.01 mm, speed 50 mm/s (nanosecond laser)

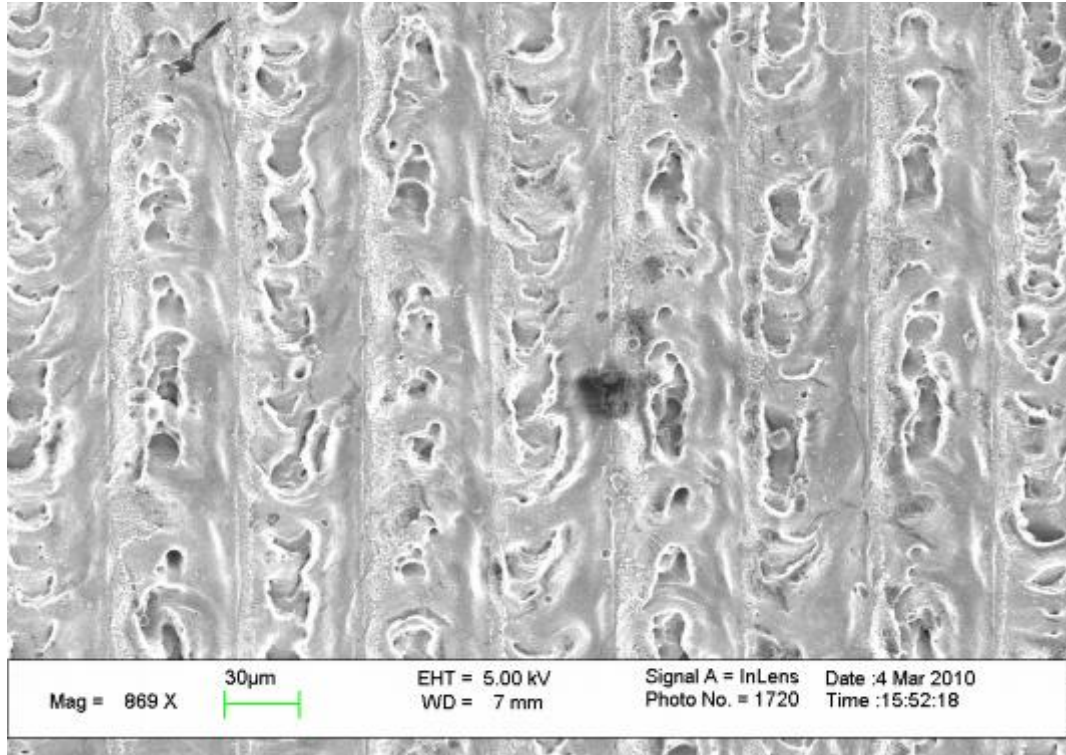


Figure 50. Fe: hatch distance 0.05 mm, speed 10 mm/s (nanosecond laser)

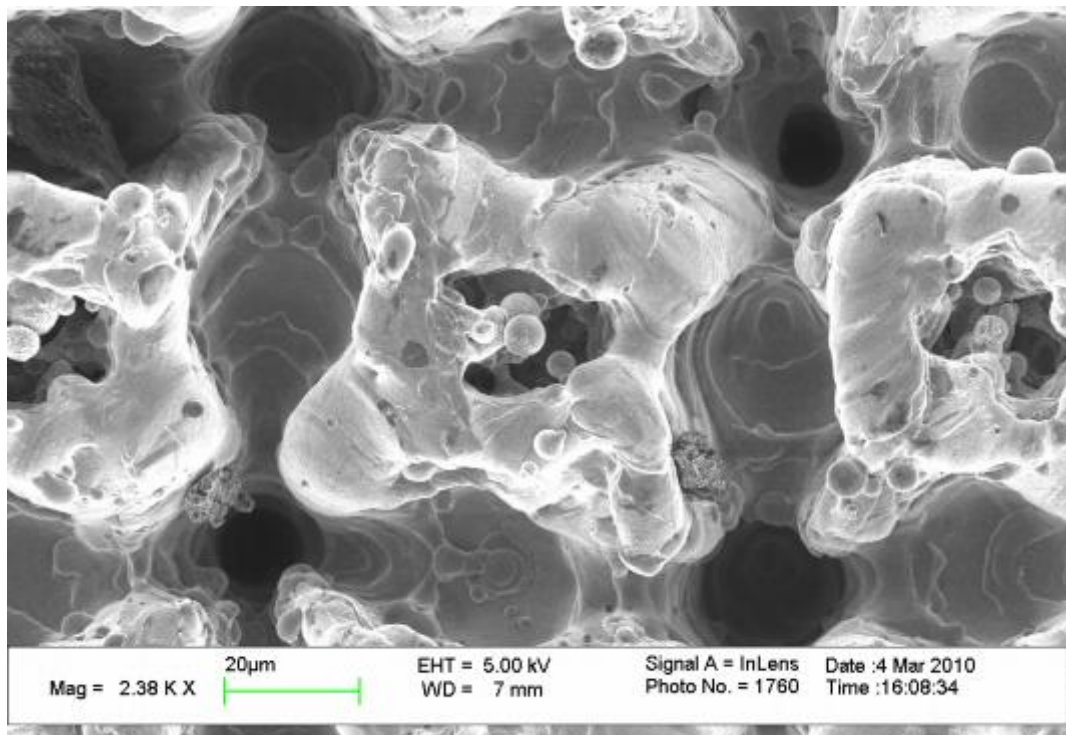


Figure 51. Fe: hatch distance 0.07 mm, speed 400 mm/s (nanosecond laser)

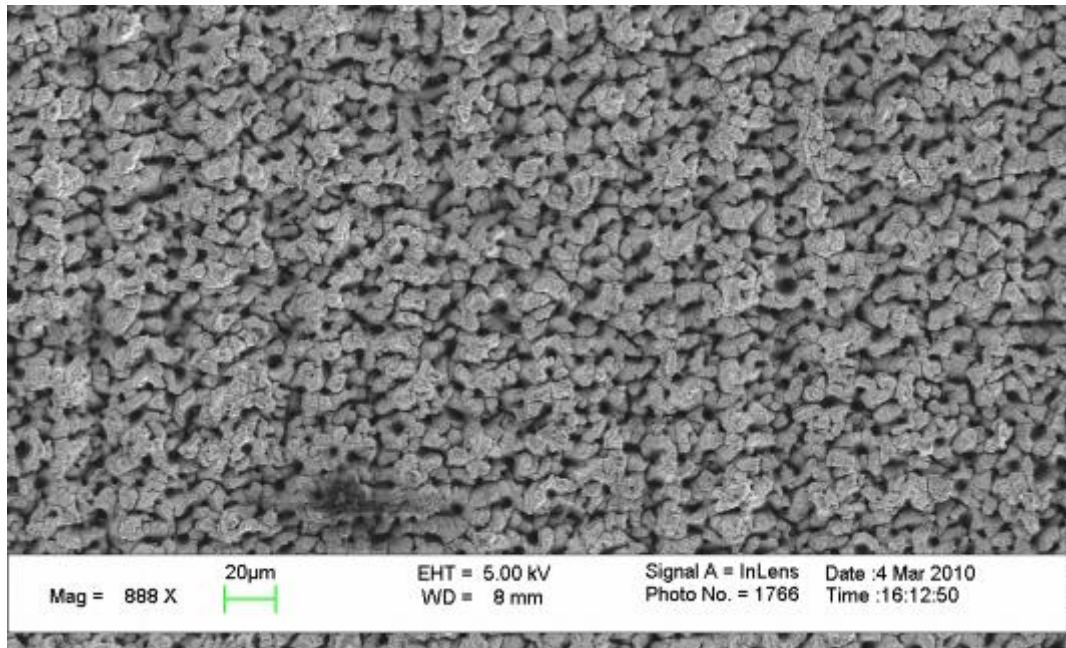


Figure 52. Fe: hatch distance 0.01 mm, speed 10 mm/s (picosecond laser)

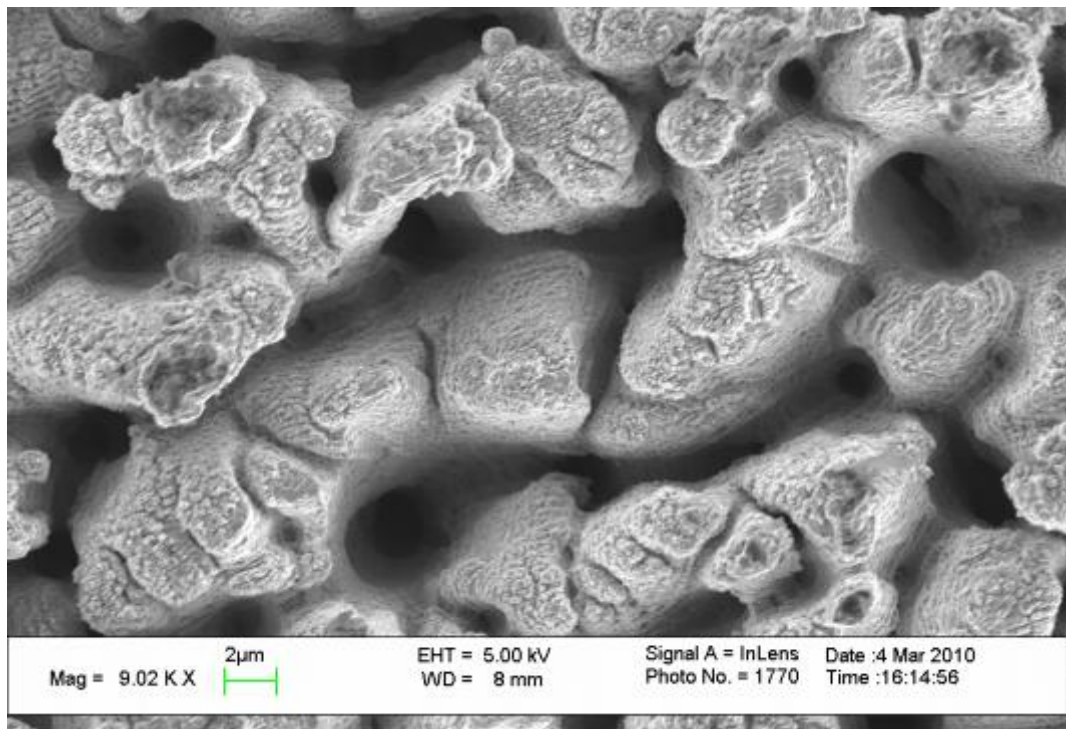


Figure 53. Fe: hatch distance 0.01 mm, speed 50 mm/s (picosecond laser)

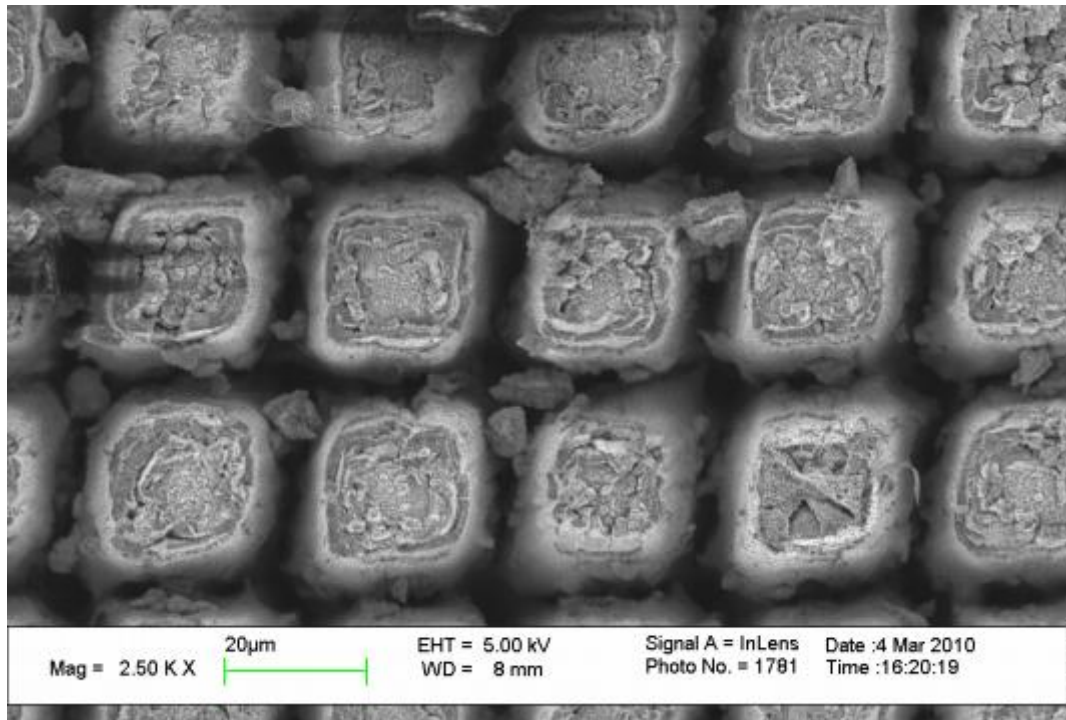


Figure 54. Fe: hatch distance 0.03 mm, speed 10 mm/s (picosecond laser)

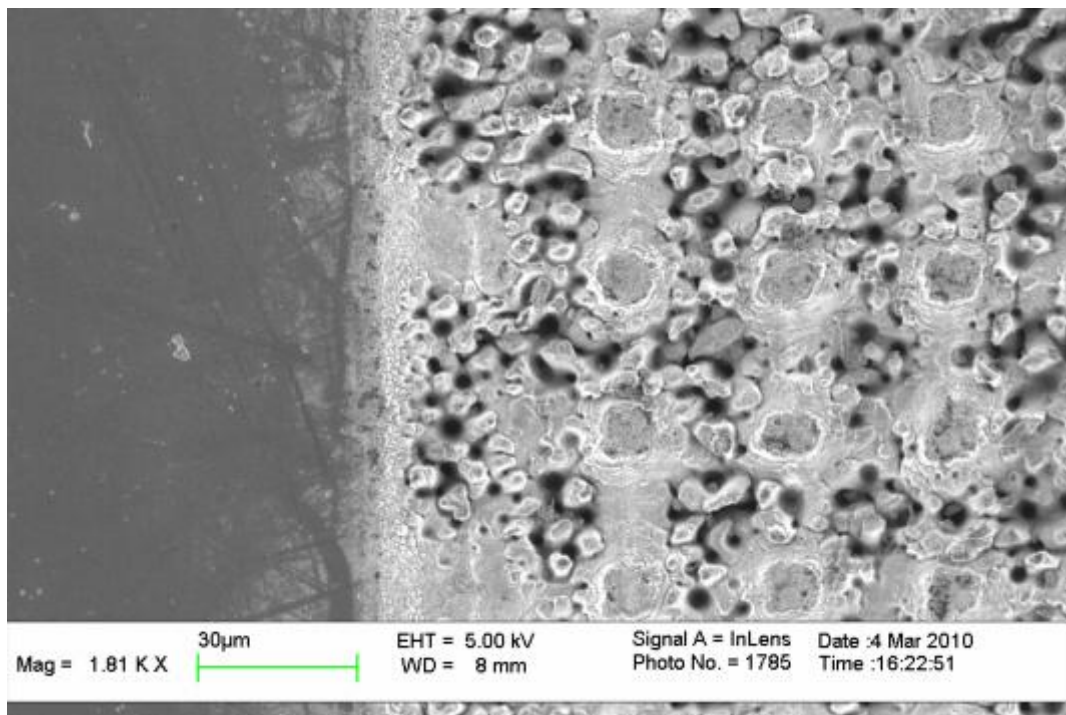


Figure 55. Fe: hatch distance 0.03 mm, speed 50 mm/s (picosecond laser)

Depths

Depths of the rectangles were estimated with an optical microscope [μm]:

Tool steel, ps-laser, 355 nm, 100 kHz, 10 repetitions

Fe, ps	0.01	0.02	0.03	0.04	0.05	0.06	0.07 mm
10 mm/s	80 μ m	40	*	*	*	*	*
20	40	30	*	*	*	*	*
50	15	15	*	*	*	*	*
100	10	10	*	*	*	*	*
200	5	0	*	*	*	*	*

* Groove width is smaller than hatch distance.

Nickel, ps-laser, 355 nm, 100 kHz, 10 repetitions

Ni, ps	0.01	0.02	0.03	0.04	0.05	0.06	0.07 mm
10 mm/s	>100	70 μ m	*	*	*	*	*
20	>100	50	*	*	*	*	*
50	50	20	*	*	*	*	*
100	30	10	*	*	*	*	*
200	20	5	*	*	*	*	*
400	10	0	*	*	*	*	*
800	5	0	*	*	*	*	*

* Groove width is smaller than hatch distance.

Silicon, ps-laser, 355 nm, 100 kHz, 10 repetitions

Si, ps	0.01	0.02	0.03	0.04	0.05	0.06	0.07 mm
10 mm/s	(140)	(60)	*	*	*	*	*
20	100 μ m	(40)	*	*	*	*	*
50	40	10	*	*	*	*	*
100	20	5	*	*	*	*	*
200	10	0	*	*	*	*	*
400	5	0	*	*	*	*	*

* Groove width is smaller than hatch distance.

() There is a lot of waste material on the surface, not removed in ultrasonic wash.

Tool steel, ns-laser, 1060 nm, 100 kHz, wf0, Exp3, 5 repetitions

Fe, ns	0.01	0.02	0.03	0.04	0.05	0.06	0.07 mm
10 mm/s	120 μ m	70	40	30	25	15	0
20	60	30	20	15	10	5	0
50	25	10	5	5	5	0	0
100	15	0	0	0	0	0	0
200	5	0	0	0	0	0	0
400	0						

Silicon, ps-laser, 1060 nm, 50 kHz, wf0, Exp3, 5 repetitions

Si, ps	0.01	0.02	0.03	0.04	0.05 mm
10 mm/s	+	+	+	+	+
20	+	+	+	+	+
50	+	+	+	+	+
100	+	+	+	+	+
200	120 μ m	100	80	40	*
400	100	80	40	*	*
800	80	50	30	*	*

+ Spikes and waste material even above surface

* Groove width is smaller than hatch distance.

Neither 50 nor 100 kHz with two repetitions made measurable depth in nickel sheets.

5.5 Comparison of rectangle depths made with different lasers

Depths of rectangles made with different lasers can be compared when powers, scanning speeds and repetitions are considered. Compared to fs-laser tests, ps-laser tests had ten times as high speeds and repetitions. So, only power correction is needed for measured ps-laser depths. The measured ns-laser depths need also repetition correction.

The following table compares rectangle depths in tool steel [μm]:

- fs-laser 0.5 W (APT40), 1 x speed, made once
- ps-laser 0.5 W, 10 x speed, 10 repetitions
- ns-laser 8 W, 10 x speed, 5 repetitions, measured depths divided by 8 ($5 \times 8 / 0.5 / 10 = 8$)

Fe: fs/ps/ns	0.01	0.02	0.03	0.04	0.05	0.06 mm
1 mm/s	50/80/15	30/40/9	25/-/5	20/-/4	15/-/3	10/-/2
2	30/40/8	20/30/4	15/-/3	10/-/2		
5	15/10/3	10/15/1				
10	10/5/2	0/10/0				

The following table compares rectangle depths in nickel [μm]:

- fs-laser 0.8 W (APT60), 1 x speed, made once, measured depths divided by 1.6 ($0.8 / 0.5 = 1.6$)
- ps-laser 0.5 W, 10 x speed, 10 repetitions

Ni: fs/ps	0.01	0.02 mm
1 mm/s	60/>100	20/70
2	40/>100	10/50
5	5/50	0/20
10	0/30	

The following table compares rectangle depths in silicon [μm]:

- fs-laser 0.5 W (APT40), 1 x speed, 2 repetitions, measured depths divided by 3.2 ($2 \times 0.8 / 0.5 = 3.2$)
- ps-laser 0.5 W, 10 x speed, 10 repetitions
- ns-laser 8 W, 10 x speed, 5 repetitions, measured depths divided by 8 ($5 \times 8 / 0.5 / 10 = 8$)

Si: fs/ps/ns	0.01	0.02	0.03	0.04	0.05 mm
5 mm/s	28/40/-	13/10/-	9/-/-	13/-/-	6/-/-
10	13/20/-	6/5/-	5/-/-	3/-/-	3/-/-
20	6/10/15	3/0/13	2/-/10	2/-/5	2/-/-
40	3/5/13	2/0/10	0/-/5		
80	2/0/10	0/0/6	0/-/4		

5.6 Holes in silicon

Test holes

Holes were made in silicon wafers (diameter 150 mm, thickness 0.38 mm, coated and uncoated) with VTT's fs-laser:

- linear x-y-table for wafer movements
- fixed optics f100 and f50
- power settings APT20, APT25, APT30, APT40 and APT55 (20, 125, 250, 500 and 800 mW)
- number of pulses 1, 2, 4, 8, 16, 32, 64, 125, 250, 500, 1000, 2000, 4000, 8000, 16000 and 32000

Diameters of through holes were measured with an optical microscope:

Using optics f100, through holes could be made by 1000xAPT55, 2000xAPT40, 2000xAPT30 and 4000xAPT25. Power setting APT25 and 4000 pulses made hole diameter 55/20 μm (in/out).

With optics f50 through holes could be made by 500xAPT55, 1000xAPT40, 2000xAPT30 and 4000xAPT25. Power setting APT30 and 2000 pulses made hole diameter 40/30 μm (in/out).

The samples were sent to VTT Espoo for characterization.

Hole matrixes

According to measurements of test holes, hole matrixes were made to coated and uncoated silicon wafers (see Figure 26):

- hole groups (11x11), pitch 0.5 mm, group size 5x5 mm
- one group (e.g. A1) made with same parameters
- 1 mm space between hole groups (e.g. A1–B1 or A1–A2)
- 4 matrixes/wafer, 1 matrix (A1–F4) made in a quarter of a wafer
- laser on time 64 minutes/matrix = 256 minutes/wafer
- working time 92 min/matrix = 6 h 8 min / wafer

The hole matrixes (16 matrixes, 4 wafers) were sent to VTT Espoo for characterization.

Laser parameters (APT/number of pulses)

F= 50	A	B	C	D	E	F
1	55/125	55/250	55/500	55/1000	55/2000	55/4000
2	40/125	40/250	40/500	40/1000	40/2000	40/4000
3	30/125	30/250	30/500	30/1000	30/2000	30/4000
4	25/125	25/250	25/500	25/1000	25/2000	25/4000

f= 100	A	B	C	D	E	F
1	55/125	55/250	55/500	55/1000	55/2000	55/4000
2	40/125	40/250	40/500	40/1000	40/2000	40/4000
3	30/125	30/250	30/500	30/1000	30/2000	30/4000
4	25/125	25/250	25/500	25/1000	25/2000	25/4000

The depth of the holes were measured from their side profiles after dicing. No polishing was done this time. Calculated values for spot sizes are $10\mu\text{m}$ for f50 optic and $20\mu\text{m}$ for the f100 optic. Beam quality is taken into account in calculations. From Table 3 one can see the intensity values for different pulse energies used.

Table 3. Intensities used with different optics and pulse energies in J/cm^2

	f50	f100
850 μJ	1082	271
525 μJ	668	167
244 μJ	311	78
117 μJ	149	37

These intensities are really high compared to many other authors drilling experiments but the aim was to drill through as fast as possible without vacuum chamber. From Figure 56 we can see that increasing pulse energy after certain point does not make drilling faster. Using f50 optic it takes 4000 pulses to get through when pulse energy is $117\mu\text{J}$ but when pulse energy is doubled the hole can be made twice as fast. 2000 pulses are enough to drill through the wafer. When again doubling the pulse energy the drilling speed is nominally faster. At $850\mu\text{J}$ drilling is not anymore faster but a lot of side effects appear. Wafer surface is heavily damaged on the edges of the hole and hole is not round anymore. This same is visible also on $525\mu\text{J}$ pulse energy.

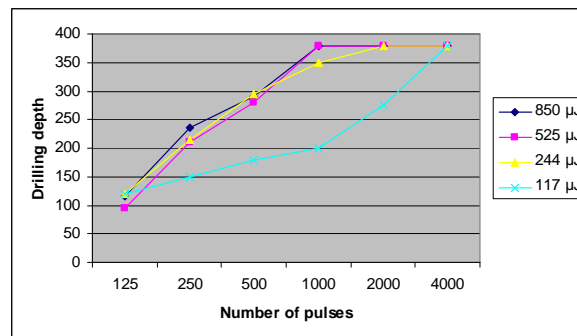


Figure 56. Drilling with f50.

J Koga et al [14] have done extensive research on laser induced breakdown of air and they found that with $20\mu\text{m}$ spot the breakdown energy at 800nm wavelength with 100fs pulse is $320\mu\text{J}$. Sound when air breakdown happens can be easily heard at $580\mu\text{J}$ level. As intensity these values are $100\text{--}185\text{ J}/\text{cm}^2$. This means that when breakdown of air happens some part of the pulse energy is lost and beam focusing changes. These experiments were made in air without target present.

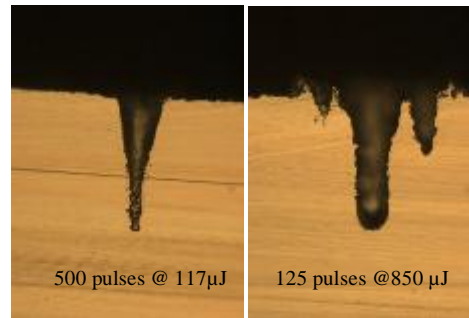


Figure 57. Drilling with $f100$. Depth on both $\sim 250 \mu\text{m}$ and on right heavy damages around the hole.

When using $f100$ optic intensities are a lot smaller and there should not be air breakdown present at the lowest pulse energies. This seems to be true due increasing pulse energy increases drilling rate. When it takes 2000 pulses for 244 μJ to go through the wafer only 1000 pulses is needed for the 525 μJ energy (Figure 58). But again 850 μJ does not help anymore and the upper face of the wafer is damaged (Figure 57).

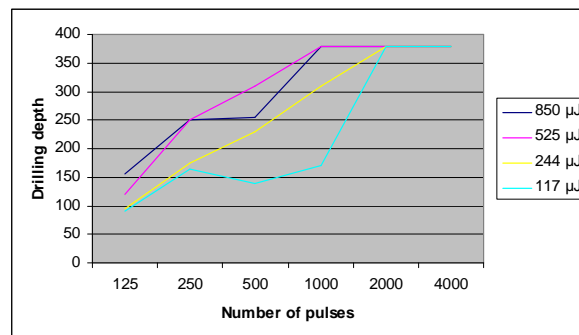


Figure 58. Drilling with $f100$ and different pulse numbers and energies.

Figure 58 has logarithmic scale on x-axis and we can see that drilling rate slows down when more pulses are inputted. At 117 μJ 500 and 1000 pulses data is misleading due depth measurement was not made from middle of hole and this is why curve is not reliable at those points.

Since drilling is done the beam focus on surface of the wafer the holes are quite conical and the additional pulses after breaking through the wafer makes the holes more cylindrical. This can be found from Figure 59. Changing the focal position would change the drilled hole geometry also.

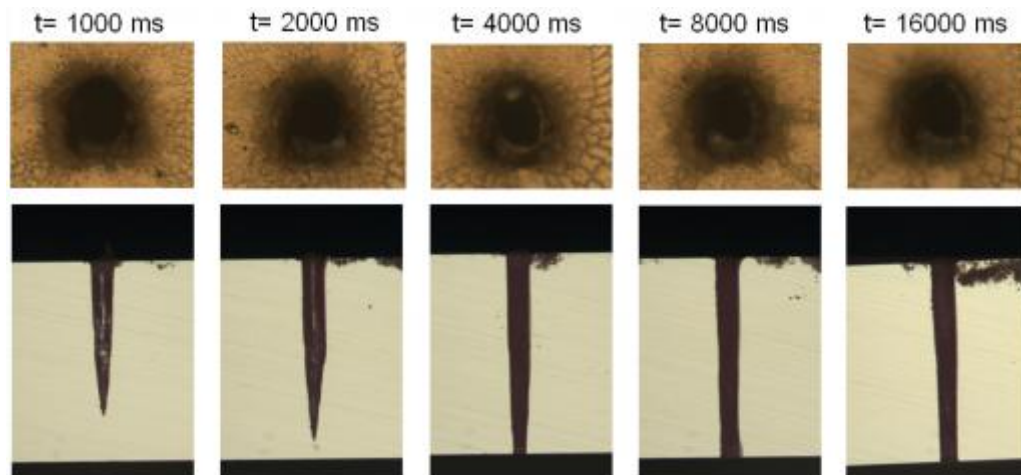


Figure 59. Holes drilled using $244\mu\text{J}$ pulse energy with $f50$ optic in focus. Pulse count from left to right 1000, 2000, 4000, 8000 and 16000 pulses per hole.

Many authors like Mizeikis et al.[15] have used vacuum chamber for femtosecond drilling experiments and it has improved drilling ability. Vacuum also removes the danger of laser induced breakdown of air or other gases. In industrial application vacuum chamber might require additional costs due part handling and vacuum pumping time which could be a challenge for the economics of the process.

Drilling of silicon was demonstrated to work well but depending on pulse energy drilling is affected by the side effects. The effects ruin the quality and will not help in enhancing the drilling speed. Drilling depth per pulse is slowed down after couple of hundred pulses a lot. Because more pulses are needed to go through the wafer it takes longer time to finish drilling.

More work is needed to be done if industrial speeds are pursued in using similar femtosecond system. Using of vacuum chamber is known to give better quality in drilling. Vacuum also makes the air breakdown problem disappear due there is not air to influence with the beam.

5.6.1 Basic drilling tests

First drilling tests showed that arbitrarily high values of fluence cannot be used for femtosecond drilling of the silicon. Using too high pulse energies resulted cracks in the material as shown in the Figure 60. In order to avoid the crack formation fluence values below 10 J/cm^2 should be used. For example, to the hole diameter of $50\ \mu\text{m}$ this correspond to the pulse energy of $200\ \mu\text{J}$. In Figure 60 is shown the holes made using values higher than above mentioned threshold fluence. The effect of the cracks can be seen clearly from the exit apertures of the holes. When using lower fluence values repeatable good quality holes without cracking can be made as shown in Figure 61.

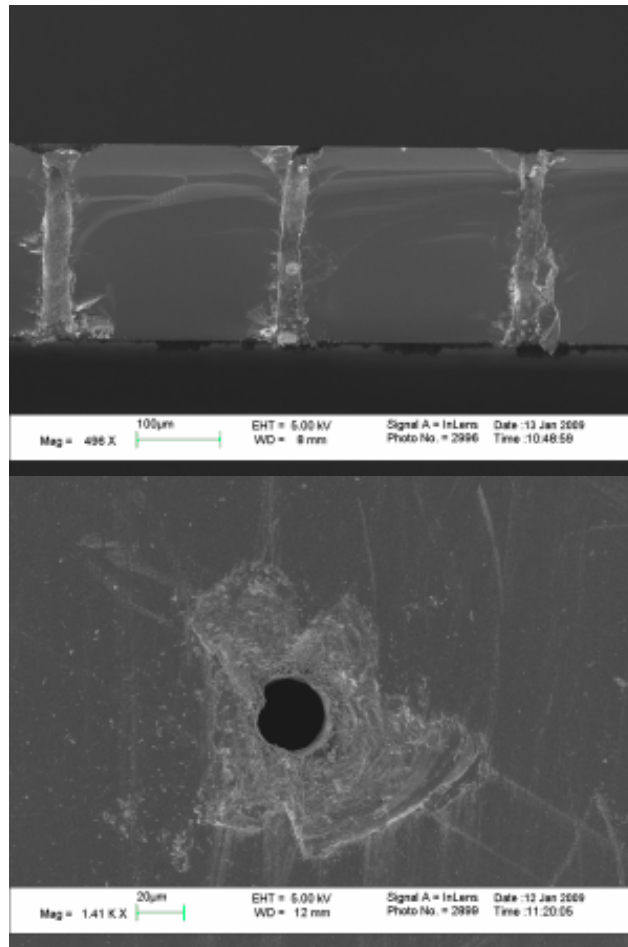
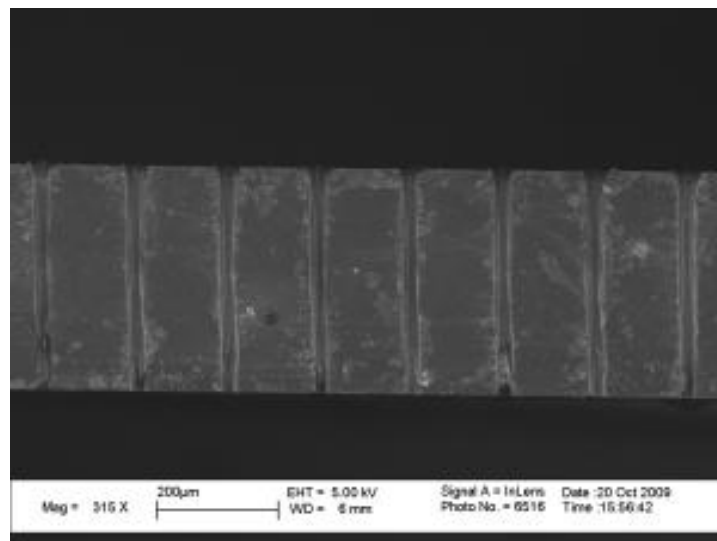


Figure 60. Holes drilled through 280 µm thick silicon wafer using pulse energy of 1 mJ and 100 pulses. Too high pulse energy results in cracks that can be seen from the mutilated exit aperture.



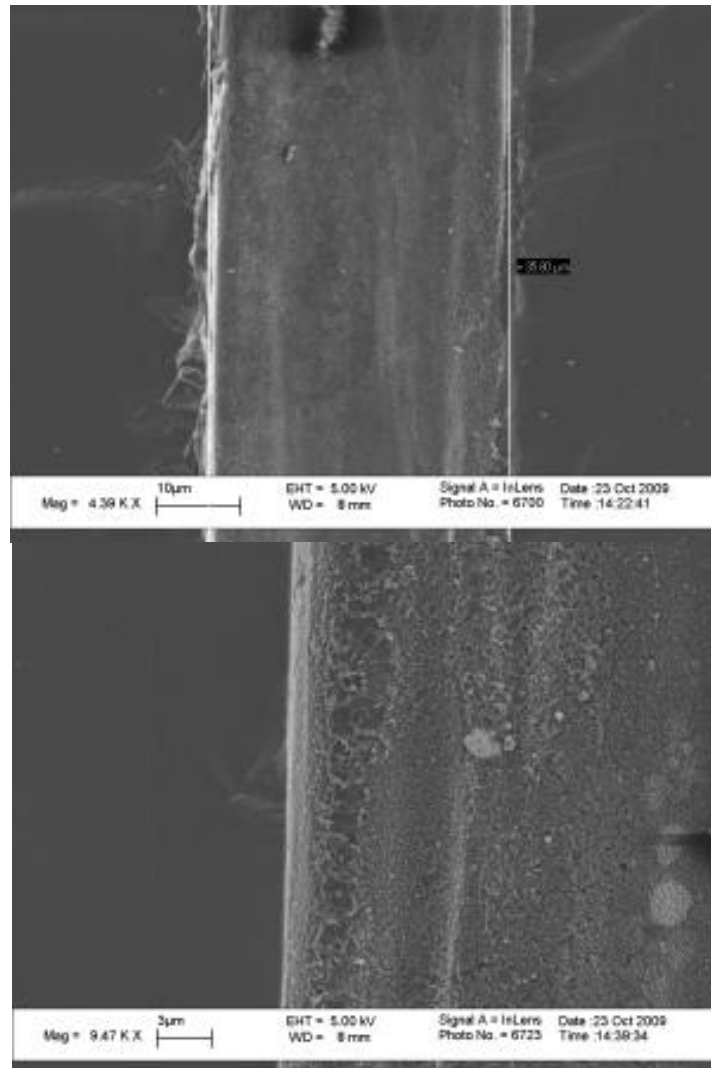


Figure 61. Holes drilled through 380 μm thick silicon wafer. Using low values of pulse energy results in a good quality, crack free and repeatable holes. Holes are made using 150 μJ pulse energy and 2000 pulses. Ablation debris was removed using BHF acid bath.

Ablation debris was removed using buffered hydrofluoric acid (BHF) bath of 30 minutes. In Figure 62 is shown the effect of the bath to debris removal on the entrance of the holes. BHF removes the debris consisting of silicon dioxide from the surface and leaves silicon untouched. Although the results are good using BHF bath for the debris removal, using water assisted ablation is far more simple and effective technique.

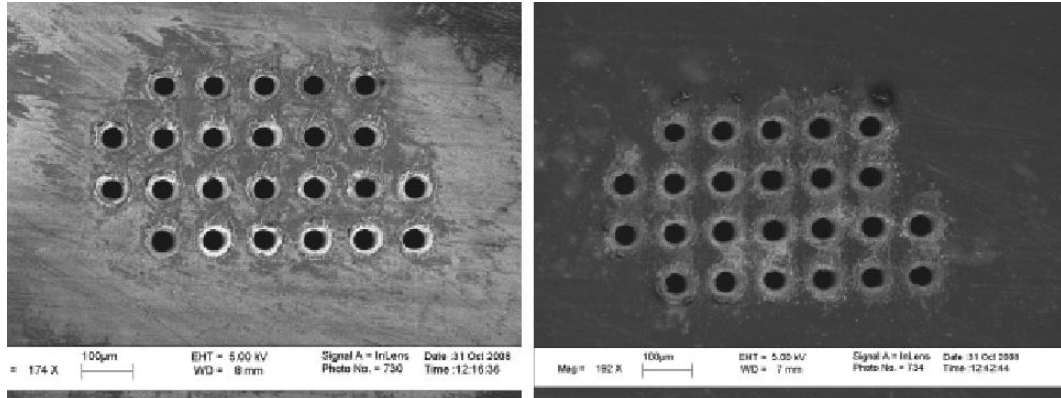


Figure 62. The effect of ablation debris removal using the hydrofluoric acid bath.

5.6.2 Water assisted drilling

During the project it was found that the water assisted ablation reduces greatly problems related to debris removal and thermal effects. By applying proper layer of water in a form of vapour to the sample surface material removal rate can be enhanced and the processing quality increased.

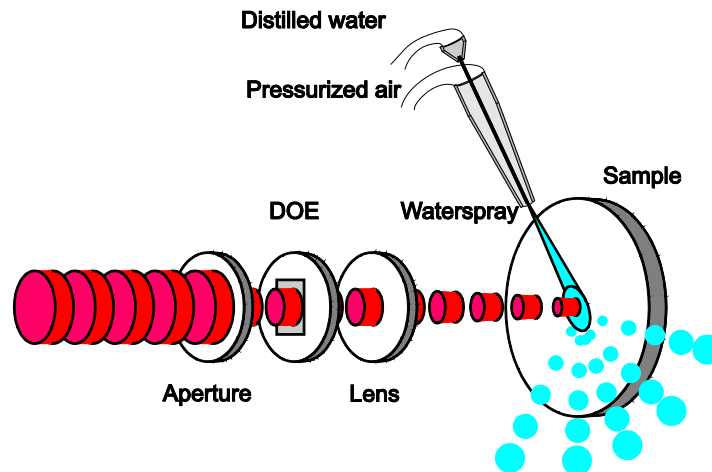


Figure 63. Schematics of the water assisted drilling.

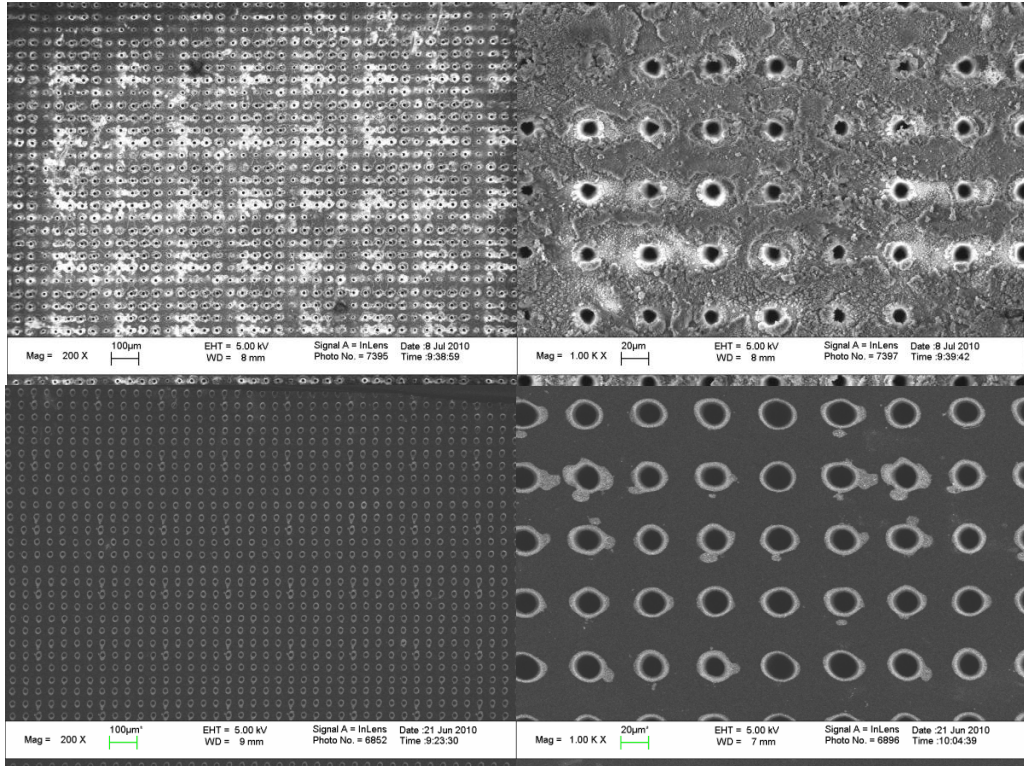


Figure 64. Quality of the drilled holes without (above) and with (below) water assisted ablation before any subsequent cleaning.

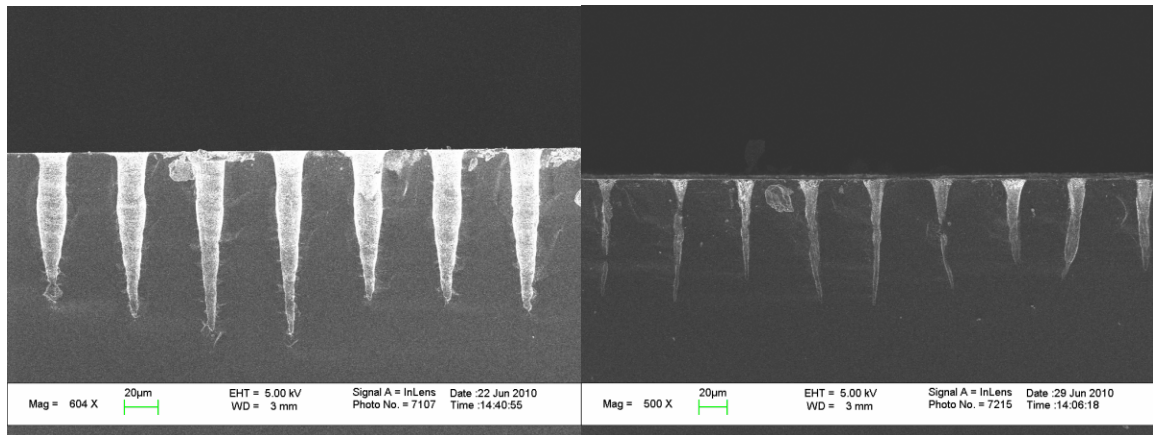


Figure 65. Compared quality of the holes with and without water assisted ablation.

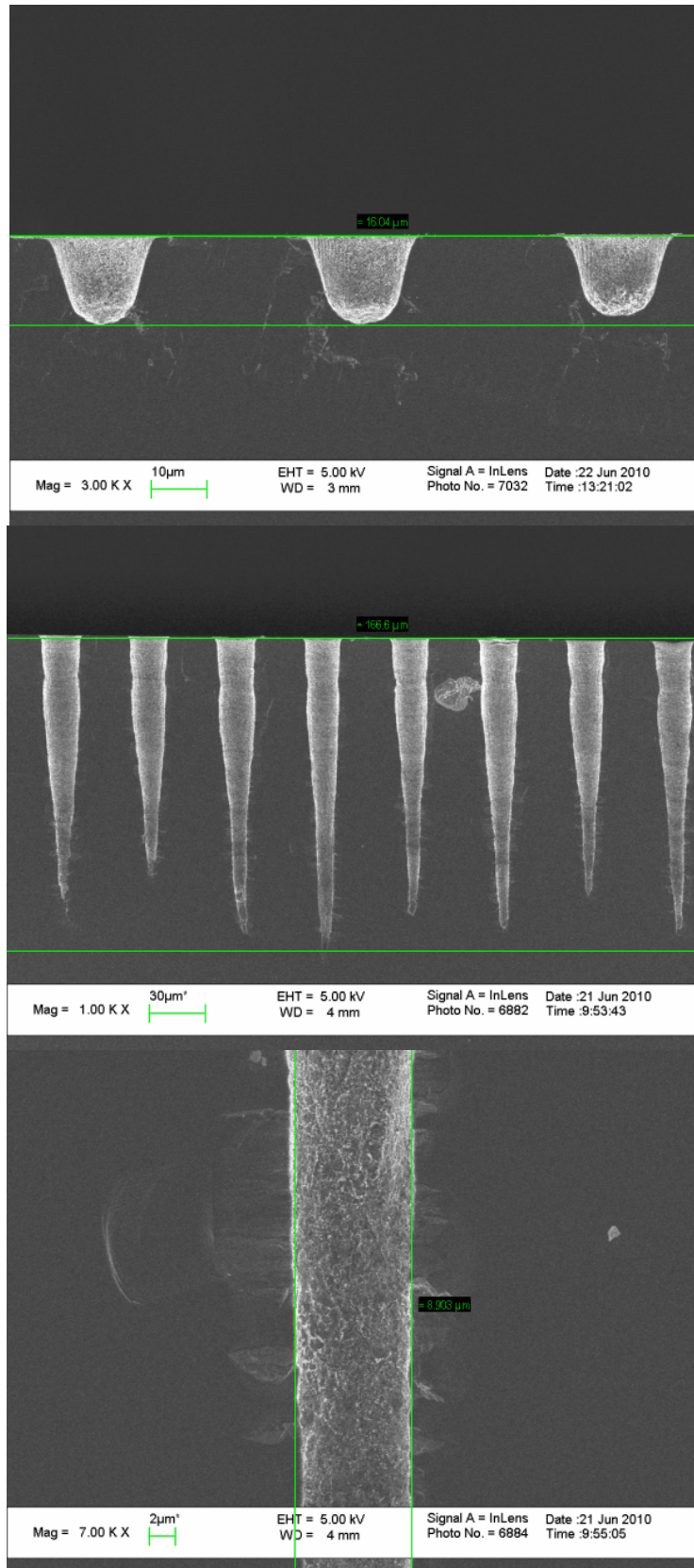


Figure 66. Ablation quality using 8 μJ and 100 (top) and 4 μJ and 4000 (middle, bottom) for pulse energy and number.

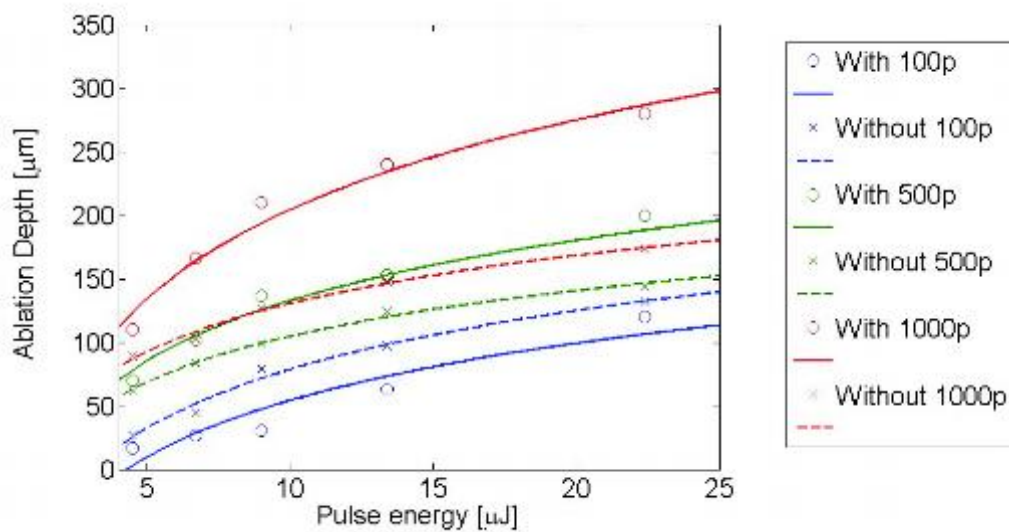


Figure 67. Measured ablation depth as a function of the energy for drilling with and without the water spray.

5.6.3 Drilling using diffractive optics

The aperture size and depth requirements of the project regarding drilling of the silicon where 15/75 μm and 30/150 μm respectively. When drilling such small apertures the energy density on the sample surface can get too high causing the cracking of the material. We found in the experiments that fluence values $F < 10 \text{ J/cm}^2$ should be used in order to avoid cracking in silicon. For example, with hole diameter of 50 μm you should use pulse energies less than 200 μJ . When having more than 3 mJ of pulse energy on the laser this means great energy losses when drilling just one hole at the time. This can be avoided using simultaneous drilling based on the diffractive optics. In Figure 68 are shown schematics of the system exploiting diffractive optics.

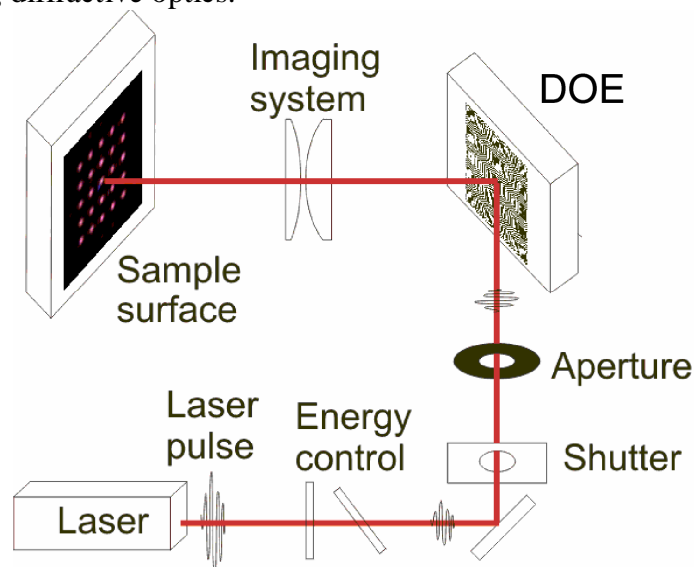


Figure 68. Schematics of the ablation system using diffractive optical element (DOE.)

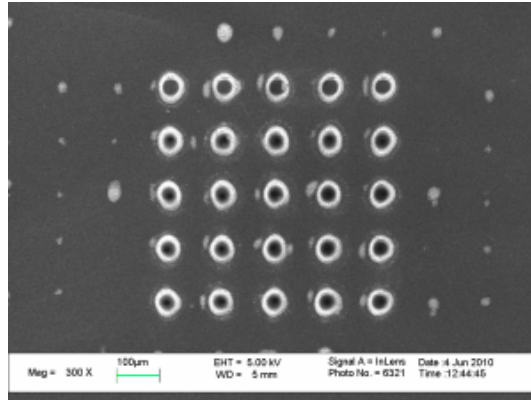


Figure 69. Simultaneously ablated 5*5 hole-matrix.

5.7 Nanoparticle measurements

5.7.1 Introduction and goal

The purpose of this experiment was to produce information about the (nano)particles generated by a femtosecond laser ablation. This included the measurement of the concentration and size distribution of the particles released from nickel target processed with fs-laser. Besides this, the work also included experiments with the local exhaust system. The aim of this part was to check if nanoparticles become dispersed into the surrounding air and to determine the performance of the local exhaust system. Finally, the efficiency of the air filter in the local exhaust system was tested to clarify the filtration efficiency for nanoparticles.

5.7.2 Description

The measurements were made at VTT Lappeenranta (Factory of the future) by using VTT's fs-laser workstation. During the experiments nickel disc target was continuously scanned with a constant power laser beam. The released particles were captured with an exhaust hood and the exhausted air was drawn through the HEPA filter inside the exhaust device. The filtered exhaust air was allowed to enter to room air. The principle of the set-up used in the study is illustrated in Figure 70.

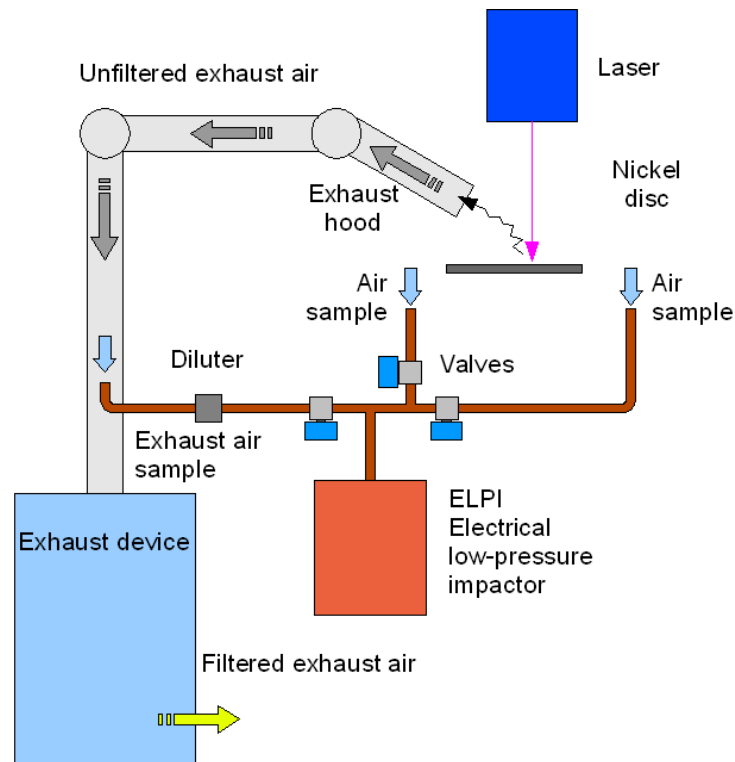


Figure 70. Principle of the measurement system.

The particle measurements were made with ELPI (Electrical low-pressure impactor) equipped with a sampling system, which was used to continuously monitor particle concentration and size distribution from three sampling points. Two of the sampling points were located in the vicinity of the nickel disc processed by the laser beam. Third sampling line was used to sample air from the exhaust duct. Because of the high particle concentration in the exhaust duct, the sampling line was equipped with a diluter which reduced the concentration by a factor of 1/25. Diluter was necessary to avoid overloading the sampling stages of ELPI analyzer.

Pneumatically operated ball valves were used to switch between sampling points in such a way that sampling time from each line was 60 s, i.e. each sampling site was monitored for one minute every three minutes. Besides ELPI measurements, some other measurement devices were used. However, these devices were used only for gathering information about the performance of direct reading particle monitors and therefore the results are not discussed in this report.

The photographs of the test set-up are shown in *Figure 71* and *Figure 72*. The photograph in *Figure 71* illustrates the location of the nickel disc, laser beam and the exhaust hood. The photograph in *Figure 72* shows the arrangement of the sampling devices.

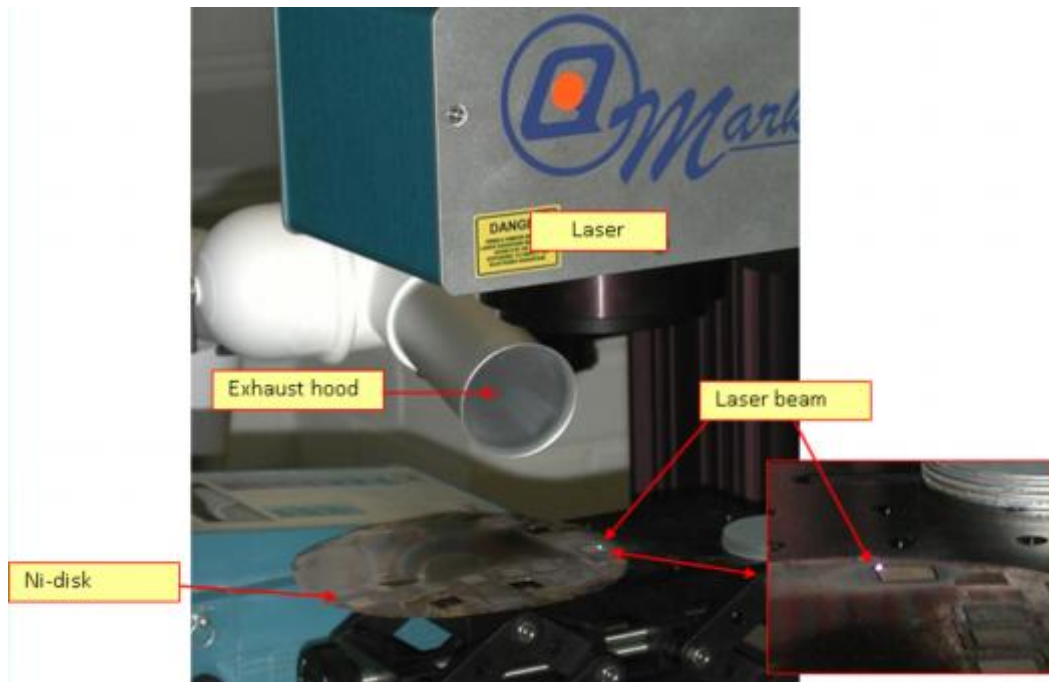


Figure 71. Photograph of the test set-up. Position of laser, nickel disc and local exhaust hood.

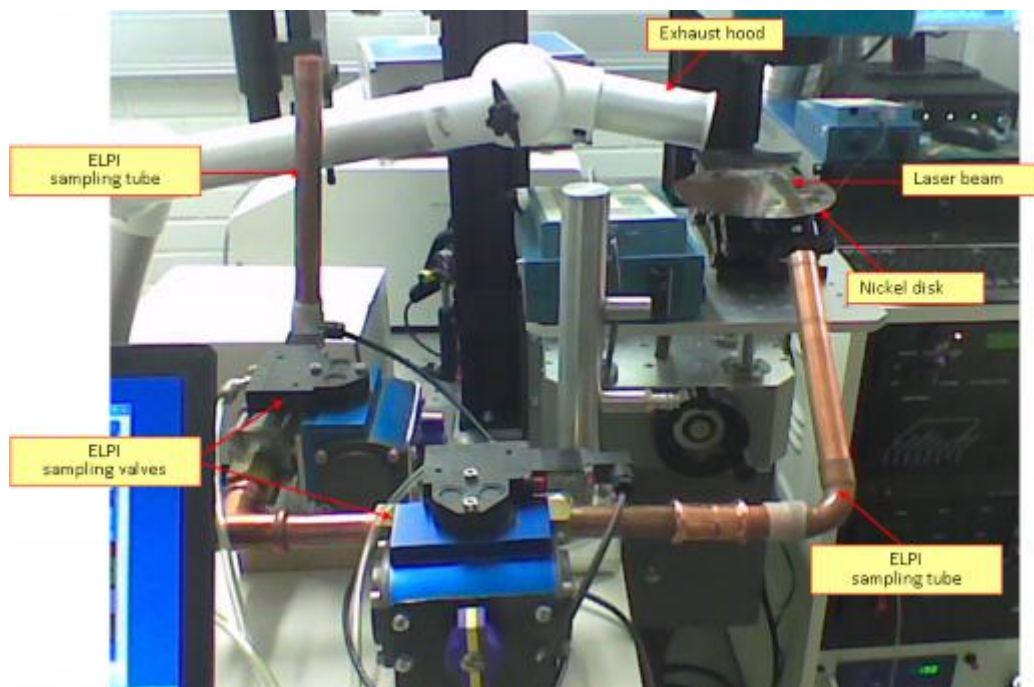


Figure 72. Arrangement of the sampling system for ELPI particle analyzer. The sampling line from the exhaust duct is not shown in this photograph.

The study also included measurements the purpose of which was to determine the removal efficiency of the local exhaust device. This measurement was made by slightly modifying the sampling system. One of the sampling lines was installed to sample air directly from the filtered air outlet of the local exhaust device (see *Figure 73*). In this way, the particle concentration in the filtered air was monitored parallel with measurements from the exhaust air and from the room air.

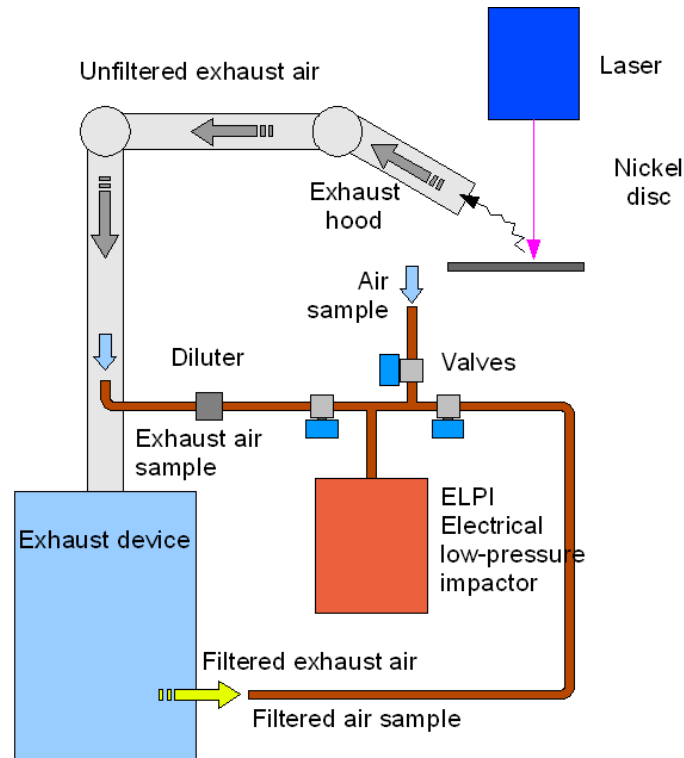


Figure 73. Principle of the sampling system used to measure particles from the outlet of the local exhaust device.

5.7.3 Measurements and results

Measurements

The measurement included three phases. The first phase was made in “normal” operation conditions, i.e. laser was used continuously at constant power and local exhaust was active, i.e. generated particles were captured by the exhaust hood. During this phase, the power of the laser switch to lower level to demonstrate the relationship between laser power and the amount of generated particles. This was, however, only a demonstration and no systematic study about the exact relationship between particle properties and laser power was made.

The purpose of the second phase was to demonstrate the importance of the proper use of the local exhaust system. The local exhaust was operated continuously but the exhaust hood was moved from its proper position further off from the particle release point. The third phase was made to check the performance of the local exhaust device. This device provides the necessary exhaust air flow and cleans the exhaust air by means of HEPA filter.

In all of these measurements ELPI analyzer was used to provide information about the particle number concentration. It must be noticed that when determining the number concentration from the ELPI readings, the density of the particles should be known. It was assumed that the particle density can be approximated by the value 2 g/cm^3 . The accuracy of this estimation may, however, be poor because no information about the morphology and composition of the particles is available. The density of nickel and nickel oxides are much higher than 2 g/cm^3 ,

but it is reasonable to assume that particles are agglomerates or aggregates with much lower effective density than the bulk density of the particle material.

Besides number concentration, also the number size distribution was determined from the results produced by the ELPI analyzer.

Results

The results from the first phase measurements show that the number concentration in the exhaust air is about 10^7 $1/\text{cm}^3$ while the corresponding concentration around the laser processing area was three orders of magnitude lower (see *Figure 74*). The results in *Figure 74* also indicate that reducing the laser power causes a clear decrease of particle concentration.

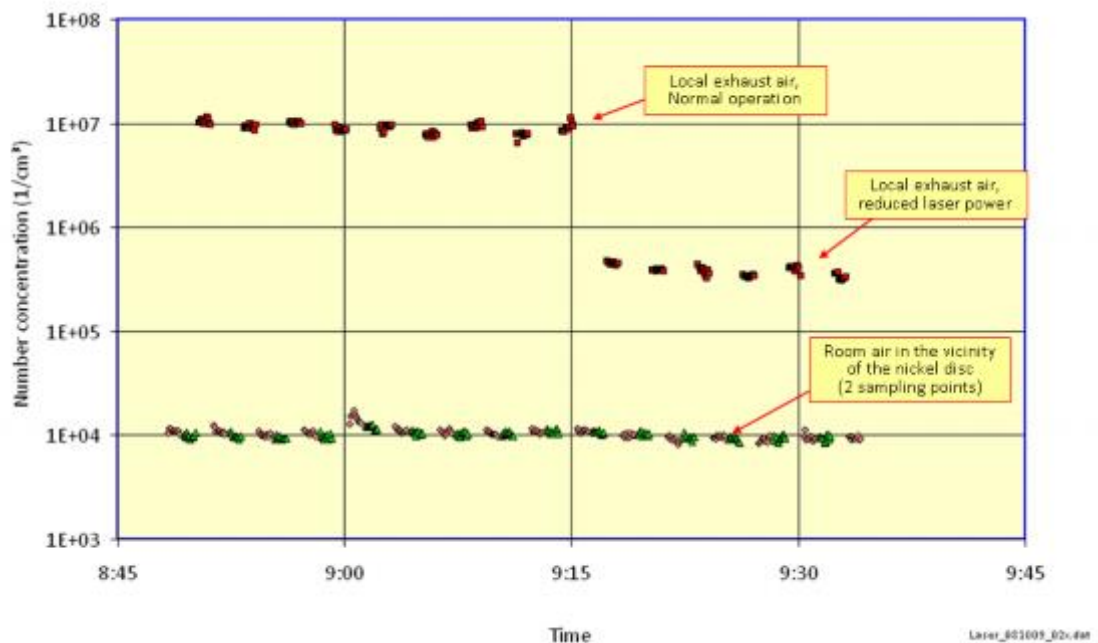


Figure 74. Particle concentration in the exhaust air in the air surrounding the laser processing area.

Figure 75 shows the particle number size distribution from the exhaust air during normal operation. According to this result, the median particle size is around 70 nm which means that most of the particles can be classified as “nanoparticles” (i.e. particles in the size range below 100 nm). It is worth noticing that the relative amount of finest particles (21 nm) is quite low. This supports the assumption that the particle concentration has been high enough to cause significant particle agglomeration.

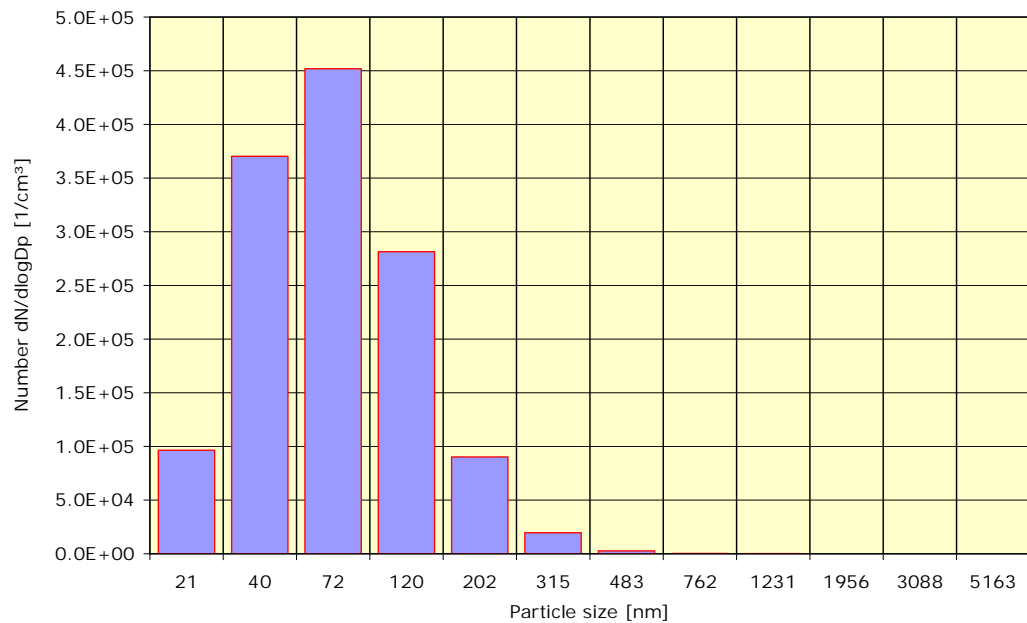


Figure 75. Particle number size distribution in exhaust air.

Figure 76 shows the results from the experiment in which local exhaust hood was moved from its proper position further off. As expected, the particle concentration drops immediately to the same level as measured in the room air. It is worth noticing that for some unknown reason, the particle concentration in room air increased during the day from about 10^4 $1/\text{cm}^3$ up to 6×10^4 $1/\text{cm}^3$. During this period with exhaust hood moved away from the proper position, practically all particles were released into the room air and it caused a concentration increase from the level of 5×10^4 $1/\text{cm}^3$ up to 10^5 $1/\text{cm}^3$. This indicates that the laser processing without the local exhaust significantly increases the particle concentration in the room air.

Figure 76 also indicates that the efficiency of the local exhaust device is quite good. The concentration in the filtered air was approximately 4×10^2 $1/\text{cm}^3$ while the concentration in the exhaust air upstream of the filter was around 6×10^6 $1/\text{cm}^3$. Thus, the removal efficiency of the filter is higher than 99.99 %.

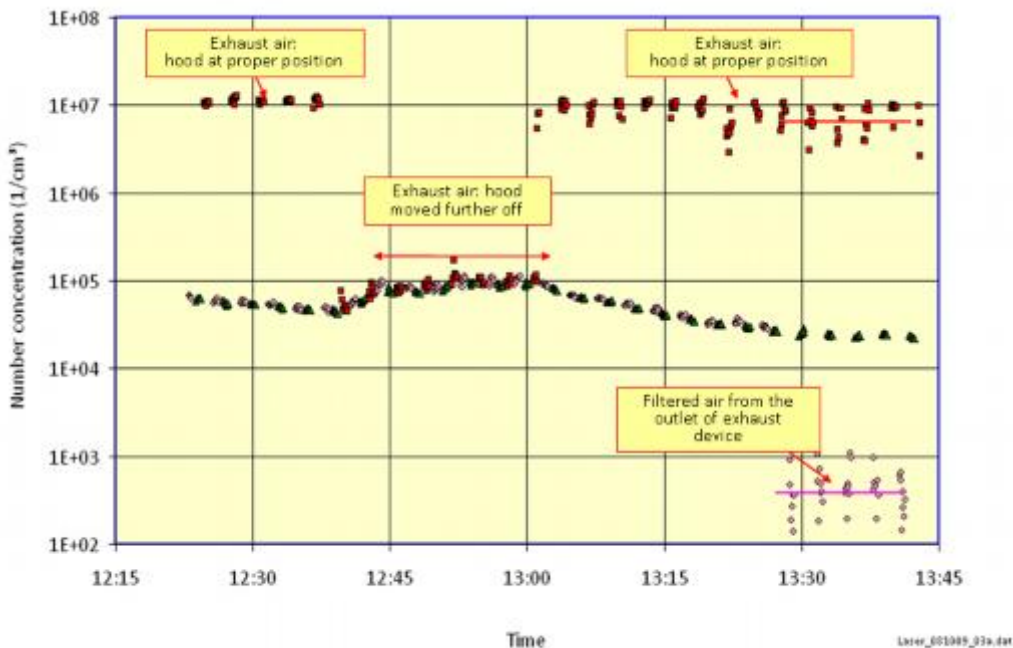


Figure 76. Particle number concentrations in the exhaust air with exhaust hood at proper position and hood moved further off, in the filtered exhaust air and in the room air.

5.7.4 Nanoparticle generation in solution

Nanoparticles of specific material have many applications, for example, in medical sciences. We tested the formation of the gold, copper, nickel, carbon, etc. nanoparticles using femtosecond ablation. Liquid (water, isopropanol) was used to collect the generated nanoparticles. The main focus was in generation of the gold nanoparticles for their suitable properties for many medical applications. The femtosecond beam was focused on surface of the gold sample that was placed inside the solution. After several minutes of ablation color of the solution turns into red indicating presence of the nanoparticle population with specific size distribution (Figure 77).



Figure 77. Gold nanoparticles in isopropanol solution.

In Figure 78 is shown the SEM image of the nanoparticles on silicon substrate when isopropanol is evaporated. The picture shows that the size of the generated gold nanoparticles varies from 100 nm down to just few nanometers. Ablation in air atmosphere results in an altered size distribution compared to one ablated in solution. In Figure 79 is shown the quite uniform assembly of gold particles ranging from 200 nm to 500 nm.

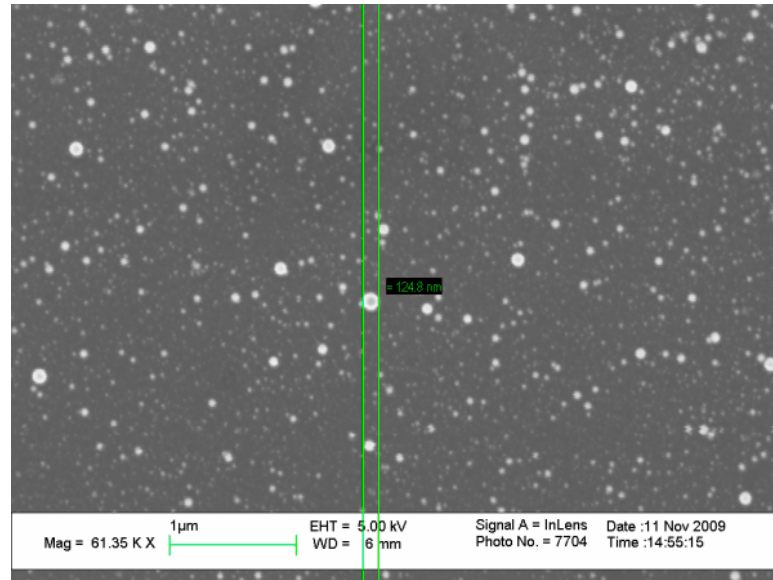


Figure 78. Gold nanoparticles made in solution on silicon substrate.

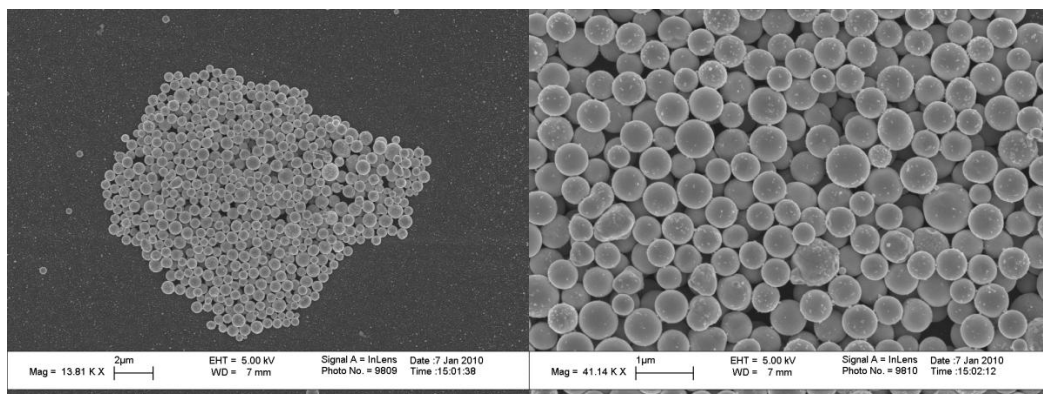


Figure 79. Gold nanoparticles made in air on silicon substrate.

5.7.5 Summary

The results of the short-term testing of the laser work station indicate that most of the generated particles can be classified as nanoparticles. The concentration in the exhaust air was 100–1000 times higher than in the room air. The particle number concentrations in the room air were in the range of 10^4 $1/\text{cm}^3$ – 6×10^4 $1/\text{cm}^3$ which cannot be regarded as “exceptionally high”, i.e. similar concentrations can be observed e.g. in urban air. The laser processing equipped with the local exhaust system did not cause any significant increase in the room air particle concentration. However, when the exhaust hood was moved from its proper position, significant contribution to the room air particle concentration was observed. The removal efficiency of the local exhaust device was above 99.99 %.

5.8 Functional surfaces

5.8.1 Hydrophobic surfaces

The wetting properties of the material can be altered by changing the surface topography. The superhydrophobic surfaces can be obtained using surface topography combining micro- and nanostructures. The reason for such enhancement of the hydrophobic properties is the reduced area fraction of the liquid-solid contact when changing the topography of the surface. These structures can be made using femtosecond laser ablation to the wide variety of material. Femtosecond laser ablation can be used for generation of both, self-organized or directly written, nano-, micro- and macrostructures. Two distinct types of surface structures were found during the project that made the surface superhydrophobic.

5.8.1.1 Self-organized structures

When ablating target surface with consecutive high fluence femtosecond pulses various self-organized structures start appearing to the sample surface. Usually these structures are considered as an undesired side-effect degrading the surface finish when using femtosecond laser for micromachining. The self-organized micro-structures consist of randomly distributed deep holes connected with ravine type formations. Average feature size of the microstructure can be controlled by laser fluence and pulse number. Note that the microstructures can be covered with self-organized nanostructures. Similar structures can be made to large selection of material including metals, alloys and semiconductors. In Figure 80 is shown example of the self-organized surface structure formed in laser-matter interaction in stainless steel.

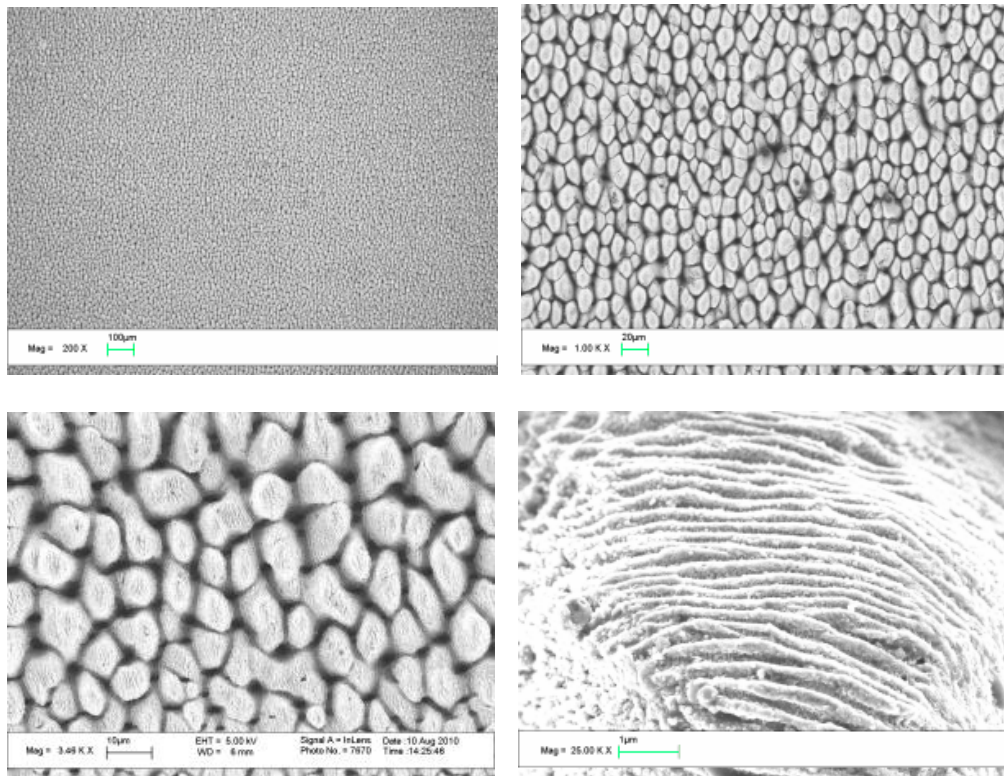


Figure 80. Sem-images of the structured surface on stainless steel with different magnifications. a. magnification of 200 times. b. magnification of 1000 times. c. magnification of 6000 times. d. magnification of 25000 times.

The hydrophobic properties of the surface are usually determined with static contact angle measurement by placing a droplet of water on a sample surface and by taking photo from which contact angle is calculated using a computer program. The surface is considered superhydrophobic if the contact angle is greater than 150° . In addition, the very low contact angle hysteresis and tilt angle indicates the self-cleaning properties for the surface. In Figure 81 is shown the contact angle measurement for polished and structured stainless steel surface shown in Figure 82. Contact angle is 80° for the polished and 152° for the structured surface.



Figure 81. Contact angle measurement of the stainless steel surface. Value of 80° is obtained for smooth surface and 152° for structured surface.

The plastic copy of the surface was made using hot-embossing.

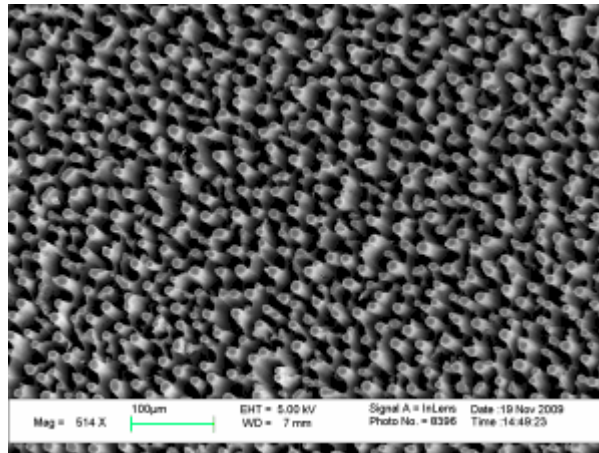


Figure 82. Sem-image of the self-organized surface structure copied to the PC plastic using hot-embossing.

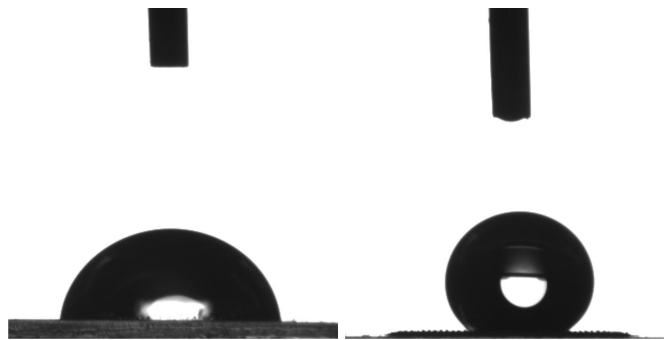
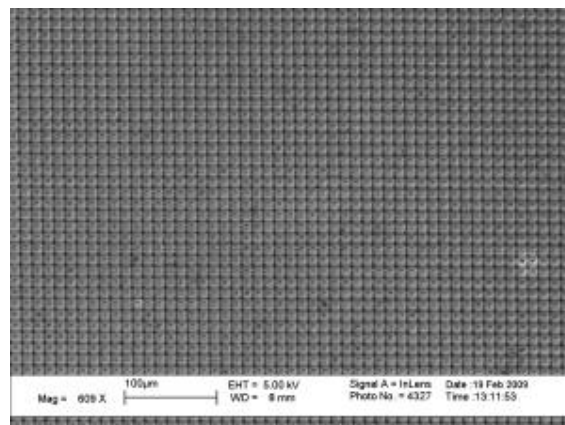


Figure 83. Contact angle measurement of the plastic surface. Value of 80° is obtained for smooth surface and 152° for structured surface.

5.8.1.2 Direct writing of the surface structures

Microstructures can be also made directly using focused fs-beam to write the desired surface texture.



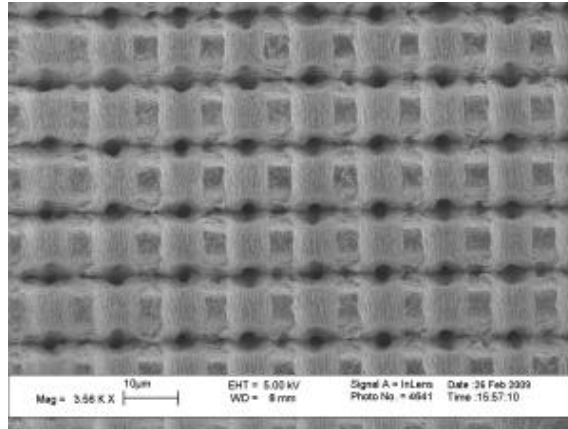


Figure 84. Two-dimensional line structure written to the surface using cylindrical lens for light focusing.

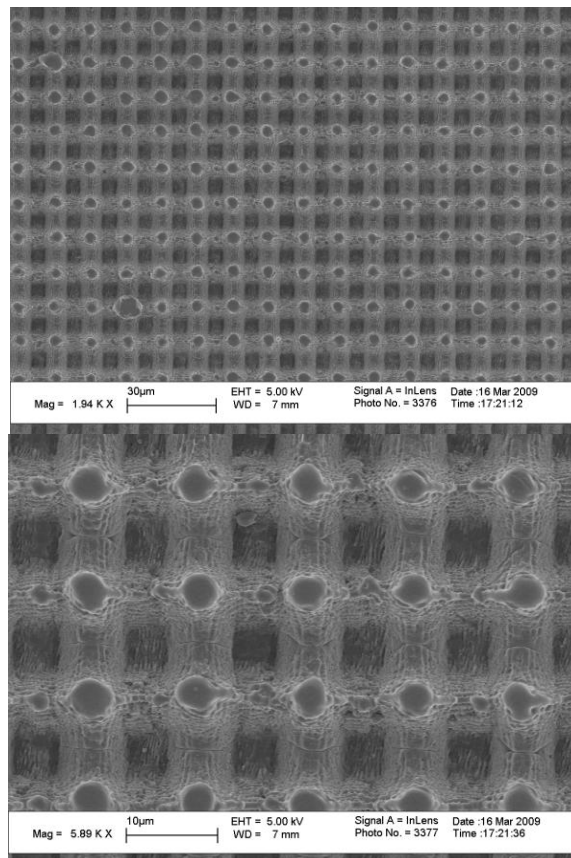


Figure 85. The injection moulded copy of the two-dimensional line structure written to the surface using cylindrical lens for light focusing.

In this project we have demonstrated the whole production chain of superhydrophobic surfaces from structured metal mould to the injection moulded plastic surface.

5.8.2 Controlling the cell adsorption using structured surface

The hydrophobic properties of the surface can also have a major role in the biomaterial adsorption at interfaces. Controlling these properties can be used to enhance desired effects, for example, cell adherence and cell migration, both important aspects of the development of biocompatible materials. The controlling of cell adsorption was tested with different surface patterning and these preliminary tests showed that the shape and position of the cells can be controlled with surface structures. In Figure 86 is shown laser written UEF logo and from the fluorescence microscope picture can be seen that the cells have refused to attach to the self-organized surface structures (Figure 80). In Figure 87 is shown how the laser written trenches affect to the shape of the attached cells. When cultivated to the surface the cell starts to expand over the surface area, but seem to be reluctant to cross deep trenches, hence it is possible, for example, elongate and orientate the cells using these structures. The osteosarcoma (U2OS) cells were used for the cultivation experiments. The cultivation was done in McCoy's 5a medium supplemented with fetal bovine serum with L-glutamine.

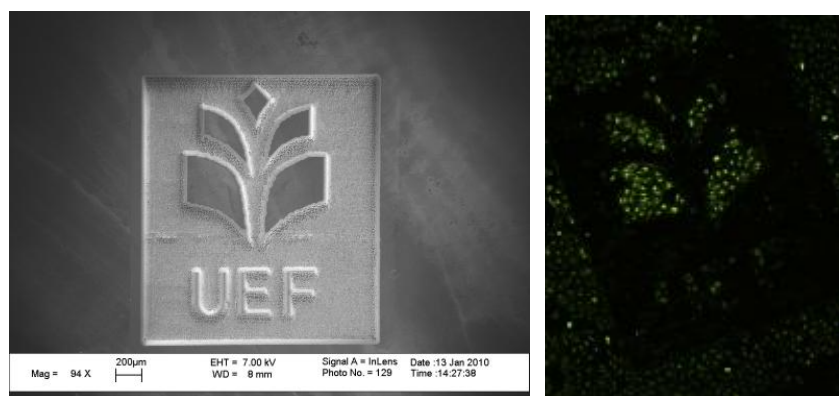


Figure 86. Laser written UEF logo. Fluorescence microscope picture shows how the cells attach only to the smooth surface and refuse to attach to the structured surface.

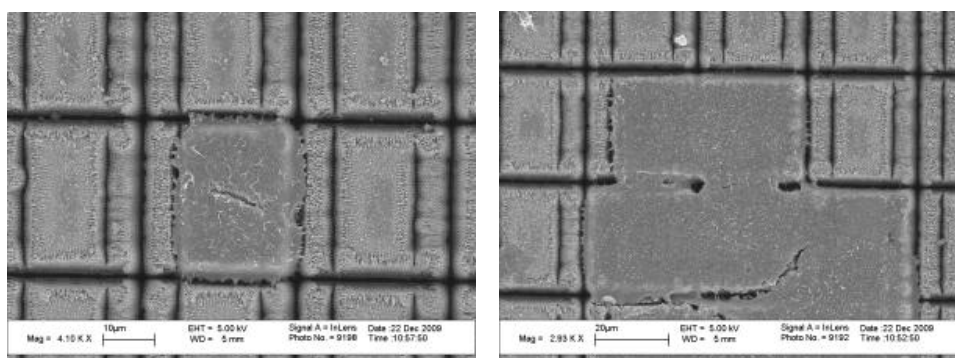


Figure 87. Laser written structures can be used to control the shape and position of the attached cells.

6 Conclusions

In this project goal was to utilize femtosecond laser processing to achieve even as small as nanoscale features. A lot of technology transfer from UEF to VTT and back was carried out during project which strengthened know how of both research organizations.

Project goals were set in the beginning of the project and during project those goals were met pretty well even though further studies would be needed to fully understand nature of femtosecond laser processing and all related phenomena. Since VTT laser group had strong competence processing with nano and pico second lasers it was really clarifying to compare femtosecond processing to these. From the results we could conclude that femtosecond processing enables even higher precision but again accuracy comes with slow processing as also with ns and ps lasers. With femtosecond laser using wrong parameters one can make really poor quality compared to carefully operated ns/ps processing so fs processing is not a thing which solves all problems. It is commonly said that in femtosecond processing laser wavelength does not play a role in processing but it really does. Only remark is that if one focuses femtosecond beam to a small spot it does process all materials but still e.g. 400 nm provides a lot better absorption to most materials than the basic 800 nm with Ti-sapphire.

Using femtosecond laser is said to give higher accuracy and this is maybe due one can really utilize the ablation threshold in a Gaussian beam. So by using different pulse energies one can make narrower groove than what spot size would presume. This also makes processing even slower.

Since the project plan and even the project name said that nanoscale structures would be done a lot of effort was put to this research. Self organizing structures were produced with less than wavelength spacing in variety of materials. Also the principles of how to control this effect into some extent were found out. Nanoscale particles were done into liquid media. These well defined particles make e.g. water to change color. Nanoscale particles that are produced during laser ablation with femtosecond laser were analyzed and results correlated well with knowledge from literature. Particles can be well under 100 nm which is in the true nanometer scale.

Building the femtosecond setups at both research places were challenging task to carry out. Since at VTT the setup was supposed to be as close to industrial case as possible the system was purchased from the laser manufacturer. This made it certain that the rental period of laser could be maximally utilized. VTT invested to the rental laser after rental period but still arrangement was good. One needs to pay more attention to femtosecond laser optics than with other lasers due pulse width tends to get longer if wrong optical components are used. Also multiple components may make the pulse longer. Using scanner did not give good beam since the beam was always distorted a bit. Also the beam was different in different places of the work field. Scanner manufacturer said this is normal to scanners when using femtosecond laser.

Functional surfaces were a big part of the project and especially the hydrophobic and hydrophilic properties were pursued. From literature the main principles how

to structurize the surface was taken as starting point. Good results were gained by laser structuring metallic surfaces. Also this effect could be copied to injection moulded samples by making an inverse structure on a mould. As high as 152° contact angles were measured. On the other hand also hydrophilic surfaces were also made when contact angle could not be measured due drop spreaded over very large area. Metallic surfaces were noticed to be hydrophilic just after processing and this effect changed over time. Depending on material the surface properties changed totally after couple of days or even up to 30 days after processing. From literature it was found out that if sample would be kept under inert atmosphere the effect would not change. Injection moulded samples did keep their properties similar days to weeks after moulding.

Using novel optical means to enhance processing speed with fs-laser was utilized successfully and compared to literature processing speed could be increased by several orders of magnitude. With diffractive optic laser drilling could be made a lot faster because several holes could be made at one pass. This parallel processing helps to avoid the problem when using femtosecond laser because high intensity pulses tend to ionize the air. Also high energy pulses end up to poor quality due effects after the pulse. When ablation is done below 10 J/cm^2 the region is called gentle ablation. This means that Ti-sapphire laser power is not used efficiently but when doing parallel processing the all power from the laser can maybe utilized.

One distinctive difference on fs processing compared to ns and ps processing can be seen in drilling for example that drilling through a sample is done after all even tough it would take time. Ns and ps laser may have a depth at which they normally stop due not so intensive laser pulses. Of course fs laser also has some limit but the effect is not so obvious.

Ti-sapphire lasers are not yet at least so rugged as the ns and ps lasers because room temperature changes can change laser operation if laser is not always on. Even tough it would be only a 5°C change in room temp could be too much. This could be a challenge for Ti-sapphire laser to survive due these used ones used had only base plate cooling and not the whole laser cooled. Another thing with the Ti-sapphire lasers is that their repetition rate cannot be raiser to a very high level and this makes them suitable for only some applications. Fiber lasers have been under heavy development and there might be the next big thing which raises femtosecond lasers up to normal production level and not just in niche applications.

For industrial production fs laser could have a lot to give but then normally high processing speed is needed and then one would like to have high repetition rate to be able to use low intensities and high speeds. Still it might be so that why use a fs laser if one could have multiple times the average power with ps laser. Fs laser has some applications in which the femtosecond pulses are needed and then one cannot make a compromise.

In the year 2010 it was showed that an fs (several hundreds of femtoseconds) laser which can provide 1200 W average power at 80 MHz. This is the state of the art but this again sets challenge for the beam guiding optics due there is so many pulses that beam has to be moving really fast or otherwise there will be a lot of heat build-up.

With a femtosecond technology one can make very interesting things but the system ruggedness is not maybe on that level needed with Ti-sapphire lasers. Maybe fiber lasers or some other lasers make the system totally reliable and push prices lower so that production with fs-laser would be more affordable.

To conclude all results in this report we could say that goals were met but a lot is still needed to do if total understanding is pursued. Femtosecond industry is still developing quite fast and new things open up new possibilities constantly and this way next year may make new applications possible.

References

- [1] 400W Yb:YAG Innoslab fs-Amplifier P. Russbuehdt, T. Mans, G. Rotarius, J. Weitenberg, H. D. Hoffmann, and R. Poprawe Optics Express, Vol. 17, Issue 15, pp. 12230-12245 (2009)
- [2] www.amphos.de
- [3] Le Harzic, R; Breitling, D; Weikert, M; Sommer, S; Föhl, C; Valette, S; Donnet, C; Audouard, E; Dausinger, F. Pulse width and energy influence on laser micromachining of metals in a range of 100 fs to 5 ps, Appl. Surf. Sci 249, 322-331, (2005).
- [4] Nolte, S; Momma, H; Jacobs, H; Tünnermann, A, Chichkov, B.N; Wellegehausen, B; Welling, H. Ablation of metals by ultrashort laser pulses, J. Opt. Soc. Am. B14, 2716-2722, (1997).
- [5] Nolte, S. Micromachining, in Fermann, M.E; Galvanauskas, A; Sucha, G (eds) Ultrafast lasers, Marcel Dekker Inc, Chapter 6, (2003).
- [6] Matsumura, T; Nakatani, T; Yagi, T. (2007) Deep drilling on a silicon plate with a femtosecond laser : experiment and model analysis. Appl. Phys. A 86, 107-114, (2007).
- [7] Charles E. Bauer and Herbert J. Neuhaus, 3D Device Integration, Proc. of the 11th Electronics Packaging Technology Conference, 2009, pp. 427-430;
- [8] Tom Jiang and Shijian Luo, 3D Integration-Present and Future, Proc. of the 10th Electronics Packaging Technology Conference, 2008, pp. 373-378
- [9] X. Zeng, X.L. Mao, R. Greif, R.E. Russo; Experimental investigation of ablation efficiency and plasma expansion during femtosecond and nanosecond laser ablation of silicon; Appl. Phys. A 80, 237-241 (2005)

- [10] Lee, Seongkuk, Yang, Dongfang and Nikumb, Suwas. Femtosecond laser micromilling of Si wafers *Applied Surface Science* 254 (2008) 2996–3005 2008
- [11] Yoo, J.H; Jeong, S.H; Greif, R; Russo, R.E. (2000) Explosive change in crater properties during high power nanosecond laser ablation of silicon, *J. Appl. Phys.*, 88, 1638-1649.
- [12] P. P. Pronko,^a) S. K. Dutta, and D. Du, Thermophysical effects in laser processing of materials with picosecond and femtosecond pulses, *J. Appl. Phys.* 78 (10), 15 November 1995
- [13] Femtosecond, picosecond and nanosecond laser ablation of solids; B.N. Chichkov, C. Momma, S- Nolte, F. von Alvensleben, A Tunnemann; *Appl. phys. A* 63, 109-115 (1996)
- [14] A. M. Rodin, J. Callaghan, N. Brennan. High Throughput Low CoO Industrial Laser Drilling Tool
http://www.emc3d.org/documents/library/technical/XSil_Laser_Drilling_A_Rodin.pdf;
- [15] Choo, K. L., Ogawa, Y., Kanbargi, G., Otra, V., Raff, L. M. and Komanduri, R. Micromachining of silicon by short-pulse laser ablation in air and under water 2004 *Materials Science and Engineering A* 372 (2004) 145–162
- [16] J. Koga et al. Simulation and experiments of the laser induced breakdown of air for femtosecond to nanosecond order pulses. *J. Phys. D: Appl. Phys.* 43 (2010) 025204
- [17] V. Mizeikis, S. Juodkazis, J-Y. Ye, A. Rode, S. Matsuo, H. Misawa, Silicon surface processing techniques for micro-systems fabrication. *Thin Solid Films* 438-439 (2003) 445-451.